Final report April 2008

WEXA: Exergy analysis for increasing the efficiency of air/water heat pumps

Elaborated by
Lukas Gasser, dipl. engineer FH
Beat Wellig, Dr. sc. techn. ETH
Karl Hilfiker, Prof. Dr. sc. techn. ETH

Lucerne University of Applied Sciences and Arts – Engineering & Architecture
CC Thermal Energy Systems & Process Engineering
Technikumstrasse 21
CH-6048 Horw

BFE
OFEN
UFE
SFOE

Preface

The WEXA study (Wärmepumpen-Exergie-Analyse - heat pump exergy analysis) was initiated by the comprehensive LOREF SFOE research project (Luftkühler-Optimierung mit Reduktion von Eis- und Frostbildung – air-cooler optimisation with reduction of ice and frost formation). In the course of the LOREF project, deeper insight was gained and it was realised that, in order to obtain an important increase in the efficiency of air/water heat pumps, all their sub-processes and the heat delivery and distribution system must also be included in an analysis.

A clear appraisal of these interrelationships can be achieved by the use of exergy analysis. Such analysis clearly shows where worthwhile potential for the optimisation for research and development can be found and how large this potential is.

Experimental exergy analyses were already carried out several years ago. In contrast to these, WEXA is a study on a theoretical basis. The study was entrusted to Lukas Gasser as a diploma thesis (Autumn 2005). With the aid of financial support provided both by the Swiss Federal Office of Energy (SFOE) and by the Lucerne University of Applied Sciences and Arts – Engineering & Architecture (HSLU - T&A), he was given the possibility of developing the study in more detail.

This work received valuable support from our team's research engineers Louis Berlinger, Martin Imholz, Rasid Sahinagic, Cornel Kuhn and Maik Albert. The extensive experience of Prof. Dr. T. Kopp, Prof. Dr. M. Ehrbar and H. J. Eggenberger also made an important contribution.

Finally, those who spurred this study on and who made sure that enough time was made available for the project are also to be cordially thanked: F. Rognon and Prof. Dr. T. Kopp from the Swiss Federal Office of Energy and Prof. J. Habegger and Prof. Dr. R Huesler from the Lucerne University of Applied Sciences and Arts.

Horw, April 2008

Karl Hilfiker, Beat Wellig

This study is also available in german.

Summary

Heating our houses is costly and still somewhat inefficient. The use of air/water heat pumps is increasing, simply because they are easy to install and operate. For house-owners, low capital expenditure for the heating system often has priority over low operating costs, so that manufacturers are also subjected to high price pressures; it is rare that a great deal of money remains for important further development. This results in the poor use of primary energy.

Heat pump systems exhibit a high potential for increasing their efficiency. The exergetic efficiency of common air/water heat pumps with on/off control amounts to about 30%. A loss-free heat pump, on the other hand, has an exergetic efficiency of 100%. Using exergy analysis, this study shows where the losses in air/water heat pumps occur, how large they are and how strongly they affect the individual sub-processes. On the basis of the exergy analysis, possibilities for making improvements are developed and the increases in efficiency to be achieved are quantified.

An energetic evaluation is necessary for making judgements on the heat pump process but does not completely suffice. The second law of thermodynamics provides information on the quality of the process. In this study, the application of the second law does not occur using abstract entropy balances but with exergy balances. The term "exergy" is easily understandable for heat pump applications: The real driving power of the compressor is higher than the driving power of an ideal (reversible) process by the sum of all exergy losses that occur. If the exergetic efficiency can be improved by further development, this will also result in an improvement in the coefficient of performance.

Basic equations for exergy loss of the heat pump as a whole, of the individual sub-processes and of the heating system were derived from elementary energy and exergy balances. These equations are suitable for representation and interpretation in T,s-diagrams as well as for numeric analyses. Four different exergetic efficiencies were defined for the evaluation of air/water heat pumps: one for the heat pump`s working fluid circuit, one with reference to the generated heating temperature for intermittently operated heat pumps with on/off control, one concerning the heating temperature continuously required by the building, and a last one that takes the desired room temperature into consideration. The exergy losses of the individual sub-processes are clearly calculated as a function of the determinant process variables. For this purpose, an analytical model was developed based on a few approximations (linearisations, series expansions) and on the thermophysical properties.

For conventional air/water heat pumps with on/off control, the generated heating capacity increases with increasing ambient temperature and the associated decrease in required heating capacity. As a result, the temperature gradients for heat transfer increase in both evaporator and condenser so that the exergy losses in the evaporator and condenser increase quasi-progressively with increasing outdoor temperature thus reducing exergetic efficiency. Further, the heating temperature generated during heat pump operation increases with increasing ambient temperature compared to that continuously required by the building, thus leading to a further exergy loss. Although this exergy loss originates outside the actual heat pump in the heat distribution system, it must, however, be attributed to the heat pump. The reason for this unfavourable behaviour of the air/water heat pump with on/off control is the unfavourable operating characteristic of the constant-speed compressor.

An important result is the increase in efficiency that can be made possible by using continuous power control (i.e. by the adaptation of the generated heating capacity to that required). In this study, continuous power control includes speed control of the compressor and of the fan. In this way, the temperature gradients of heat transfer in the evaporator and condenser that are encountered when ambient temperatures rise can be reduced effectively. In addition, the generated heating temperature

almost always corresponds to that required when this control strategy is used. The temperature lift is distinctly reduced in comparison with on/off control thus leading to a clear increase in coefficient of performance.

The power of the fan in common air/water heat pumps with on/off control is relatively small when compared with the power of the compressor. Nevertheless, it can reduce the seasonal performance factor and the annual average exergetic efficiency for air/water heat pumps with continuously controlled compressors considerably because the fans used often work at a low efficiency. If such fans operate quasi-continuously, a considerable reduction of energetic efficiency will result. In such cases, it is worthwhile equipping the fan with continuous control. If the fan is under continuous control along with the compressor, the efficiency of the fan has a considerably lower influence on the perfomance of the overall system. In this case, the seasonal performance factor can, approximately, be doubled in comparison to that of the air/water heat pump with on/off control. An important precondition for the implementation of the continuous control is the availability of efficient, continuously controllable compressors and fans. Appropriate developments are being made on the part of the manufacturers of compressors and fans. Furthermore, improved expansion valves are needed which permit lower vapour superheating in the evaporator.

This study focuses on air/water heat pumps. Many of the findings concerning the calculation of exergy losses in the heat pump and the heating system can be transferred directly to other heat pump systems.

Hopefully, this study will provide an impulse for further discussion and efforts in the area of efficient building heating systems, both by heat pump and component manufacturers as well as on the subsequent design and construction of buildings. Finally, this study should influence the further consideration of exergy analysis in the education of designers and engineers as well as in the continuing education of current professionals.

Zusammenfassung

Das Heizen unserer Häuser ist aufwändig und noch wenig effizient. Der Einsatz von Luft/Wasser-Wärmepumpen nimmt zu, mithin weil sie einfach zu installieren und betreiben sind. Für Hausbesitzer haben häufig niedrige Investitionskosten für das Heizsystem Vorrang vor tiefen Betriebskosten, so dass auch die Hersteller starken Preisdruck erfahren und für markante Weiterentwicklungen selten viel übrig bleibt. Die Folge ist eine schlechte Nutzung der Primärenergie.

Wärmepumpensysteme weisen ein grosses Potenzial für Effizienzsteigerungen auf. Der exergetische Wirkungsgrad heutiger Luft/Wasser-Wärmepumpen mit Ein/Aus-Regelung beträgt rund 30%. Die verlustfrei arbeitende Wärmepumpe hat hingegen einen exergetischen Wirkungsgrad von 100%. Diese Studie zeigt mittels Exergie-Analyse auf, wo die Verluste in Luft/Wasser-Wärmepumpen entstehen, wie gross sie sind und wie stark sich diese auf die einzelnen Teilprozesse auswirken. Auf Basis der Exergie-Analyse werden Verbesserungsmöglichkeiten erarbeitet und die damit erzielbaren Effizienzsteigerungen quantifiziert.

Die energetische Bewertung ist für die Beurteilung eines Wärmepumpen-Prozesses notwendig, aber nicht hinreichend. Über die Prozessgüte gibt der zweite Hauptsatz der Thermodynamik Auskunft. In dieser Studie erfolgt die Anwendung des zweiten Hauptsatzes nicht mit abstrakten Entropie-Bilanzen, sondern mit Exergiebilanzen. Der Begriff „Exergie“ ist für Wärmepumpen-Anwendungen leicht verständlich: Die reale Antriebsleistung des Kompressors ist um die Summe aller auftretenden Exergieverluste grösser als die Antriebsleistung des idealen (reversiblen) Prozesses. Kann der exergetische Wirkungsgrad durch gezielte Weiterentwicklungen verbessert werden, hat dies auch eine Verbesserung der Leistungszahl zur Folge.

Aus elementaren Energie- und Exergiebilanzen wurden Grundgleichungen für die Exergieverlust-Berechnungen für die Wärmepumpe als Ganzes, für die einzelnen Teilprozesse sowie für das Heizsystem hergeleitet. Diese Gleichungen eignen sich für die Darstellung und Interpretation in T,s-Diagrammen sowie für numerische Analysen. Es wurden vier verschiedene exergetische Wirkungsgrade zur Bewertung der Luft/Wasser-Wärmepumpe definiert: einer für den Wärmepumpenkreislauf, einer bezüglich der *erzeugten* Heiztemperatur bei intermittierend arbeitenden Anlagen mit Ein/Aus-Regelung, einer bezüglich der vom Gebäude kontinuierlich *erforderlichen* Heiztemperatur, und ein letzter berücksichtigt die gewünschte Raumtemperatur. Die Exergieverluste der einzelnen Teilprozesse werden mathematisch übersichtlich in Abhängigkeit der relevanten Prozessgrössen berechnet. Dazu wurde ein analytisches Modell basierend auf wenigen Approximationen (Linearisierungen, Reihenentwicklungen) und Stoffdaten entwickelt.

Bei konventionellen Luft/Wasser-Wärmepumpen mit Ein/Aus-Regelung steigt mit zunehmender Umgebungstemperatur und somit abnehmender erforderlicher Heizleistung die erzeugte Heizleistung. Als Folge davon steigen die Temperaturgefälle für die Wärmeübertragung in Verdampfer und Kondensator, so dass die Exergieverluste in Verdampfer und Kondensator mit steigender Aussentemperatur quasi progressiv zunehmen und so den exergetischen Wirkungsgrad reduzieren. Weiter wird die während dem Wärmepumpen-Betrieb *erzeugte* Heiztemperatur mit steigender Aussentemperatur gegenüber der vom Gebäude kontinuierlich *erforderlichen* zunehmend grösser, wodurch ein weiterer Exergieverlust entsteht. Dieser Exergieverlust entsteht ausserhalb der eigentlichen Wärmepumpe im Heizwärme-Verteilsystem, muss aber der Wärmepumpe angerechnet werden. Ursache für dieses ungünstige Verhalten der Luft/Wasser-Wärmepumpe mit Ein/Aus-Regelung ist die ungünstige Betriebscharakteristik des drehzahlkonstanten Kompressors.

Ein wichtiges Ergebnis ist, dass durch eine kontinuierliche Leistungsregelung (d.h. durch die Anpassung der *erzeugten* an die *erforderliche* Heizleistung) eine markante Effizienzsteigerung

möglich ist. Die kontinuierliche Leistungsreglung beinhaltet in dieser Studie die Drehzahlregelung des Kompressors und des Ventilators. Dadurch können die Temperaturgefälle für die Wärmeübertragung in Verdampfer und Kondensator mit zunehmender Aussentemperatur wirksam reduziert werden. Ausserdem entspricht die *erzeugte* Heiztemperatur mit dieser Regelstrategie stets nahezu der *erforderlichen*. Der Temperaturhub wird gegenüber der Ein/Aus-Regelung markant reduziert, wodurch die Leistungszahl deutlich ansteigt.

Die Ventilatorleistung herkömmlicher Luft/Wasser-Wärmepumpen mit Ein/Aus-Regelung ist gegenüber der Kompressorleistung verhältnismässig klein. Trotzdem kann diese bei Luft/Wasser-Wärmepumpen mit kontinuierlich leistungsgeregeltem Kompressor die Jahresarbeitszahl und den exergetischen Jahreswirkungsgrad beträchtlich reduzieren, denn oft arbeiten die eingesetzten Ventilatoren mit geringer Effizienz. Wenn solche Ventilatoren quasi im Dauerbetrieb arbeiten, erfolgt dadurch eine starke Reduktion der energetischen Effizienz. In diesem Fall lohnt es sich, auch den Ventilator mit einer kontinuierlichen Leistungsregelung auszustatten. Wird zusätzlich zum Kompressor auch der Ventilator geregelt, hat die Effizienz des Ventilators einen wesentlich geringeren Einfluss auf die Güte des Gesamtsystems. In diesem Fall kann die Jahresarbeitszahl im Vergleich zu derjenigen der Luft/Wasser-Wärmepumpe mit Ein/Aus-Regelung ungefähr verdoppelt werden. Eine wichtige Voraussetzung für die Realisierung der kontinuierlichen Leistungsregelung ist die Verfügbarkeit von effizienten, kontinuierlich regelbaren Kompressoren und Ventilatoren. Entsprechende Entwicklungen sind von Seiten der Kompressor- und Ventilator-Hersteller im Gange. Des Weiteren sind verbesserte Expansionsventile erforderlich, welche geringe Dampfüberhitzungen im Verdampfer erlauben.

In dieser Studie stehen Luft/Wasser-Wärmepumpen im Zentrum. Vielen Erkenntnisse bezüglich Exergieverlust-Berechnungen der Wärmepumpe und des Heizsystems können jedoch direkt auf andere Wärmepumpen-Systeme übertragen werden.

Es ist zu hoffen, dass die vorliegende Studie ein Anstoss für weitere Diskussionen und Anstrengungen im Bereich effiziente Gebäudeheizung ist, sowohl auf der Seite der Wärmepumpen und Komponenten-Hersteller als auch bei den Gebäudetechnik-Planern und Installateuren. Schliesslich wäre es wünschenswert, wenn das Thema Exergie-Analyse vermehrt in die Ausbildung einfliessen würde.

Table of contents

1 Heating systems using heat pumps - required versus generated heating capacity and heating temperature

1.1 Energetically efficient heating using heat pumps

Interest in heat pumps for heating purposes is generally high and will probably increase further depending on how the situation of energy demand develops. In the (Swiss) heating market for buildings, the heat pump has not yet, however, reached that level of proliferation that could be expected from its ecological advantages. The building heating market exhibits various handicaps that inhibit and oppose such widespread use: Energy prices, above all for primary energy, are still low and, for house-owners, low capital expenditure for the heating system often has priority over low operating costs; heating systems on a combustion basis are very well known, optimised in their operation and cheap from the investment point of view. This means that the manufacturers of heat pumps are faced with enormous competition and, in particular, a strong pressure on prices exists under which the potential for substantial further developments clearly suffers. In order to effectively counter the bad use of primary energy through the use of more efficient and more ecological heating systems, however, increased investment and effort are necessary not only in the further development of alternative heating systems in general, but more importantly of heat pumps too.

Heat pumps for the *heating of buildings* were first successfully implemented in Switzerland in 1939/40, namely in Zurich, for the Congress House, the City Hall and an indoor swimming pool. This was a result of Switzerland not being able to import sufficient coal during the war. The heating of residential buildings with heat pumps began between 1973 and 1978 as a result of the oil crises. In order to arrive at a functioning integral heating system using this technology, however, long-term developments were necessary. These efforts were initiated and supported by the Swiss Federal Office of Energy.

In recent years, the *Swiss Federal Office of Energy* (SFOE) has once again taken on the task of promoting the use of heat pumps in the heating of buildings. One of the most important conditions for the increased proliferation of heat pumps for heating purposes lies in the substantial increase of their efficiency. Therefore, the SFOE launched several research projects in this area (included the study presented here); whereby optimal economical efficiency and ecological concerns are considered.

Heat pumps still have a large potential for improvement in their energy performance. In around 1980, the seasonal performance factor (SPF) of air/water heat pumps was somewhat less than two, in 2005 about three. Is that good? A thermodynamically exact evaluation can be made using *exergetic efficiency*. During the same period of time this has increased from around 20% to 30% - an ideal heat pump working without any losses has an *exergetic efficiency* of 100%.

The aim of the study presented here is, using *exergy analysis,* to systematically show *where* the losses in heat pumps occur, *how large* they are and, also, how strongly these losses affect the other sub-processes of heating systems that use heat pumps. All evaluations of thermodynamic efficiency use the two terms *exergy loss* and *exergetic efficiency*. The exergy concept does not receive the attention it deserves in the field of heating engineering, even though the concept of *exergy losses* is easily understandable for heat pumps and refrigeration plants: The *actual* (mechanical or electrical) drive power is higher than the *ideal* (reversible) drive power by precisely the sum of all *exergy losses* of the sub-processes.

Four important sources of *exergy loss* can be found in heat pumps*:* On the one hand in the compressor and expansion valve (throttle) due to *drop in pressure* caused by working fluid flow and, on the other hand, in the evaporator and condenser due to the *temperature gradients* required for heat transfer.

In thermal power engineering, the perceived *potential* for energetic and economical *improvement* is frequently to be found where the *part of the total exergy loss* is highest. This also applies to heat pumps. The *exergy loss* of the working fluid in the expansion valve is relatively small but higher in the evaporator when transferring heat (from ambient air to the evaporating working fluid). The *temperature gradient* is relevant here.

In the case of conventional air/water heat pumps with on/off control, the *generated* heating capacity paradoxically increases with increasing ambient temperature and the associated decrease in *required* heating capacity. This means that the temperature gradients for heat transfer also increase. As a consequence, the heating temperature *generated* by the heat pump in intermittent operation (on/off control) is higher than that continuously *required* by the building. As a result, a further loss of exergy of heat transfer results because of the increasing and decreasing heating temperature during the heat pump’s heating cycle when it is switching between on and off and back to on again. This means that the exergetic efficiency deteriorates for intermittent operation. This state of affairs is analysed in this study and offers a starting point for important improvements.

Great progress in electrical engineering and electronics and also in compressor and fan technology opens new possibilities for the process control of heat pumps. Lower overheating in the evaporator with electronically controlled expansion valves already permits *lower maximum temperature lifts*. In particular, important improvements in *thermal efficiency* and (in the longer-term) economic efficiency result from the *continuous power control of the compressor* - and also, in the case of air/water heat pumps, of the *fan* - in that the *generated* heating capacity is continuously adapted to the heating capacity actually *required* and therefore, of course, the heating temperature *generated* by the heat pump is also continuously adapted to that *required*. As a result, the formation of frost on the fin tube evaporator, the effort for defrosting and the temperature difference are also reduced at the same time.

1.2 On the thermodynamics of heating

Currently, heating is still mainly done by using the chemical combustion energy contained in mineral oil, natural gas or biomass. The *transformation* of *energy* into heating heat occurs almost completely in accordance with the *1st law of thermodynamics;* the *thermal efficiency* is over 90% and, in the case of electric heaters, virtually 100%. On the other hand, the *exergetic efficiency* is only 5%, i.e. incredibly low. This quantification results from the *2nd law of thermodynamics*. A simple illustration on this: Mechanical and electrical energy are of forms of energy with a high quality rating and that of chemical energy is of a similar *quality* too. On the other hand, *heat as a form of energy* exhibits an inferior *energy quality,* this being dependent on its temperature relative to ambient temperature. The *quality* of the heat energy Q with an absolute temperature T in relation to a (defined) ambient temperature T_A is quantified by the term *exergy of heat* E_Q (cf. section 2.2). The associated formula is:

$$E_Q = Q \cdot \frac{T - T_A}{T} = Q \cdot \left(1 - \frac{T_A}{T}\right) = Q \cdot \eta_C \tag{1}$$

or, formulated as exergy and heat flows:

$$\dot{E}_Q = \dot{Q} \cdot \frac{T - T_A}{T} = \dot{Q} \cdot \left(1 - \frac{T_A}{T}\right) = \dot{Q} \cdot \eta_C \tag{2}$$

η_C is the *Carnot factor*. For very high temperatures, it approaches the value of 1 and therefore: $E_Q = Q$. If, however T tends toward T_A, E_Q approaches zero.

At an ambient temperature of 0°C (273 K), a heating capacity of 100 kW at 20°C (293 K) has an exergy flow of 7 kW; the Carnot factor is 7%. The corresponding *exergetic efficiency* of an electric heater is 7% (referred to the electricity supply in the house).

The following table shows the relationship between exergy E_Q and heat Q for a selection of temperatures ϑ in relation to $\vartheta_A = 0°C$.

ϑ in °C	0	10	20	40	100
$\frac{E_Q}{Q} \equiv \eta_C$	0%	3.5%	6.8%	12.8%	26.8%
$COP_{rev} = \frac{\dot{Q}}{P_{rev}} = \frac{1}{\eta_C}$	-	28.6	14.7	7.8	3.7

Tab. 1-1: $E_Q / Q = \eta_C$ *und* COP_{rev} *mit* $\vartheta_A = 0°C$

This ratio factor E_Q / Q is important because it represents the minimum *exergy expenditure* for heating. It will be shown later that this relationship represents the minimum expenditure of mechanical or electrical power P_{rev} for the *required*[1] heating capacity $\dot{Q}_H^*$ when using an ideal heat pump [1]. The reciprocal value is accordingly the *best possible coefficient of performance for a reversible air/water heat pump* with reference to the *required* heating temperature T_H^*:

$$COP_{rev\,e}^* = \frac{T_H^*}{T_H^* - T_A} = \frac{T_H^*}{\Delta T_{Lift\ ideal}} = \frac{1}{\eta_{Ce}^*} \quad (3)$$

It follows from this formula that the *ideal coefficient of performance* is reciprocal to the temperature lift ΔT_{Lift}. This is approximately valid for a typical heat pump. This means that doubling the temperature lift cuts the *coefficient of performance* in half.

Analogous to Eq. (3) the following applies to the maximum or *reversible coefficient of performance of the best possible (ideal) heating system using air/water heat pumps* with reference to the room temperature T_R desired:

$$COP_{rev\,HS} = \frac{T_R}{T_R - T_A} \quad (4)$$

Therefore, the *required* heating temperature T_H^* (average *required* heating water temperature) ideally exactly corresponds to the room temperature T_R. The building services engineering planner should to bear this fact in mind when designing a heating system using a heat pump.

---

[1] All variables that refer to heating capacities required and heating temperatures required are designated with a star * superscript.

A fascinating of the heat pump is that the heating capacity $\dot{Q}_H$ is obtained with a relatively small amount of mechanical driving power P and the difference can be taken as heat flow $\dot{Q}_A$ from the colder environment. Fig. 1-1 shows the energy flow diagram ($\dot{Q}_{A_{rev}}$; P_{rev}; $\dot{Q}_H$) and the *heating exergy flow* $\dot{E}_{Q_H}$ of an *ideal* heat pump and Fig. 1-2 that of a *typical* heat pump. Both operate with the same temperatures (T_A and T_H) and the same *generated* heating capacity $\dot{Q}_H$. In both cases, therefore, $\dot{E}_{Q_H}$ is the same: indeed $\dot{E}_{Q_H} = P_{rev}$. However $P > P_{rev}$ and $\dot{Q}_A < \dot{Q}_{A_{rev}}$. The exergy flow $\dot{E}_{Q_A}$ from the environment is in both cases zero.

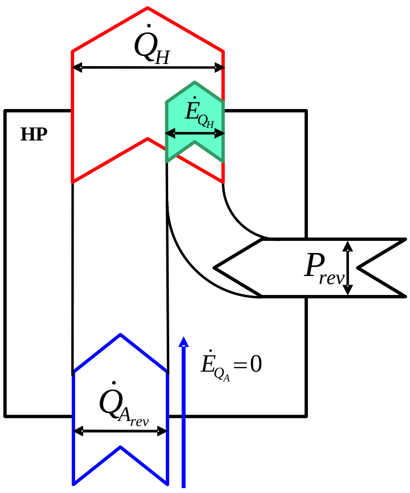

Fig. 1-1: Energy and exergy flow diagram of an ideal heat pump

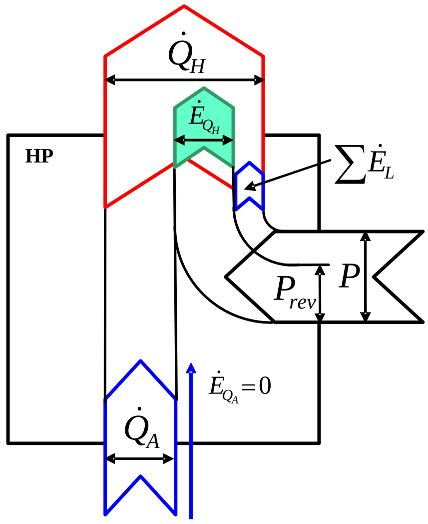

Fig. 1-2: Energy and exergy flow diagram of a real world heat pump

The idea of the heat pump process (and therefore of the refrigeration process too) is 150 years old and originates from the imaginative physicist Thomson, otherwise known as Lord Kelvin (1824 - 1907). The professional world distrusted this idea; Kelvin discovered that the principle of the heat pump is only the inversion of the reversible heat engine. This had already been conceived by the young Sadi Carnot in 1826.

A systematical representation of the thermodynamics of heating has been supplied by Baehr in two contributions made in 1980 [1] [2]. In these, the distribution of the heat and exergy requirements over time during the annual heating season is determined. Among other things, the behaviour of compression heat pumps under partial load is examined and, in particular, the problem of the drifting gradient between the heating capacity *required* by the heating system and the heating capacity *generated* by the heat pump.

1.3 Annual heating requirements and its exergy expenditure necessary

The dimensioning of a heating system depends on the *minimum ambient temperature defined*. From this, the *maximum heating capacity required* for the building $\dot{Q}_{max}^*$ can be calculated in accordance with its thermal insulation; in addition, the *maximum temperature lift* for the heat pump can also be calculated. For economical and thermodynamic evaluations, however, representative atmospheric temperature characteristics over the whole year (taken from statistical records) are the decisive factor. The cumulative frequency distribution (in days per year) against average daytime temperature can be considered as a suitable representation. This daily average of the external air temperature is defined as *ambient temperature* T_A both in exergy analysis and, consequently, in this study too: It serves as a reference temperature (cf. chapter 2). The cumulative frequency distribution function of the ambient temperature for Zurich is shown in Fig. 1-3, shown from the *coldest day* through to the *hottest day* in the year (taken from measurements made from 1990 to 2000).

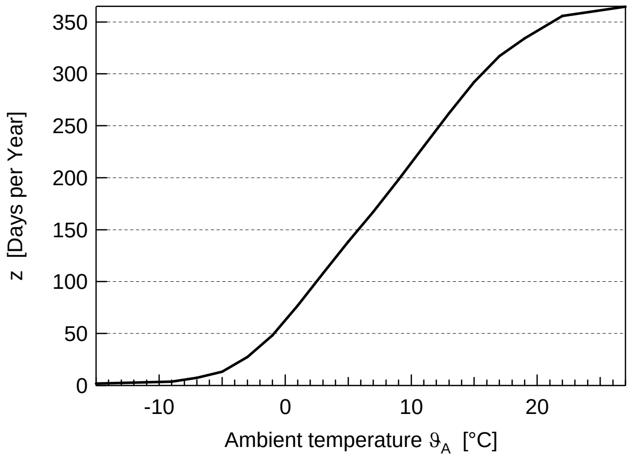

Fig. 1-3: Cumulative frequency distribution function for the ambient temperature in Zurich (1990-2000)

The *distribution over time* of the *required* heating capacity $\dot{Q}_H^*$ results from the particular ambient temperature. In Fig. 1-4 this is represented as $\dot{Q}_H^* / \dot{Q}_{max}^*$ over the year, once more in the direction of cold to warm. The shaded area below represents the annual amount of heat required for heating in relation to $\dot{Q}_{max}^*$. On the right-hand side of the diagram, the ambient temperature is shown as the ordinate. The heating limit temperature here is 20°C.

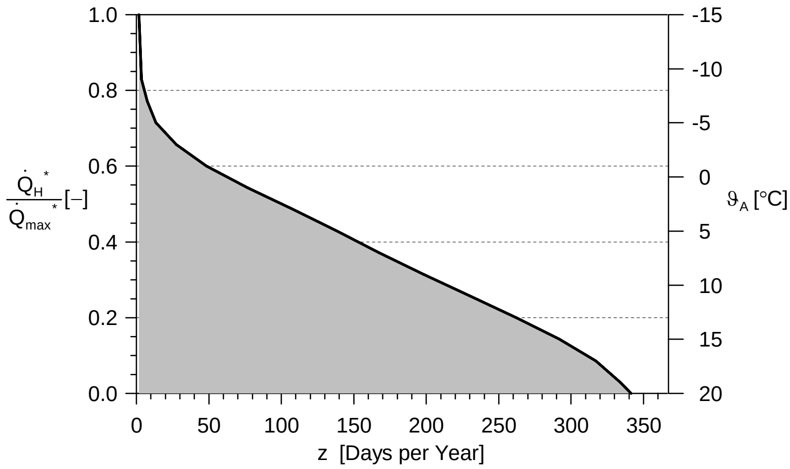

Fig. 1-4: Distribution of heating requirements over time in days per annum as shown in Fig. 1-3

The *exergy of the heat needed for heating* for a *required* heating temperature T_H^* at an ambient temperature of T_A is determined by the *Carnot factor:*

$$\dot{E}_{Q_H}^* = \dot{Q}_H^* \cdot \frac{T_H^* - T_A}{T_H^*} = \dot{Q}_H^* \cdot \eta_{Ce}^* \tag{5}$$

The distribution of the *exergy flow required for heating*, $\dot{E}_{Q_H}^*$ over the year, as far as the *required* heating capacity and heating temperature are concerned, is shown in Fig. 1-5, namely as the relation $\dot{E}_{Q_H}^* / \dot{Q}_H^*$. This corresponds to the distribution of the *Carnot factor* over time for the year. The heating temperatures 20°C, 40°C and 60°C are shown as parameters. In this way increasing *exergy expenditure* for higher heating temperatures is clearly shown. A good building insulation indeed reduces exergy expenditure for heating because $\dot{Q}_H^*$ is lowered. Further, a heating system operating at lowest possible heating temperatures demands less exergy. When heating with heat pumps, heat losses in the heating distributing system are usually insignificant; *exergy losses* resulting from temperature gradients for heat transfer, however, are not.

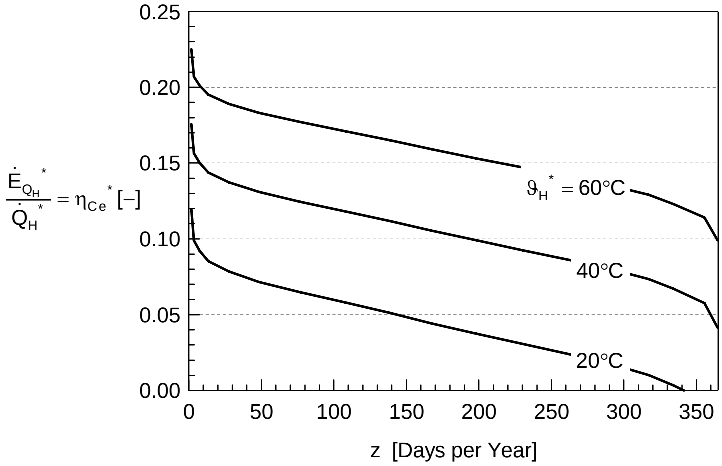

Fig. 1-5: Distribution of the exergy flow required for heating in days per year for the required heating capacity is shown in Fig. 1-4 and Eq. (5), i.e. $\dot{E}_{Q_H}^*$ *is always calculated using the appropriate ambient temperature*

Fig. 1-6 shows the comparison between both the distribution of heating and exergy requirements over time in days per annum, both being referred to $\dot{Q}_{max}^*$. The distribution of exergy requirements over time is shown for a *required* heating temperature of ϑ_H^* = 40°C.

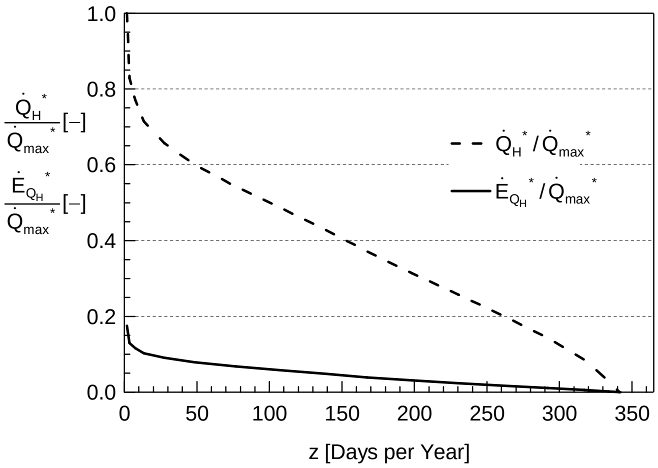

Fig. 1-6: Distribution of the heating and exergy requirements in days per annum according to Fig. 1-3

In the case of an ideal heat pump, the *minimum (reversible)* driving power[2] corresponds exactly to the exergy flow $\dot{E}_{Q_H}^*$ *required* for heating (cf. Fig. 1-1 and Fig. 1-2). In the case of traditional heating systems (e.g. electrical or oil-fired heating), on the other hand, the entire *required* heat flow $\dot{Q}_H^*$ has to be provided by electrical energy and/or by the combustion of chemical energy.

[2] In this study the exergy losses occurring during the generation of electricity are not taken into account.

1.4 Heating temperature and temperature lift in relation to ambient temperature

From the energy point of view, the lower the temperature lift, the more effective the heat pumps are for heating. The coefficient of performance is approximately inversely proportional to the temperature lift (cf. section 1.2). The temperature lift is *minimal,* when the heat *generated* by the air/water heat pump can be delivered at just the *required* room temperature T_R .

$$\Delta T_{Lift\ min} = T_R - T_A \quad (6)$$

In reality, however, the temperature lift is increased by all the temperature gradients necessary for heat transfer, i.e. those in the evaporator for heat transfer from the ambient by $\Delta T_E \approx T_A - T_E$, in the condenser for the transfer of the heating capacity to the heating-circuit water by around $\Delta T_C \approx T_C - T_H$ and, finally, from the heating water to the room air by around $\Delta T_R \approx T_H - T_R$. Therefore, for a heating system with an air/water heat pump, the *effective temperature lift* is given by:

$$\Delta T_{Lift} = \Delta T_{Lift\ min} + \Delta T_E + \Delta T_C + \Delta T_R \quad (7)$$

These three temperature gradients are, essentially, the cause of *exergy losses* and correspondingly increase the *exergy expenditure* in the heat pump necessary for heating.

The subdivision of the temperature gradients shown in Eq. (7) for the delivery of the heat is still insufficient for a clear judgement if the heat is continuously *required* but only *generated* intermittently by conventional on/off-controlled heat pumps. Consequently, it is important to distinguish between the *required* and the *generated* heating temperatures. In this study, we make the assumption that heat distribution (in the heating distribution system) is done using heating water and, therefore, we distinguish between the *heating (water) temperature generated* T_H and the *heating (water) temperature required* T_H^*. The first one, T_H, is intermittent in the case of heat pumps with on/off control, the second one, T_H^*, is continuous. This non-stationary process in the heating distribution system can be easily handled in a practice-oriented way; this will be done in section 1.5. For the delivery of the heat required for heating purposes, three temperature gradients are introduced:

$$\Delta T_C = T_C - T_H ; \quad \Delta T_H = T_H - T_H^* ; \quad \Delta T_R = T_H^* - T_R \quad (8), (9), (10)$$

In accordance with the law for stationary heat transfer, the temperature gradient ΔT_i for a heat flow of $\dot{Q}_i$ can be influenced by the heat exchanger surface area A_i

$$\Delta T_i = \frac{\dot{Q}_i}{k_i \cdot A_i} \quad (11)$$

whereby i can be replaced by E or C for the evaporator or condenser, respectively.

Subsequently, small temperature gradients must be compensated for with larger heat exchanger surfaces. Moreover, a certain minimum temperature gradient is needed in the evaporator for the *superheating required* for the functioning of the expansion valve.

Another point must be considered for the development of optimised air/water heat pumps: the *behaviour of the air/water heat pump under part load*, i.e. when the ambient temperature ϑ_A is higher than the design temperature $\vartheta_{A\,min}$ reducing the *heat flow required* for heating purposes. To look at this we must consider the *characteristics of the heat distribution and delivery system* which includes first the *required heating capacity* and, second the *heating capacity generated* by the air/water heat pump.

As the *heat flow* required for heating the building is approximately proportional to the difference between room temperature and ambient temperature ($T_R - T_A$) the following is valid:

$$\frac{\dot{Q}_H^*(T_A)}{\dot{Q}_{max}^*} = \frac{T_R - T_A}{T_R - T_{A\,min}} \tag{12}$$

After a modification according to Raiss [3], the following applies for the transfer of the heat into the room being heated:

$$\frac{\dot{Q}_H^*(T_A)}{\dot{Q}_{max}^*} = \frac{T_R - T_A}{T_R - T_{A\,min}} = \left(\frac{T_H^* - T_A}{T_{Hmax}^* - T_{A\,min}}\right)^{\frac{1}{m}} \tag{13}$$

From the relation (13) the following applies for the heating temperature *required* in relation to the ambient temperature:

$$T_H^*(T_A) = T_R + \left(T_{Hmax}^* - T_R\right)\cdot\left(\frac{T_R - T_A}{T_R - T_{A\,min}}\right)^m \tag{14}$$

For radiator heating units, Raiss [3] indicates for the empirically determined exponent m = 0.75. For well-designed floor heating systems, this exponent is closer to one.

Three such *required heating temperatures* T_H^* dependent on the ambient temperature according to Eq. (14) are shown in Fig. 1-7. The parameters are $\vartheta_{A\,min} = -15°C$ and the maximum heating temperatures $\vartheta_{Hmax}^* = 30°C, 45°C$ and $60°C$.

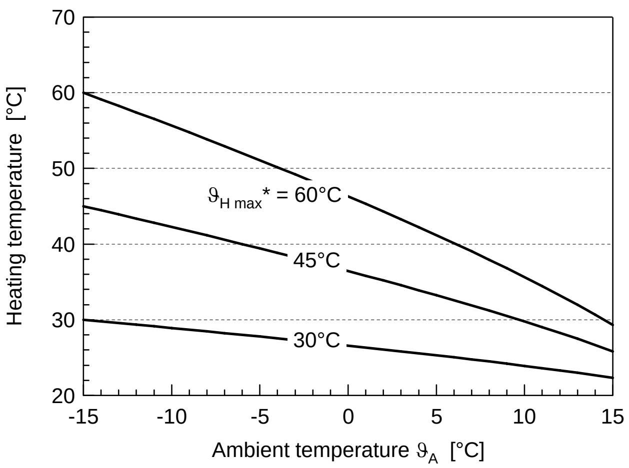

Fig. 1-7: Curves of required heating temperature as a function of ambient temperature

From this, it becomes obvious that in the case of unfavourably-designed heat distribution and delivery systems, the gradient of the *required temperature lift* for heat pumps is greatly reduced when ambient temperatures increase. This fact should be kept in mind when attempting to increase the efficiency of heat pumps.

For the *yearly evaluation* of heating systems with air/water heat pumps, the distribution of the heating temperature and ambient temperature *over the annual heating season* is a decisive factor. Heat pump manufacturers show in their advertising that the coefficient of performance of the heat pump increases with the ambient temperature. Can one, however, also expect an improvement in exergetic efficiency for part load?

This does not apply up to now to so-called conventional air/water heat pumps (with on/off control). On the contrary, with higher ambient temperatures the compressor delivers a higher mass flow of working fluid. As a result, the heating capacity *generated* by the heat pump increases, and consequently higher temperature gradients are found in the evaporator and condenser. Accordingly, the temperature lift *generated* decreases less significantly with increasing ambient temperature in comparison to the *required* (ideal) temperature lift (cf. Fig. 1-8). This means that the *external exergetic efficiency* of conventional air/water heat pumps decreases with increasing ambient temperature.

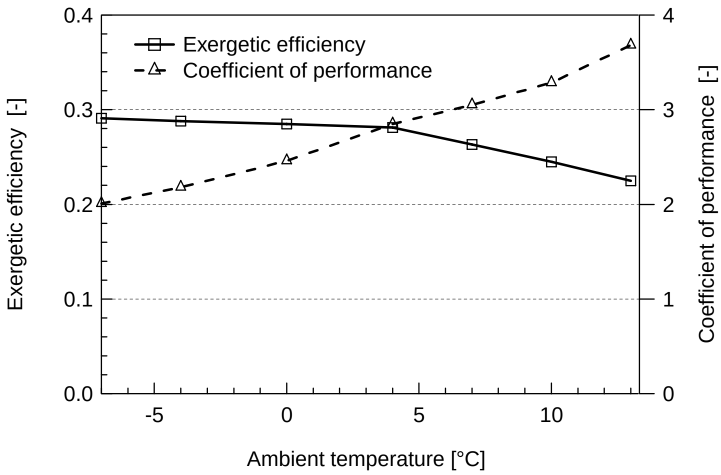

Fig. 1-8: Coefficient of performance and exergetic efficiency of a real-world air/water heat pump with on/off control according to measurements ($\dot{Q}_{H\,nom} = 7\,kW$ *)*

Curves of the coefficient of performance and the exergetic efficiency in relation to ambient temperature calculated from measurements [4] are shown in Fig. 1-8 for an air/water heat pump with 7 kW nominal heating capacity. Although the coefficient of performance increases from 2 to 3.7 for 0°C to 13°C, the exergetic efficiency falls, however, from 0.29 to 0.22. An increase in exergetic efficiency should be strived for which will come with and an even larger increase in coefficient of performance for decreasing *required* heating capacity of rising ambient temperatures.

1.5 Divergence of required and generated heating temperature and heating capacity for heat pumps with on/off control

The above section shows that an increase in ambient temperature reduces both the *required* heating capacity and the *required* heating temperature. On the other hand, the behaviour of conventional heat pumps, whose compressor is driven with constant speed, is exactly the opposite, the lower the heating capacity and the heating temperature *required* by the building, the higher the heating capacity and temperature *generated*. This peculiarity will be analysed for the operating characteristics of heat pumps (with on/off control) in the chapter 5. The control of heating capacity is achieved by switching on and off (on/off control). A cycle consists of the operating period $(t_1 - t_0)$ and the standstill period $(t_2 - t_1)$, cf. Fig. 1-9. Assuming constant *required* heating capacity $\dot{Q}_H^*$ during the heating cycle $(t_2 - t_0)$ and constant *generated* heating capacity $\dot{Q}_H$ during the operating period $(t_1 - t_0)$ the following condition applies:

$$\dot{Q}_H^* \cdot (t_2 - t_0) = \dot{Q}_H \cdot (t_1 - t_0) = Q_H^* = Q_H \tag{15}$$

The two amounts of heat within a cycle must be identical (heat losses taken to be negligible), cf. Fig. 1-9. In practice these are the mean values of the heat flows.

We define the *heat flow ratio* υ in relation to *required* heating capacity $\dot{Q}_H^*$ with:

$$\upsilon = \frac{\dot{Q}_H}{\dot{Q}_H^*} \geq 1 \tag{16}$$

Which means that the *heat pump operation ratio* f is:

$$f = \frac{t_1 - t_0}{t_2 - t_0} = \frac{1}{\upsilon} \leq 1 \tag{17}$$

Fig. 1-9 shows the resulting temperature curves. T_H^* is the *required* heating temperature which, along with $\dot{Q}_H^*$, is determined by T_A, T_R and the heating curve of the building. As the *generated* heating temperature T_H is larger than T_H^*, exergy losses result in the heat distribution system. - These losses are identified separately and are caused by the on/off operation of the heat pump.

The heat pump is turned on as soon as the return temperature has dropped to a predetermined value and then *generates* the amount of heat Q_H during the operating period. During this operating period, the *generated* supply and return temperatures (T_{SP} and T_{RT}) increase as the heat flow *generated* is larger than that *continuously required* by the building $\dot{Q}_H^*$. The arithmetic mean value of the supply and return temperatures are used as the heating temperature.

The *generated* return temperature averaged over the operating time ($\overline{T}_{RT}$) corresponds to the one continuously *required* by the building T_{RT}^* (in accordance with the heating curve of the building).

From now on in this study, the supply, return and heating temperatures (T_{SP}, T_{RT}, T_H) will be represented by the values of the delivered temperatures averaged over time ($\overline{T}_{SP}$, $\overline{T}_{RT}$, $\overline{T}_H$).

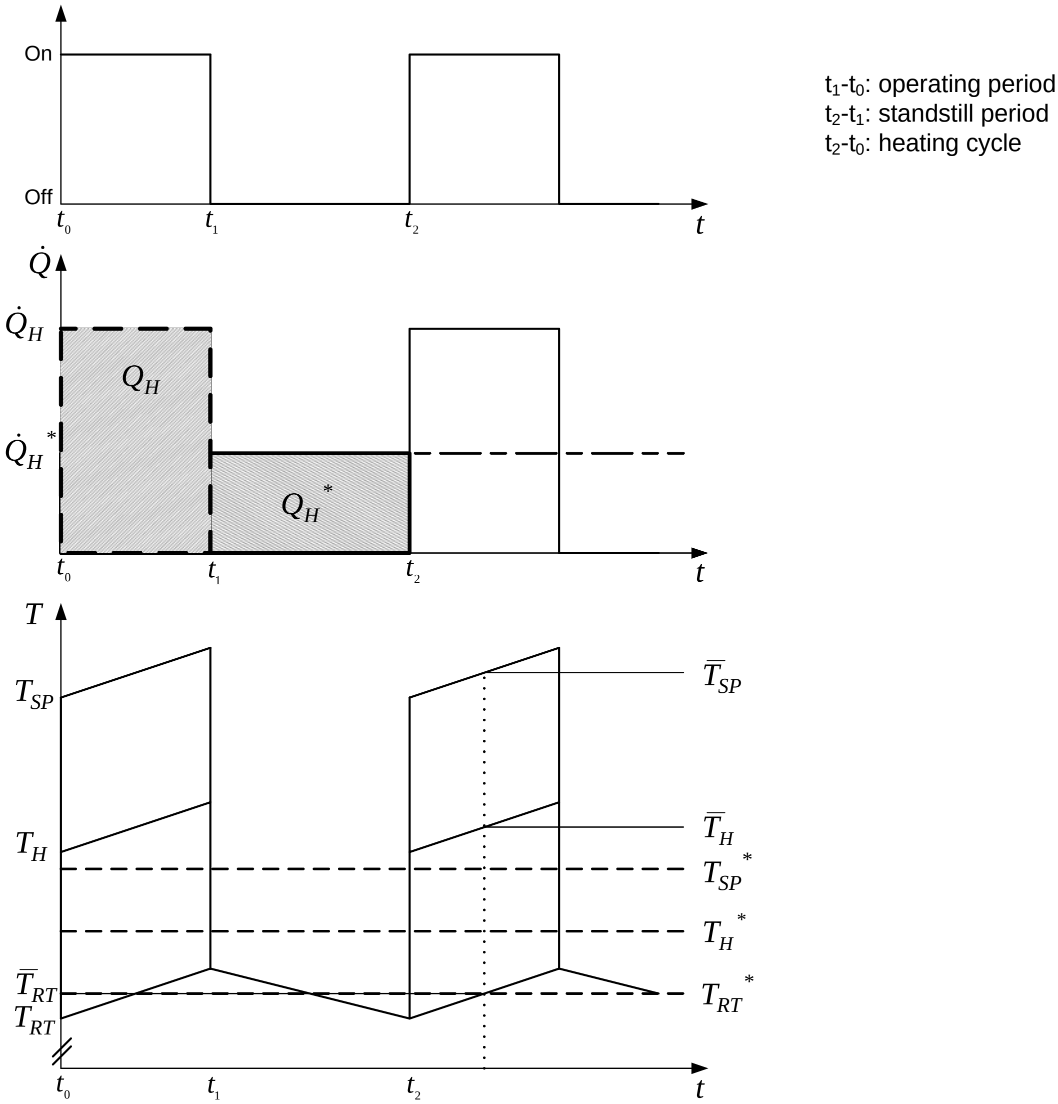

Fig. 1-9: Behaviour over time of the air/water heat pump with on/off control

1.6 General comparison between air/water and ground-source heat pumps

Air/water heat pumps require only low investments, are easy to install and are, today, reliable in their operation. They are *not* subject to official approval and in the future will run with less noise as a result of improved air-flow guidance and better fans. They exhibit the following disadvantages when compared to heat pumps with geothermal heat tubes otherwise known as ground source heat pumps:

- Heat extraction from air is more complex than from water (or brine): Its specific heat capacity ($c_{pAir} \approx 1/4 \cdot c_{pW}$), its density ($\rho_{Air} \approx 1/1000 \cdot \rho_W$) and its thermal conductivity ($\lambda_{Air} \approx 1/25 \cdot \lambda_W$) are unfavourable. With air as a heat source, the evaporators have to be manufactured as voluminous fin tube heat exchangers with a fan. When water is the source on the other hand, plate heat exchangers can be used.
- While cooling the outside air to below 4°C, and sometimes already by 7°C, ice and/or frost forms on the evaporator/lamella air heat-exchanger. This reduces the flow of air, the generated heat-flow, the coefficient of performance and the exergetic efficiency during the heating process. Periodic defrosting procedures are necessary. For this purpose, intricate technical equipment is necessary, and a certain part of the heat generated is needed for use as defrosting energy.
- At low outside temperatures, air/water heat pumps have to provide a far greater temperature lift compared to heat pumps with geothermal heat tubes. The heat pump must be designed for certain *minimal temperature* conditions $\vartheta_{A\,min}$ i.e. the *required* heating capacity must be maximal for this state: $\dot{Q}_{max}{}^{*}$. Although this operating state occurs only rarely, this has further consequences for conventional heat pumps with on/off control, as the instantaneous heating capacity *generated* under part-load conditions increases with increasing ambient temperature: The temperature gradients for heat transfer in the evaporator and condenser increase, therefore reducing the exergetic efficiency of the air/water heat pump in part-load operation. At the same time, ice and frost formation also increases in the fin tube heat-exchanger. The consequence of this: the *annual average exergetic efficiency* and the *seasonal performance factor* of air/water heat pumps are less than those of ground-source heat pumps, since the source temperature of a geothermal heat probe heat pump is more or less constant over the yearly heating season, and lies in the area of 7°C to 12°C.

Disadvantages also exist for ground source heat pumps: A secondary water loop is required with an additional temperature gradient for heat transfer. This means that capital expenditure is considerably higher. In autumn and spring, outdoor air is often warmer than the ground. Air/water heat pumps profit from this fact.

Which of the two heat sources for a heat pump heating system is more superior depends of course on the local yearly temperature characteristics and the local geothermal situation. It should be noted here that for both systems an important potential for further development is still available, whereby that for air/water heat pumps seems to be higher. The key to an increase in efficiency for both systems can be found in the *continuous control* of *the heating power* of the heat pump with which the *generated heating capacity* is adapted more or less continuously to the heating capacity *required* by the building. This can be achieved by continuous control of the heat pump compressor’s speed. In the case of air/water heat pumps, moreover, it is also sensible to adjust the fan’s rotational speed. By taking both these measures frost formation on the fin tube heat exchanger is reduced or even avoided under the neuralgic frost formation conditions of 4°C to 7°C [5]. Also, noise emissions are reduced by such control measures.

With a lot of experimental effort, Eggenberger has developed the "Pioneer" air/water heat pump [6] with continuous power control. This should pave the way for the introduction of this new technology.

1.7 This study's objectives and approach

Provide a basis for an increase of the efficiency of air/water heat pumps by using exergy analysis

The *2nd law of thermodynamics* determines the *quality of thermodynamic processes*. It states that all technical processes are *non-reversible* (irreversible). In thermodynamics, one must not speak of energy losses (in accordance with the 1st law) but may speak of *irreversible increases in entropy* (according to Clausius, 1822–1888). Instead of evaluating the *quality* of thermodynamic processes with abstract entropy balances, *exergy analysis is more suitable for our purposes*. Its results are easy to follow and immediately demonstrate possibilities for improvement in thermodynamic efficiency because, using *exergy analyses, exergy losses* can be determined for both complete systems and their subsystems. For heating and cooling systems, *exergy losses* always mean that additional mechanical work is necessary in comparison with ideal process in which no *exergy losses* occur.

In this study, *exergy balances* will be calculated for the whole heat pump process and all sub-processes. In order to do this, we aim to clearly show the exergy losses mathematically in relation to the relevant process variables and their effect on other sub-processes. For this purpose, suitable approximations will be made, e.g. where permissible by linearisation or by series expansions. The resulting inaccuracies will always be checked by means of thermo-physical properties from solid equations of state. For calculations on frost formation and, therefore, transient process variables, only numeric calculation methods are available. This of course also applies to the calculation of coefficients of performance and of the exergetic efficiency of the heat pump.

The main result of this study is to demonstrate the distinct increase in efficiency made possible by controlling the power of compressor and fan. Such performance control consists of two measures to be taken for the air/water heat pump. Primarily, the rotational speed of the compressor and fan should be continuously controlled so that the heating capacity *generated* is equal to that *required*. The heat pump will hardly switch on and off anymore. For certain outdoor air temperature ranges, periodic defrosting may still be necessary. During the heating cycle between the periodical defrosting, the fan power should be adjusted as a second measure for maximising of the coefficient of performance and the exergetic efficiency. (These two measures have already been successfully implemented in the prototype of the “Pioneer” heat pump by Eggenberger [6].)

This study will stimulate relevant research in the fields of heat and mass transfer, frost formation, fan and compressor engineering and the development of control systems. We hope that heat pump manufacturers will actively co-operate in using these new possibilities and so make a contribution to the development of thermally efficient and economically optimised air/water heat pump heating systems. This Study will also serve as a means to provide many heating engineers with an understanding on the exergy-evaluation of heating systems.

2 Thermodynamic basics

Thermodynamics is often regarded as being abstract theory. Its two principal laws are formulated using accurately defined terms. In this study, the energy forms *work*, *heat* and *energy of substances* and *power*, *heat-flow* and *enthalpy of substance flow* are employed in our *energy balances*. The *2nd law* is needed to correctly judge the efficiency of thermal processes. Here, these will not be performed as *entropy analyses* (as in physics) but as *exergy analyses. Exergy analyses* are easily understandable for technical processes and the results are interpretable; in particular, the *benefits of the possibilities for improvement* can be grasped directly and their economical effects can also be quantified.

2.1 Energy and exergy

Energy has two aspects: *Quantity and quality*. The *1st law* of thermodynamics states that energy is never lost in *transformations;* as far as its *quantity* is concerned. But energy can lose its *quality:* through dissipative drops of pressure in a fluid, through temperature gradients in heat transfer, through differences in the humidity of chilling air caused by the condensation or de-sublimation of water vapour (generally known as *mass transfer*).

The term *exergy* was introduced in 1952 by Rant [7] as *energy's ability to perform work* and this for every form of energy.

In accordance with this definition *mechanical* and *electrical energy* consist entirely of *exergy*. This also applies approximately to *chemical energy* such as combustibles [8]. These three are regarded as forms of energy of physically high quality: They can be converted completely into work without any loss and also be converted one hundred percent into each other (cf. Fig. 2-1).

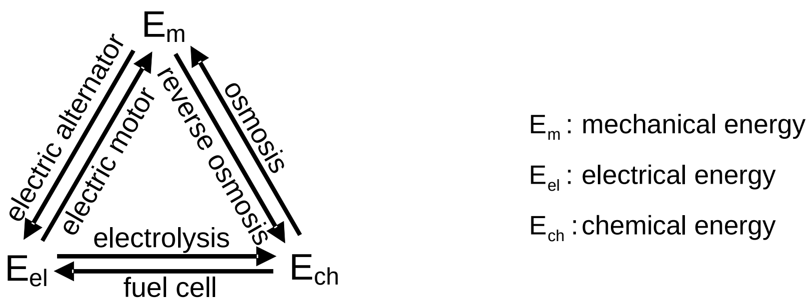

Fig. 2-1: Energy consisting of pure exergy and its reversible transformation

The situation concerning the energy *of heat* and *substances* is different: Only a part of it is *exergy,* that is its ability to perform work in relation to ambient conditions; the other part of the energy is called *anergy.* This means that heat at ambient temperature and fluids at ambient temperature and pressure have no exergy.

For mixtures of substances, exergy depends on, in addition to temperature and pressure, their composition.

We need equations for the calculation of exergy from two forms of energy: heat and substances. These will be explained in chapters 2.2 and 2.3.

The 2nd law can be formulated in a way that is easy to follow:

- For all *reversible* (and therefore loss-free) transformations of energy, *exergy* is conserved.
- In the case of all *irreversible* (real) processes, exergy is lost. This decrease in exergy is referred to as *exergy loss.*

For illustration, the energy and exergy flow diagram of an adiabatic fluid flow is shown in Fig. 2-2. Here, pressure is reduced by throttling from p_1 to p_2 (kinetic energies are considered negligibly small). The energy flow of the fluid remains unchanged in spite of the decrease in pressure $\dot{H} = \dot{H}_1 = \dot{H}_2$. On the other hand the exergy flow of the fluid is decreased from $\dot{E}_1$ to $\dot{E}_2$. This decrease in exergy flow can be easily considered as an *exergy loss flow* $\dot{E}_L$.

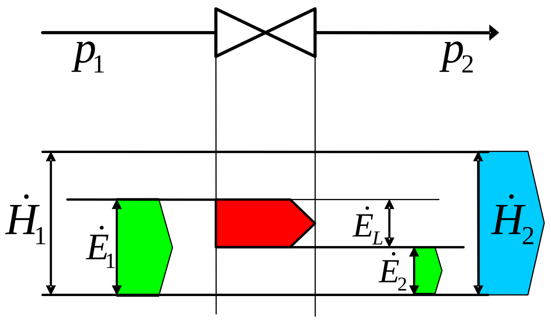

$$\dot{H}_1 = \dot{H}_2 \qquad (1^{st}\ \text{law})$$

$$\dot{E}_L = \dot{E}_1 - \dot{E}_2 \qquad (2^{nd}\ \text{law})$$

Fig. 2-2: Adiabatic throttling of a fluid flow

For steady-state flow processes, the exergy loss flow is always the difference between all input and output exergy flows for the system under consideration.

2.2 The exergy of heat

From a heat flow $\dot{Q}$ with a temperature T, the maximum power P_{rev} can be won by the use of the reversible *Carnot* heat engine. The amount is additionally dependent on the ambient temperature T_A. The energy difference must be rejected to the environment as heat flow $\dot{Q}_A$. Fig. 2-3 shows the appropriate energy and exergy flows.

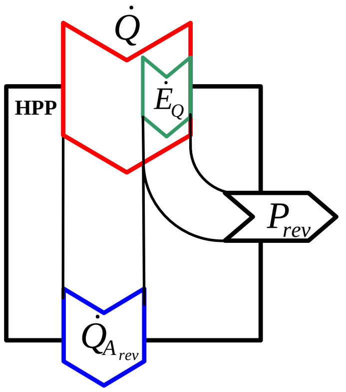

The following apply:

$$P_{rev} = \dot{Q} - \dot{Q}_{A_{rev}} \qquad (1^{st}\ \text{law})$$

$$\frac{\dot{Q}}{T} = \frac{\dot{Q}_{A_{rev}}}{T_A} \qquad (2^{nd}\ \text{law})$$

Fig. 2-3: Energy and exergy flow diagram for a reversible heat and power plant (clockwise Carnot process)

By eliminating $\dot{Q}_{A_{rev}}$ it follows that:

$$P_{rev} = \dot{Q} \cdot \left(1 - \frac{T_A}{T}\right) = \dot{Q} \cdot \eta_C \qquad (18)$$

$$\eta_C \equiv \frac{P_{rev}}{\dot{Q}} = 1 - \frac{T_A}{T} = \frac{T - T_A}{T} \qquad \text{(Carnot factor)} \qquad (19)$$

In this way, we obtain the exergy flow $\dot{E}_Q$, that is the ability of the heat flow $\dot{Q}$ to perform work. $\dot{E}_Q$ *is identical with* P_{rev} *:*

$$\dot{E}_Q \equiv P_{rev} = \dot{Q} \cdot \left(1 - \frac{T_A}{T}\right) = \dot{Q} \cdot \frac{T - T_A}{T} \qquad (20)$$

$\dot{E}_Q$ is therefore proportional to $\dot{Q}$ and dependent on the temperature T of the heat flow $\dot{Q}$ and also dependent on the ambient temperature T_A. (Tab. 1-1 on page 11 gives numeric examples of this)

2.2.1 Exergy loss when transfering heat

For the transfer of a (fixed) heat flow $\dot{Q}$ through a wall with a surface area A, a *temperature gradient* of ΔT *is* required: According to the law of heat transition (from a fluid 1 through a wall to a fluid 2), the following relation is valid:

$$\dot{Q} = k \cdot A \cdot \Delta T \qquad (21)$$

As a result, an *exergy loss flow* $\dot{E}_L$ occurs. This is dependent on the user temperature T, the temperature gradient ΔT and the ambient temperature T_A. From Eq. (20) and Fig. 2-4 the following is valid for the case $T > T_A$:

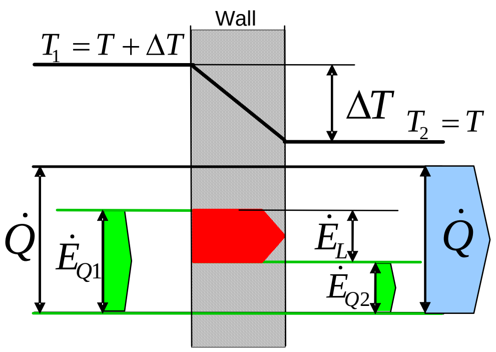

$$\dot{E}_L = \dot{E}_{Q_1} - \dot{E}_{Q_2} = \dot{Q} \cdot T_A \cdot \frac{\Delta T}{T \cdot (T + \Delta T)} \qquad (22)$$

$$\dot{E}_L \approx \dot{Q} \cdot T_A \cdot \frac{\Delta T}{T^2} \qquad (23)$$

Fig. 2-4: Energy and exergy flow diagram for heat transmission through a flat wall

Equation (23) yields the important result that the *exergy loss flow* for the heat transmission is proportional to the temperature gradient ΔT and is approximately inversely proportional to the square of the user temperature T (if ΔT is small compared with T). It is quite evident that the exergy loss flow $\dot{E}_L$ is directly proportional to the heat flow $\dot{Q}$.

In air/water heat pumps without continuous control of the generated heating capacity, ΔT and $\dot{Q}$ in the condenser and evaporator adjust themselves according to the compressor characteristic and depending on the ambient temperature. Taking this aspect into account, it follows from Eq. (21) and (23) that the exergy loss flow in a heat exchanger with a surface area A and an overall heat transfer coefficient k is dependent on the square of the temperature gradient ΔT:

$$\dot{E}_L = k \cdot A \cdot T_A \cdot \frac{\Delta T^2}{T^2} \qquad (24)$$

In Eq. (23) and (24) different positions are taken when making calculations or interpretations. Equation (23) is suitable for design considerations and Eq. (24) for interpretation in the case of part-load.

For the electrical power of an ohmic resistor R the following is valid:

$$P = U \cdot I = I^2 \cdot R = \frac{U^2}{R} \qquad (25)$$

Now, which is valid? $P \sim R$ or $P \sim R^{-1}$? This depends on the point of view! If the current is fixed, the power is proportional to the resistance, if the voltage is kept constant, however, the power is inversely proportional to the resistance.

2.3 Exergy of mass flows

Mass and mass flows with a temperature T and pressure p contain exergy if work can be won from them until they reach the dead state (T_A and p_A). Consequently, it is clear that mass at ambient conditions, such as outside air with T_A and p_A, have no exergy. But energy can still be *extracted* from mass at dead state (as in the case of a heat pump from ambient air). However, they are themselves not able to cause any transformations by themselve alone.

The exergy of a mass can be calculated trough a *reversible* process bringing the mass to the (defined) dead state. If, however, work must be supplied in order to bring the mass to ambient conditions, its exergy is negative.

The *exergy flow* $\dot{E}$ of *a mass flow* is given by [8].

$$\boxed{\dot{E} = \dot{m} \cdot [h - h_A - T_A \cdot (s - s_A)]} \tag{26}$$

And for a unit mass flow the specific exergy of mass is:

$$\boxed{e = h - h_A - T_A \cdot (s - s_A)} \tag{27}$$

The specific enthalpy h and the specific entropy s of the mass are determined by T, p, h_A and s_A on the one hand, and by T_A and p_A as thermal state variables on the other. For mixtures of substances with variable composition, as in the case of partial condensation or de-sublimation, information on their composition is additionally needed. Kinetic and potential energy are also pure exergy. They are, however, negligibly small for our considerations. Chemical reactions are, naturally, also excluded here.

Equation (27) can be easily verified for *ideal gases* from the T,s-diagram (Fig. 2-5). Gas with a temperature T and a pressure p is initially used in an isentropic turbine down to T_A and produces the work $h - h_A$; it is then used isothermally from the intermediate pressure p_Z down to p_A, where the work $T_A \cdot (s_A - s)$ is won.

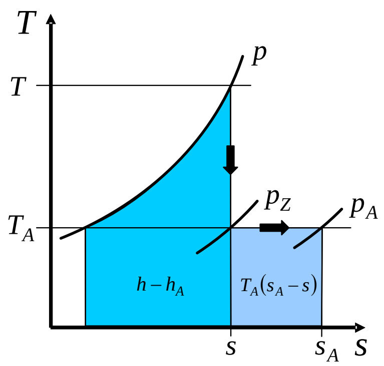

Fig. 2-5: T,s-diagram

For *perfect gases,* the specific exergy e can be directly calculated from T, T_A, p and p_A with the properties c_p and R. From Eq. (27) the following can be stated:

$$e = c_p \cdot (T - T_A) - T_A \cdot \left(c_p \cdot \ln \frac{T}{T_A} - R \cdot \ln \frac{p}{p_A} \right) \tag{28}$$

Similarly, for *incompressible liquids*

$$e = c_p \cdot \left[(T - T_A) - T_A \cdot \ln \frac{T}{T_A} \right] + v \cdot (p - p_A) \tag{29}$$

whereby in our study the term for flow work is negligible in comparison with the first expression, due to the temperature change.

The *exergy of moist air* is, finally, additionally dependent on the humidity content x and on the ambient humidity x_A.

$$e = \left[(c_{pAir} + c_{pSt} \cdot x) \cdot \left(T - T_A - T_A \cdot \ln \frac{T}{T_A} + (R_{Air} + R_{St} \cdot x) \cdot T_A \cdot \ln \frac{p \cdot (0.622 + x_A)}{p_U \cdot (0.622 + x)} + \left(R_{St} \cdot x \cdot T_A \cdot \ln \frac{x}{x_A} \right) \right) \right] \tag{30}$$

2.3.1 Exergy loss in mass flows

Exergy losses in mass flows mainly occur as a result of dissipative drops of pressure in such flows. For adiabatic throttling, the following serves as an example (cf. Fig. 2-2),

$$\boxed{\dot{E}_L = \dot{E}_1 - \dot{E}_2 = \dot{m} \cdot (e_1 - e_2) = \dot{m} \cdot T_A \cdot (s_2 - s_1) = \dot{m} \cdot T_A \cdot s_{irr12}} \tag{31}$$

respectively for unit mass flow

$$\boxed{e_L = T_A \cdot (s_2 - s_1) = T_A \cdot s_{irr12}} \tag{32}$$

as the change in enthalpy is zero. s_{irr12} is the *irreversible entropy generation*.

3 Energy and exergy balances for the heat pump process

In this chapter, basic equations suitable for the *calculation of exergy losses* are developed on the basis of the elementary energy and exergy balances discussed in chapter 2. This is done both for the heat pump as a whole as well as for its individual sub-processes. One *internal* and three *external exergetic efficiencies* are defined. In chapter 4, the equations set up here will be developed further and used to analyse the relevant factors of heat pump operation.

3.1 Evaluations made on the heat pump process

In order to clearly evaluate the effects of exergy losses, various exergetic efficiencies will be defined. An evaluation is made on the relationship between *usable* exergy and the exergy *actually used* independent of heating capacity; this is less than one for typical heat pumps and exactly one in the borderline case where no exergy losses occur. The four exergetic efficiencies defined in the following sections refer to the corresponding temperatures of the heat used for heating purposes.

Fig. 3-1 shows the heat pump cycle with the four elementary sub-processes (evaporation, compression, condensation, expansion) - but without the heat delivery system for rooms. Fig. 3-2 provides a survey of the relevant and representative temperatures.

Three *energy flows* can be found at the external interfaces of the air/water heat pump: At the evaporator it is the *heat flow* $\dot{Q}_A$ from the environment, the *internal power* P_i is passed on to the working fluid by the compressor and, in the condenser, the working fluid passes on the *heating capacity* $\dot{Q}_H = \dot{Q}_A + P_i$ to heating circuit's water.

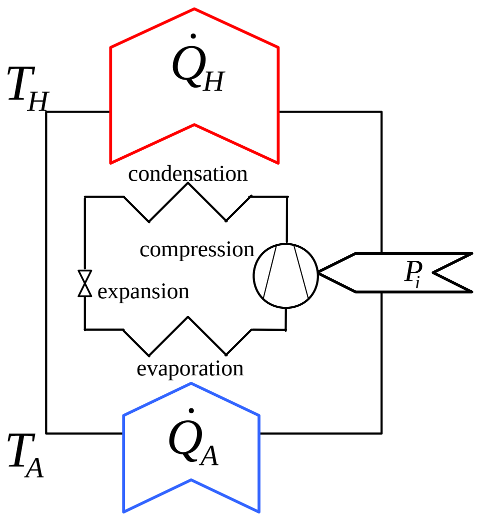

Fig. 3-1: Heat pump circuit with energy flows

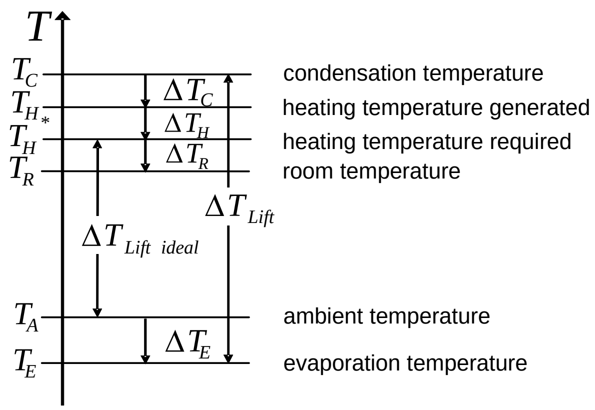

Fig. 3-2: Temperatures in the heat pump process

The associated energy and exergy flow *diagram* is shown in Fig. 3-3. The heat flow $\dot{Q}_A = \dot{Q}_E$ in the evaporator is transmitted from ambient air with the temperature T_A over an average temperature gradient ΔT_E to the working fluid with the temperature T_E. In a similar way, the condenser transfers the *generated* heat flow $\dot{Q}_H$ from the working fluid with a temperature of T_C via an average temperature gradient ΔT_C to the heating water with the average *generated* temperature T_H.

The temperature gradients in the evaporator and condenser ΔT_E and ΔT_C cause the *exergy losses* $\dot{E}_{LE}$ and $\dot{E}_{LC}$. In addition to the exergy losses during heat transfer, further exergy loss occurs *in the working fluid,* mainly in the compressor, $\dot{E}_{LCp}$, and in the expansion valve, $\dot{E}_{LEx}$. The latter two together are designated as the *internal exergy loss* $\dot{E}_{Li}$ of the heat pump:

$$\dot{E}_{Li} = \dot{E}_{LCp} + \dot{E}_{LEx} \tag{33}$$

For the clear illustration of the exergy loss flows in the heat pump process, the driving power P_i is not represented to scale in Fig. 3-3.

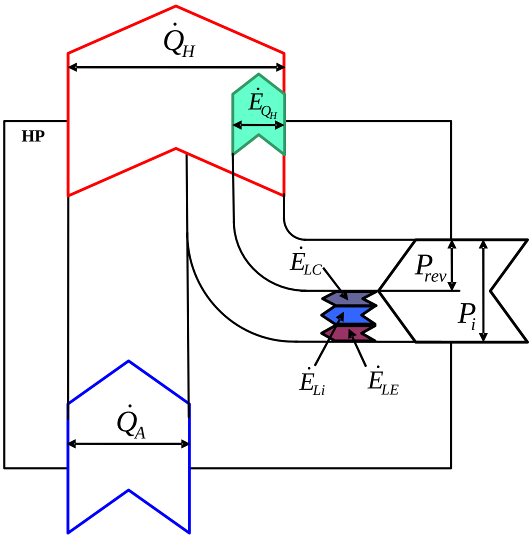

Fig. 3-3: Energy and exergy flow diagram of a real-world heat pump

As far as energy is concerned, heat pumps are characterised by their (instantaneous) *coefficient of performance* COP and their *seasonal performance factor* SPF .

$$COP = \frac{\dot{Q}_H}{P_{el}} \qquad SPF = \frac{\int_0^{365d} \dot{Q}_H \cdot dt}{\int_0^{365d} P_{el} \cdot dt} \tag{34}$$

Fig. 3-4 shows the coefficients of performance of a particular air/water heat pump determined by experiments [4]. They increase with higher ambient temperatures. They can vary considerably between the products of different manufacturers.

The *best possible coefficient of performance* COP_{rev} of a *reversible* heat pump is the reciprocal of its *Carnot factor*, because the ideal heat pump is the reverse process of the ideal heat engine (cf. chapter 2.2).

The *reversible internal coefficient of performance of a heat pump working ideally* is determined by the (self-adjusting) evaporation and condensation temperatures (T_E and T_C):

$$COP_{rev\,i} = \frac{T_C}{T_C - T_E} = \frac{1}{\eta_{Ci}} \tag{35}$$

The best possible *external coefficient of performance of a reversible air/water heat pump with reference to the generated heating temperature* T_H at an ambient temperature of T_A is determined by:

$$COP_{rev\,e} = \frac{T_H}{T_H - T_A} = \frac{1}{\eta_{Ce}} \tag{36}$$

As far as the *required* heating temperature T_H^* is concerned, the following is valid:

$$COP_{rev\,e}{}^{*} = \frac{T_H{}^{*}}{T_H{}^{*} - T_A} = \frac{1}{\eta_{Ce}{}^{*}} \tag{37}$$

If the entire heating system could be operated without exergy losses, one could calculate the maximum reversible coefficient of performance with T_A and the room temperature T_R from:

$$COP_{rev\,HS} = \frac{T_R}{T_R - T_A} = \frac{1}{\eta_{CHS}} \tag{38}$$

In order to thermodynamically evaluate the quality of a (irreversible) air/water heat pump correctly, the *exergetic efficiency* η_{ex} is introduced: the exergy flow $\dot{E}_{Q_H}$ of the heat for heating purposes is referred to the mechanical and/or electrical power P absorbed.

$$\eta_{ex} = \frac{\dot{E}_{Q_H}}{P} \tag{39}$$

For loss-free (reversible) heat pumps

$$P = P_{rev} = \dot{E}_{Q_H} \tag{40}$$

and therefore

$$\eta_{ex\,rev} = 1$$

The *internal exergetic efficiency of the heat pump* provides judgement on the closed-loop process gone through by the heat pump's working fluid in the evaporator and condenser with fluid temperatures T_E and T_C:

$$\eta_{ex\,i} = \frac{\dot{Q}_H \dfrac{T_C - T_E}{T_C}}{P} = COP \cdot \eta_{Ci} \tag{41}$$

For the *external exergetic efficiency of the generated heating temperature* T_H, the exergy of the *generated* heating capacity $\dot{Q}_H$ is referred to the *generated* heating temperature T_H in the condenser:

$$\eta_{ex\,e} = \frac{\dot{Q}_H \dfrac{T_H - T_A}{T_H}}{P} = COP \cdot \eta_{Ce} \tag{42}$$

As already shown in section 1.5 for on/off controlled heat pumps, the intermittent *generated* heating capacity $\dot{Q}_H$ is higher than the continuously *required* heating capacity $\dot{Q}_H{}^{*}$ by the factor υ. Consequently, the *generated* heating temperature T_H is also higher than that *required,* which means that an additional loss of exergy results. This non-steady state loss of exergy can be computed from the exergy balance over a heating cycle $(t_2 - t_0)$. The continuously *required* amount of exergy for a building at $T_H{}^{*}$ is:

$$E_{Q_H}{}^{*} = Q_H{}^{*} \cdot \frac{T_H{}^{*} - T_A}{T_H{}^{*}} = \dot{Q}_H{}^{*} \cdot (t_2 - t_0) \cdot \frac{T_H{}^{*} - T_A}{T_H{}^{*}} = \dot{Q}_H \cdot \frac{t_2 - t_0}{\upsilon} \cdot \frac{T_H{}^{*} - T_A}{T_H{}^{*}} \tag{43}$$

and the amount of work in the compressor is:

$$W = P \cdot (t_1 - t_0) = P \cdot \frac{t_2 - t_0}{\upsilon} \tag{44}$$

In this way we can calculate, as a third evaluation method, the *external exergetic efficiency of the required heating temperature* for an on/off controlled air/water heat pump as a mean value over the heating period ($t_2 - t_0$):

$$\eta_{exe}{}^{*} = \frac{E_{Q_H}{}^{*}}{W} = \frac{\dot{Q}_H \frac{T_H{}^{*} - T_A}{T_H{}^{*}}}{P} = COP \cdot \eta_{Ce}{}^{*} \tag{45}$$

For T_H the arithmetic mean value of the supply and return temperatures of the heating water is used (the deviation from the thermodynamic average temperature is minimal).

As in Eq. (45), a fourth evaluation of the *external exergetic efficiency of a heating system with an air/water heat pump* (exergetic efficiency of the heated building) is referred to the ambient temperature T_A along with the room temperature T_R required:

$$\eta_{exHS} = \frac{\dot{Q}_H \frac{T_R - T_A}{T_R}}{P} = COP \cdot \eta_{CHS} \tag{46}$$

The *external exergetic efficiency of the required heating temperature* also takes the exergy losses occurring in the heat delivery system (e.g. floor heating) into consideration. These are not to be attributed to the heat pump.

With the Eq. (41), (42), (45) and (46) the exergetic efficiency can, in practice, be easily determined from the product of the coefficient of performance and the *Carnot factor.* For it, the relevant coefficient of performance is determined experimentally in each case. A rough but thermodynamically sound assessment of heat pump performance is thus made possible in a simple way.

The *coefficient of performance* determined from experiments [4] made on an air/water heat pump of 7 kW nominal heating capacity and the *external exergetic efficiency of the generated heating temperature* are represented in Fig. 3-4 against ambient temperature, always immediately after defrosting, i.e. before frost formed in the fin tube evaporator.

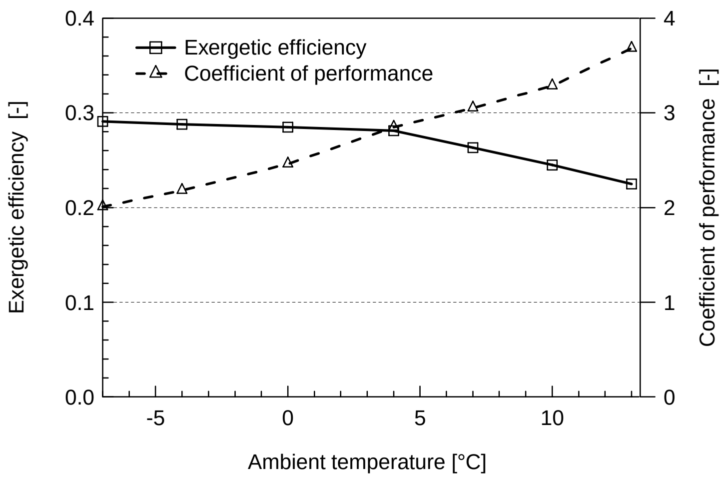

Fig. 3-4: Coefficient of performance and exergetic efficiency of a real-life air/water heat pump on the basis of measurements ($\dot{Q}_{H\,nom} = 7\,kW$)

From this it follows that:

- The exergetic efficiency of the air/water heat pump with nearly 30% is only moderately good.
- In the case of "part-load", i.e. with higher ambient temperature than the minimum ambient temperature, the exergetic efficiency gets worse. The opposite should be possible for such operating states as the heat exchangers need lower temperature gradients and therefore permit smaller temperature lifts!

3.2 Balances of the sub-processes of the heat pump working fluid

The power requirements P_i *(internal compressor power*) of the heat pump are higher than the *reversible drive power* P_{rev} by the *sum of all exergy loss flows* occurring $\dot{E}_{Ltot}$:

$$P_i = P_{rev} + \dot{E}_{Ltot} = P_{rev} + \dot{E}_{LCp} + \dot{E}_{LC} + \dot{E}_{LEx} + \dot{E}_{LE} \qquad (47)$$

The main exergy losses in a simple compression heat pump are: $\dot{E}_{LCp}$ in the compressor, $\dot{E}_{LC}$ in the condenser, $\dot{E}_{LEx}$ in the expansion valve and $\dot{E}_{LE}$ in the evaporator. These are separately derived here from elementary exergy balances. In chapter 4, they are then computed dependent on the relevant influencing factors in order to be able to quantify the possibilities for the exergetic improvement of the heat pump in detail. Further sources of loss such as those found in mechanical and electrical drives as well as fan power (in the case of air/water heat pumps with forced convection), needs not to be considered at this point.

The influence of *exergetic efficiency* can now clearly be seen from the total exergy loss. In general, this will be referred to in the following as the *internal compressor power* P_i.

$$\eta_{ex} = \frac{\dot{E}_{Q_H}}{P_i} = \frac{\dot{E}_{Q_H}}{P_{rev} + \dot{E}_{Ltot}} \qquad (48)$$

As $\dot{E}_{Q_H} = P_{rev}$, it follows that

$$\eta_{ex} = \frac{1}{1 + \frac{\dot{E}_{Ltot}}{\dot{E}_{Q_H}}} = 1 - \frac{\dot{E}_{Ltot}}{P_i} \qquad (49)$$

Using Eq. (41), the *internal exergetic efficiency of the heat pump* can be determined by:

$$\eta_{ex\,i} = \frac{1}{1 + \frac{\dot{E}_{LCp} + \dot{E}_{LEx}}{\dot{E}_{Q_H}}} = 1 - \frac{\dot{E}_{LCp} + \dot{E}_{LEx}}{P_i} \qquad (50)$$

According to Eq. (42), the *external exergetic efficiency of the generated heating temperature* can be evaluated with:

$$\eta_{ex\,e} = \frac{1}{1 + \frac{\dot{E}_{LCp} + \dot{E}_{LEx} + \dot{E}_{LE} + \dot{E}_{LC}}{\dot{E}_{Q_H}}} = 1 - \frac{\dot{E}_{LCp} + \dot{E}_{LEx} + \dot{E}_{LE} + \dot{E}_{LC}}{P_i} \qquad (51)$$

In Fig. 3-5 the heat pump process is represented by a detailed representation of the individual state points of the heat pump working fluid in the T,s-diagram. Evaporation and condensation are taken as being isobar-isotherm. In the evaporator, *vapour superheating* ΔT_{cGsh} occurs. In the compressor, *vapour superheating* ΔT_{hGsh} with reference to T_C occurs along with *condensate subcooling* ΔT_{Csc} .

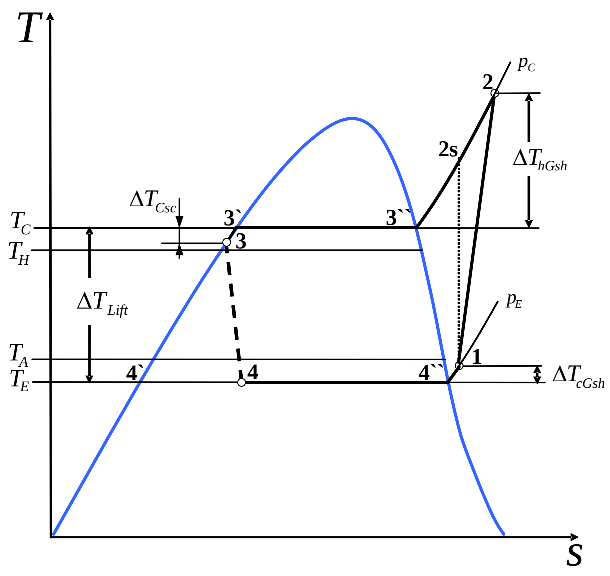

Fig. 3-5: T,s-diagram with state points noted

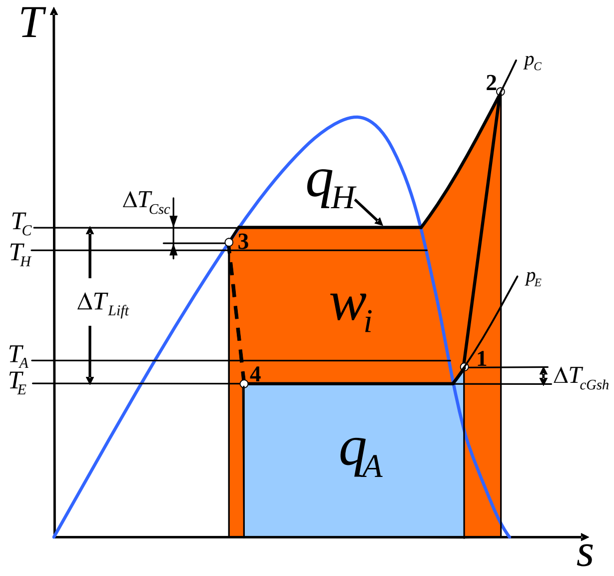

Fig. 3-6: T,s-diagram with specific heats and drive work

From point 1 to point 2, the *gaseous working fluid* is compressed from the evaporation pressure p_E to the higher condensation pressure p_C, so that it can be condensed at a temperature level of T_C.

In the condenser (point 2 to point 3), the superheated vapour is saturated, condensed and somewhat subcooled. At the same time the heating water is heated from the return temperature to the supply temperature and, thus, the heating capacity is transferred to the heating water circuit.

Subsequently, the pressure of the liquid, slightly subcooled working fluid is relieved in the expansion valve from condensation pressure p_C to the lower evaporation pressure p_E, whereby wet steam (point 4) results.

In the (fin tube) evaporator, the working fluid is evaporated and slightly superheated by taking up heat from the environment. Water vapour in the ambient air passing through air/water heat pump's fin tube evaporator condenses as the air stream is cooled to below its saturation temperature (dew point) so that condensate and/or frost forms on the fins of the evaporator. The transmitted heat flow $\dot{Q}_A = \dot{Q}_E$ therefore consists of two components, i.e. the sensible heat flow $\dot{Q}_{Es} = \dot{Q}_{As}$ and the latent heat flow $\dot{Q}_{El} = \dot{Q}_{Al}$.

Fig. 3-6 shows the specific heats $q_A = q_E$ and $q_H = q_A + w_i$ and the specific internal drive work w_i, represented areas in the T,s-diagram.

3.2.1 Balances for the compressor

For the *adiabatic compression* from $p_1 = p_E$ to $p_2 = p_C$ the enthalpy flow of the working fluid is raised by the *internal compressor power* P_i (passed on to the fluid). The exit enthalpy and the exit temperature depend on the *isentropic compressor efficiency* η_s.

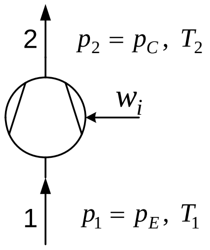

Fig. 3-7: Sketch of the compression principle

$$P_i = \dot{H}_2 - \dot{H}_1 = \dot{m}_f \cdot (h_2 - h_1) = \dot{m}_f \cdot \frac{1}{\eta_s} \cdot (h_{2s} - h_1) \quad (52)$$

and for unit mass flow of the working fluid:

$$w_i = h_2 - h_1 = \frac{1}{\eta_s}(h_{2s} - h_1) \quad (53)$$

The *exergy* in the working fluid is also raised by P_i. This rise is once more dependent on the *isentropic compression efficiency* η_s. The exergy loss flow $\dot{E}_{LCp}$ of the working fluid in the compressor is the difference between its *input* and *output exergies*:

$$\dot{E}_{LCp} = (P_i + \dot{E}_1) - \dot{E}_2 = P_i + (\dot{E}_1 - \dot{E}_2) \quad (54)$$

Using Eq. (52) and (53), it follows that:

$$\dot{E}_{LCp} = \dot{m}_f \cdot T_A \cdot (s_2 - s_1) \quad (55)$$

$$e_{LCp} = T_A \cdot (s_2 - s_1) = T_A \cdot s_{irr12} \quad (56)$$

The exergy loss is therefore determined by the ambient temperature and the *irreversible increase in entropy* $s_2 - s_1 = s_{irr12}$ in the compressor. The effect of the *isentropic compressor efficiency* η_s is implicitly contained in s_{irr12}. In Fig. 3-8, the specific exergy loss of the compression e_{LCp} according to Eq. (56), as well as the subsequent mathematically described exergy losses of the other sub-processes, are represented as areas in the T,s-diagram.

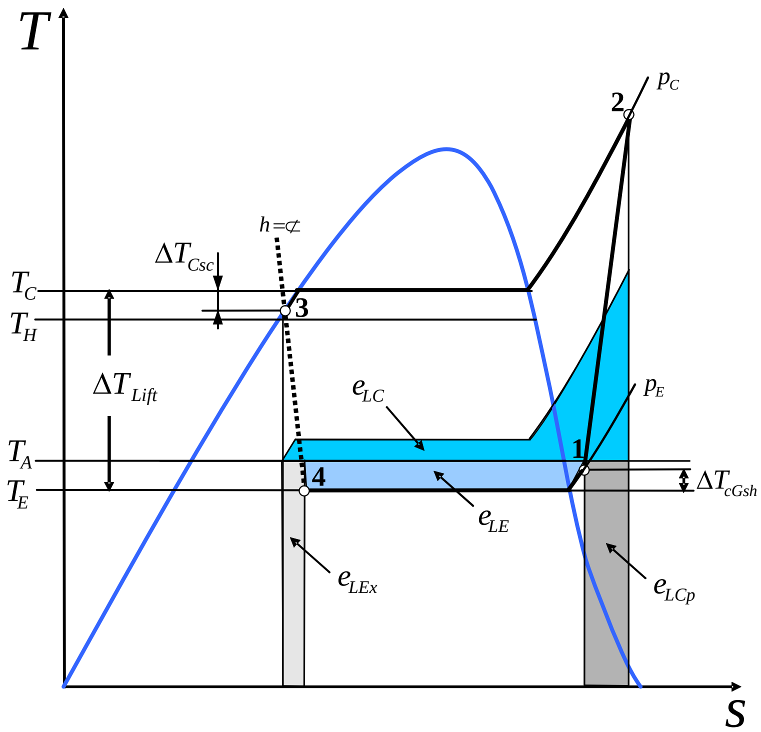

Fig. 3-8: T,s-diagram of the heat pump process with specific exergy losses (not to scale)

3.2.2 Balances for the condenser

In the condenser, the superheated vapour is saturated, condensed and, possibly, slightly subcooled and, thus, the heating-circuit water is heated up from the return temperature T_{RT} to the *generated* supply temperature T_{SP}. Assuming negligibly low heat losses, the following applies for the condenser:

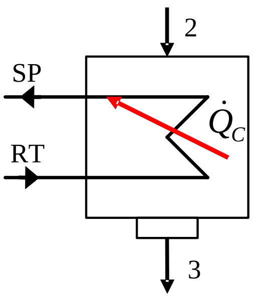

Fig. 3-9: Sketch of the condenser principle

$$\dot{Q}_C = \dot{m}_f \cdot (h_2 - h_3) = \dot{Q}_H = \dot{m}_{HW} \cdot c_{pHW} \cdot (T_{SP} - T_{RT}) \quad (57)$$

and, for the entire heat pump

$$\dot{Q}_H = \dot{Q}_E + P_i \quad (58)$$

The *exergy loss in the condenser* is determined from three different control volumes: the first control volume is suitable for numeric analyses, the other two are used for analytical illustration and for interpretation.

Adiabatic control volume

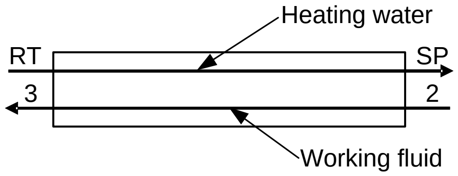

Fig. 3-10: Adiabatic control volume for the condenser

The exergy of the working fluid decreases from $\dot{E}_2$ to $\dot{E}_3$ and the exergy in the heating water increases from $\dot{E}_{RT}$ (return) to $\dot{E}_{SP}$ (supply). The *exergy loss flow in the condenser* is given by the exergy balance:

$$\dot{E}_{LC} = \left(\dot{E}_2 + \dot{E}_{RT}\right) - \left(\dot{E}_3 + \dot{E}_{SP}\right) = \left(\dot{E}_2 - \dot{E}_3\right) + \left(\dot{E}_{RT} - \dot{E}_{SP}\right) \quad (59)$$

If the pressure losses in the two fluids are disregarded, the exergy loss only results from the temperature gradients for heat transfer (that is for vapour saturation, condensation and condensate subcooling). Consequently, the following is valid for the decrease of exergy flow in the working fluid according to (26):

$$\dot{E}_2 - \dot{E}_3 = \dot{m}_f \cdot \left[h_2 - h_3 - T_A \cdot \left(s_2 - s_3\right)\right] \quad (60)$$

In each case, both the specific enthalpies (h_2 and h_3) and the specific entropies (s_2 and s_3) of the working fluid are defined as state variables by T and p. The increase in exergy in the heating water (whilst disregarding of the pressure loss) can be computed directly from the return temperature and the *generated* supply temperature using Eq. (28).

$$\dot{E}_{SP} - \dot{E}_{RT} = \dot{m}_{HW} \cdot c_{pHW} \left[T_{SP} - T_{RT} - T_A \cdot \ln\frac{T_{SP}}{T_{RT}}\right] \quad (61)$$

These two last Eq. (61) and (60) will be used for numerical calculations (evaluation of measured values).

Diabatic control volume for the working fluid

In the condenser, the *exergy flow of the generated heating capacity* $\dot{E}_{Q_H}$ is transferred at the *generated* heating temperature T_H:

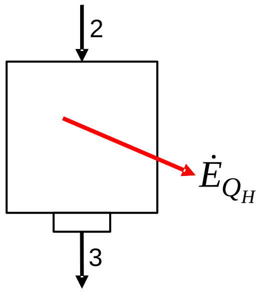

$$\dot{E}_{Q_H} = \dot{Q}_H \cdot \frac{T_H - T_A}{T_H} \quad (62)$$

Fig. 3-11: Diabatic control volume for the condenser

For the calculation of the *generated* heating temperature T_H, it is sufficient to use the arithmetic mean value of the *generated* supply and return temperature of the heating water circuit:

$$T_H = \frac{1}{2} \cdot (T_{SP} + T_{RT}) \tag{63}$$

From the exergy balance of this control volume, the *exergy loss flow in the condenser* can now also be calculated from:

$$\dot{E}_{LC} = \dot{E}_2 - \dot{E}_3 - \dot{E}_{Q_H} \tag{64}$$

And for unit mass flow of the working fluid of the heat pump:

$$e_{LC} = e_2 - e_3 - e_{Q_H} = h_2 - h_3 - T_A \cdot (s_2 - s_3) - q_H \cdot \left(1 + \frac{T_A}{T_H}\right) \tag{65}$$

Since $h_2 - h_3 = q_H$ (cf. Fig. 3-6), it follows that:

$$e_{LC} = q_H \cdot \frac{T_A}{T_H} - T_A \cdot (s_2 - s_3) \tag{66}$$

The *specific exergy loss in the condenser* e_{LC} is represented in Fig. 3-8 in the T,s-diagram (according to Eq. (66)) as an area. The specific heat for heating purposes q_H in the T,s-diagram (cf. Fig. 3-6) is, in this case, corrected by a factor T_A / T_H and has $T_A(s_2 - s_3)$ subtracted from it.

Condenser surface as a control volume

A simple analytical interpretation of the exergy loss in the condenser is possible without including vapour superheating and condensate subcooling (The error is of no great importance here and is corrected later). The working fluid would condense at the temperature T_C for pure fluids or it suffers a temperature drop of around ΔT_{GC} (Temperature glide in the condenser) for mixtures such as R407C.

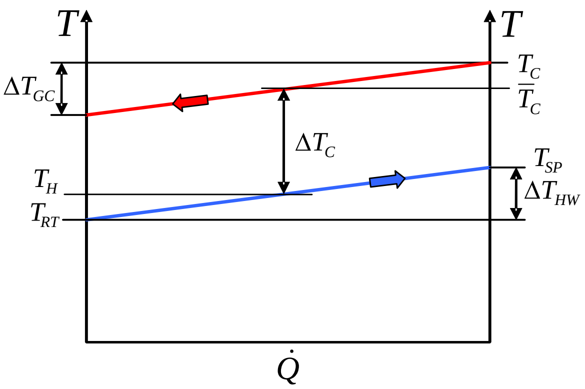

Fig. 3-12: $T,\dot{Q}$ -diagram for the condenser

In counter-flow (or cross-counter-flow), the heating water is heated up from the return temperature T_{RT} to the *generated* supply temperature T_{SP}. An average condensation temperature $\overline{T}_C$, a *generated* heating temperature T_H and, therefore, an *average temperature gradient* $\Delta T_C = \overline{T}_C - T_H$ are represented in Fig. 3-12. Consequently, the *exergy loss flow in the condenser* is quantified according to Eq. (22):

$$\dot{E}_{LC} = \dot{Q}_H \cdot T_A \cdot \frac{\Delta T_C}{T_H \cdot \overline{T}_C} = \dot{Q}_H \cdot T_A \cdot \frac{\Delta T_C}{T_H \cdot (T_H + \Delta T_C)} \approx \dot{Q}_H \cdot T_A \cdot \frac{\Delta T_C}{{T_H}^2} \tag{67}$$

The exergy loss flow in the condenser for a *generated* heating capacity $\dot{Q}_H$ is therefore approximately proportional to the temperature gradient ΔT_C. If, however, for typical on/off heat pumps in part-load operation, the temperature gradient ΔT_C and the *generated* heating capacity $\dot{Q}_H$ regulate themselves in accordance with the heat pump's characteristic, one obtains by using Eq. (23) for a condenser with a surface A_C and an overall heat transfer coefficient k_C :

$$\dot{E}_{LC} \approx T_A \cdot k_C \cdot A_C \cdot \frac{\Delta T_C{}^2}{T_H{}^2} \tag{68}$$

From this point of view, the *exergy loss flow in the condenser is proportional* to the square of the temperature gradient ΔT_C. In chapter 5 it will be shown that for typical on/off-heat pumps ΔT_C increases with increasing ambient temperatures. (A_C remains, of course, constant and k_C varies only by a comparatively small degree - cf. section 5.1).

3.2.3 Balances for the expansion valve

Throttling from $p_3 = p_C$ to $p_4 = p_E$ occurs quasi-adiabatically and therefore isenthalpically.

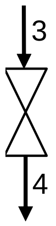

$$\dot{H}_4 = \dot{H}_3 \tag{69}$$

and

$$h_4 = h_3 \tag{70}$$

Fig. 3-13: Sketch of the expansion valve

The exergy loss flow in the expansion valve is computed using (31):

$$\dot{E}_{LEx} = \dot{E}_3 - \dot{E}_4 = \dot{m}_f \cdot T_A \cdot (s_4 - s_3) \tag{71}$$

$$e_{LEx} = T_A \cdot (s_4 - s_3) \tag{72}$$

In the T,s-diagram Fig. 3-8 the *specific exergy loss* in the expansion valve e_{LEx} is interpreted as an area; it shows that the exergy loss over the expansion valve can be reduced by subcooling the condensate a little. The quantitative effect of this is examined in section 4.2.

3.2.4 Balances for the evaporator

a) In the case of the sole transfer of heat from the heat-source side

The following considerations apply to heat pumps which take up their *source heat* at ambient temperature T_A. This applies for air/water heat pumps without air pre-heating. In the fin tube evaporator the ambient air is cooled from $T_A = T_{Air\,I}$ to $T_{Air\,O}$. Here, it is also assumed that the humidity of the air does not change, i.e. no partial condensation or de-sublimation occurs and that only pure heat transfer occurs (e.g. when operating with dry air). Consequently, the following is valid for the heat flow transmitted from ambient air to the working fluid:

$$\dot{Q}_A = \dot{Q}_E = \dot{m}_{Air} \cdot c_{pAir} \cdot (T_{Air\,I} - T_{Air\,O}) = \dot{m}_f \cdot (h_1 - h_4) \tag{73}$$

The exergy losses occurring in the evaporator are derived from various control volumes, as in the case of the condenser.

Adiabatic control volume

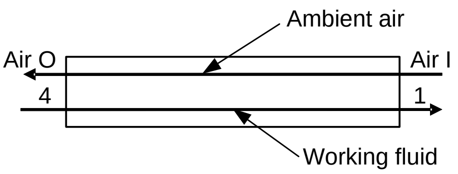

Fig. 3-14: Evaporator adiabatic control volume

In the evaporator, exergy losses occur because of the temperature gradient necessary for heat transfer. The air cooled down to below ambient temperature contains *exergy of cold* $\dot{E}_{Air\,O}$ (with positive sign) and is transferred unused to the environment. The exergy of the input stream of air $\dot{E}_{Air\,I}$ is by definition zero. Consequently, the *exergy loss flow in the evaporator* is given by:

$$\dot{E}_{LE} = \left(\dot{E}_4 + \dot{E}_{Air\,I}\right) - \left(\dot{E}_1 + \dot{E}_{Air\,O}\right) = \dot{E}_4 - \dot{E}_1 - \dot{E}_{Air\,O} \tag{74}$$

The exergy flow in the air exhausted is calculated according to (28):

$$\dot{E} = \dot{m}_{Air} \cdot \left(c_{pAir} \cdot (T - T_A) - T_A \cdot \left(c_{pAir} \cdot \ln\frac{T}{T_A} - R_{Air} \cdot \ln\frac{p}{p_A} \right) \right) \tag{75}$$

For a simple interpretation of the exergy loss in the evaporator, the exergy of the outputted, chilled air is neglected. The specific exergy loss in the evaporator is therefore:

$$e_{LE} = e_1 - e_4 = h_1 - h_4 - T_A \cdot (s_1 - s_4) \tag{76}$$

The above equation e_{LE} is shown once more in the T,s-diagram in Fig. 3-8 as an area.

Evaporator surface as a control volume

As in the case of the condenser, a simple analytical interpretation of the exergy losses without vapour superheating is made for the evaporator. The working fluid could be a pure substance that evaporates at a temperature of T_E or a mixture that therefore experiences an increase in the evaporation temperature by the so-called temperature glide ΔT_{GE}.

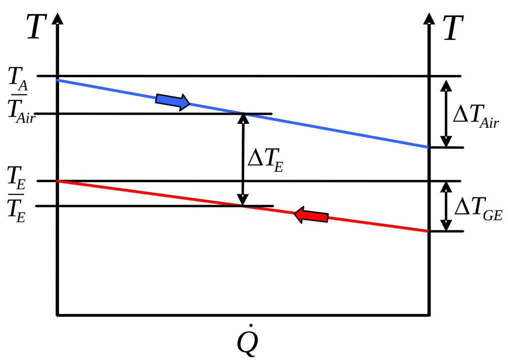

Fig. 3-15: $T,\dot{Q}$-diagram for the evaporator

In Fig. 3-15, it is assumed that the working fluid evaporates in the cross counter-flow and the ambient air cools down from T_A by ΔT_{Air}. $\overline{T}_E$ is the average evaporation temperature, $\overline{T}_{Air}$ is the average air temperature and $\Delta T_E = \overline{T}_{Air} - \overline{T}_E$ is the *average temperature gradient* for heat transfer. The resulting exergy loss flow in the evaporator is, according to Eq. (22):

$$\dot{E}_{LE} = \dot{Q}_E \cdot T_A \cdot \frac{\Delta T_E}{\overline{T}_E \cdot \left(\overline{T}_E + \Delta T_E\right)} \approx \dot{Q}_E \cdot T_A \cdot \frac{\Delta T_E}{\overline{T}_E^{\,2}} \approx \dot{Q}_E \cdot \frac{\Delta T_E}{T_A} \tag{77}$$

And, for an interpretation in the case of part load:

$$\dot{E}_{LE} \approx k_E \cdot A_E \cdot \frac{\Delta T_E^{\,2}}{T_A} \tag{78}$$

From the point of view of Eq. (77), the exergy loss flow in the evaporator is proportional to the heat transfer temperature gradient ΔT_E for a heat flow of $\dot{Q}_E$. In accordance with Eq. (78) however, the exergy loss in the evaporator is proportional to the square of the temperature gradient ΔT_E. Further interpretations on this subject can be found in chapter 5.

In order to determine the exergy loss in the evaporator through the transfer of heat more precisely, e.g. by taking the temperature glide of the working fluid and the superheating into consideration, one must base on the differential exergy loss. Consequently, it follows that:

$$\dot{E}_{LE} = \int d\dot{E}_{LE} = T_A \cdot \int \frac{T_{Air} - T_E}{T_{Air} \cdot T_E} \cdot d\dot{Q} \approx T_A \cdot \sum_{i=1}^{n} \frac{T_{Air\,i} - T_{E\,i}}{T_{Air\,i} \cdot T_{E\,i}} \cdot \Delta\dot{Q}_i \tag{79}$$

b) During heat and mass transfer from the heat source side

With ambient air as a source of heat and, above all, if it is not preheated, the air not only transfers heat when cooling but also through partial condensation or partial desublimation when its moisture content is decreased.

If saturation is achieved while cooling the air, from this point on water vapour precipitation occurs, either as condensate or frost or ice. In passing through the fin tube evaporator the air temperature decreases from $T_A = T_{Air\,I}$ down to $T_{Air\,O}$ and its humidity decreases from $x_A = x_{Air\,I}$ to $x_{Air\,O}$ (LOREF [5]). In the case of partial condensation (i.e. during the formation of condensate), the following applies for the heat flow $\dot{Q}_A$:

$$\dot{Q}_A = \dot{Q}_E = \dot{m}_{Air} \cdot \left(c_{pAir} \cdot \left(T_{Air\,I} - T_{Air\,O}\right) + \left(x_{Air\,I} - x_{Air\,O}\right) \cdot \left[r_{E_w} + c_{pSt} \cdot \left(T_{Air\,I} - T_{Air\,O}\right) - c_{pCd}\left(T_{Cd} - 273.15\right)\right]\right) \tag{80}$$

In Eq. (80) r_{E_w} stands for the specific enthalpy of evaporation of water, c_{pAir} for the specific heat capacity of dry air, c_{pSt} for the specific heat capacity of water vapour (at air temperature), c_{pCd} for the specific heat capacity of the condensate (i.e. water) and T_{Cd} for the temperature of the condensate precipitated. The two last terms in the square brackets (Eq. (80)) are in comparison to r_{E_w} negligibly small. Consequently, the following is approximately valid in the case of partial condensation:

$$\dot{Q}_A = \dot{Q}_E = \dot{m}_{Air} \cdot \left(c_{pAir} \cdot \left(T_{Air\,I} - T_{Air\,O}\right) + r_{E_w}\left(x_{Air\,I} - x_{Air\,O}\right)\right) \tag{81}$$

Similarly, in the case of partial desublimation (i.e. during the formation of frost), the following is valid:

$$\dot{Q}_A = \dot{Q}_E = \dot{m}_{Air} \cdot \left(c_{pAir} \cdot \left(T_{Air\,I} - T_{Air\,O}\right) + r_{S_w}\left(x_{Air\,I} - x_{Air\,O}\right)\right) \tag{82}$$

In this case, r_{S_w} stands for the specific enthalpy of sublimation of water, i.e. the sum of the specific enthalpy of evaporation r_{E_w} and the specific enthalpy of solidification r_{Sd_w}. From now on, r_i will be used for r_{S_w} and r_{E_w}.

The heat flow $\dot{Q}_A$ is now divided into a sensible part and a latent part. For the sensible heat flow $\dot{Q}_{As}$ the following is valid:

$$\dot{Q}_{A\,s} = \dot{m}_{Air} \cdot c_{pAir} \cdot \left(T_{Air\,I} - T_{Air\,O}\right) \tag{83}$$

Similarly, for the latent heat flow $\dot{Q}_{Al}$:

$$\dot{Q}_{Al} = \dot{m}_{Air} \cdot r_i \cdot \left(x_{Air\,I} - x_{Air\,O}\right) \qquad (84)$$

For the total heat flow $\dot{Q}_A$, therefore, it follows that:

$$\dot{Q}_A = \dot{Q}_{As} + \dot{Q}_{Al} \qquad (85)$$

The sensible heat flow is transferred from ambient air to the air-side evaporator surface by an average temperature gradient of ΔT_E and the latent heat flow via an average moisture gradient Δx_E. It follows from the energy balance on the working fluid side that:

$$\dot{Q}_A = \dot{Q}_E = \dot{m}_f \cdot \left(h_1 - h_4\right) \qquad (86)$$

In the following, the equations concerning the adiabatic control volume necessary for the calculation of exergy losses are given for a simple evaluation of given measuring data. If partial condensation or desublimation occurs in the fin tube evaporator one must consider the exergy of moist air.

Adiabatic control volume

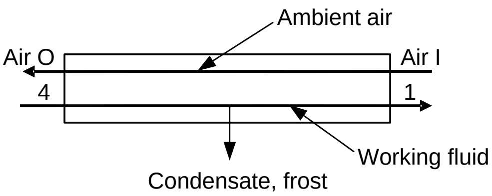

Fig. 3-16: Adiabatic control volume of the evaporator

The exergy loss flow can once more be calculated using the input and output exergy flows of the working fluid and the moist air and, therefore, the following applies:

$$\dot{E}_{LE} = \left(\dot{E}_4 + \dot{E}_{Air\,I}\right) - \left(\dot{E}_1 + \dot{E}_{Air\,O}\right) = \dot{E}_4 - \dot{E}_1 - \dot{E}_{Air\,O} \qquad (74)$$

Here, the exergy flow of the moist air is given by Eq. (30):

$$\dot{E} = \dot{m}_{Air} \cdot \left[\left(c_{pAir} + c_{pSt} \cdot x\right) \cdot \left(T - T_A - T_A \cdot \ln\frac{T}{T_A} + \left(R_{Air} + R_{St} \cdot x\right) \cdot T_A \cdot \ln\frac{p \cdot (0.622 + x_A)}{p_A \cdot (0.622 + x)} + \left(R_{St} \cdot x \cdot T_A \cdot \ln\frac{x}{x_A}\right)\right)\right] \qquad (87)$$

3.3 Balances for the heat pump including the heating water circuit

If the heating water circuit (heat delivery and distribution system) is also considered, two further exergy losses occur in addition to the exergy losses of the four elementary sub-processes of the compression heat pump. For these, $\eta_{ex\,e}^{*}$ and η_{exHS} are defined.

3.3.1 Exergy loss in the heat distribution system

The transient processes involved in the heat distribution system have already been explained in section 1.5 and conceptually defined using the *heat-flow ratio* with reference to the *required* heating capacity

$$\upsilon = \frac{\dot{Q}_H}{\dot{Q}_H^{*}} \geq 1 \qquad (88)$$

and the heat pump operating ratio:

$$f = \frac{t_1 - t_0}{t_2 - t_0} = \frac{1}{\upsilon} \le 1 \qquad (89)$$

An average exergy loss flow $\dot{E}_{LHS}$ in this heat distribution system should now be derived, namely for the intermittently *generated* heating capacity $\dot{Q}_H$. The reason for relating $\dot{E}_{LHS}$ to $\dot{Q}_H$ and not $\dot{Q}_H^*$ can be found in the fact that the exergetic efficiencies are appropriately related to the internal compressor power P_i.

For derivation purposes the balance of the *amounts* of energy and exergy transferred to the heating system during a whole heating cycle $(t_2 - t_0)$ will be considered. During the period $(t_1 - t_0)$ the *generated* heating capacity $\dot{Q}_H$ is passed on to the heating water circuit in a steady-state manner at an (average) *generated* heating temperature T_H and, during the period $(t_2 - t_0)$, the *required* heating capacity $\dot{Q}_H^*$ is carried away by the heating water circuit at the (average) *required* heating temperature T_H^*. Consequently, a fictitious heat store (HS) is included in the model (cf. Fig. 3-17).

a) Schematic of the heating water circuit with a fictitious heat store WS

b) Derivation of the exergy loss

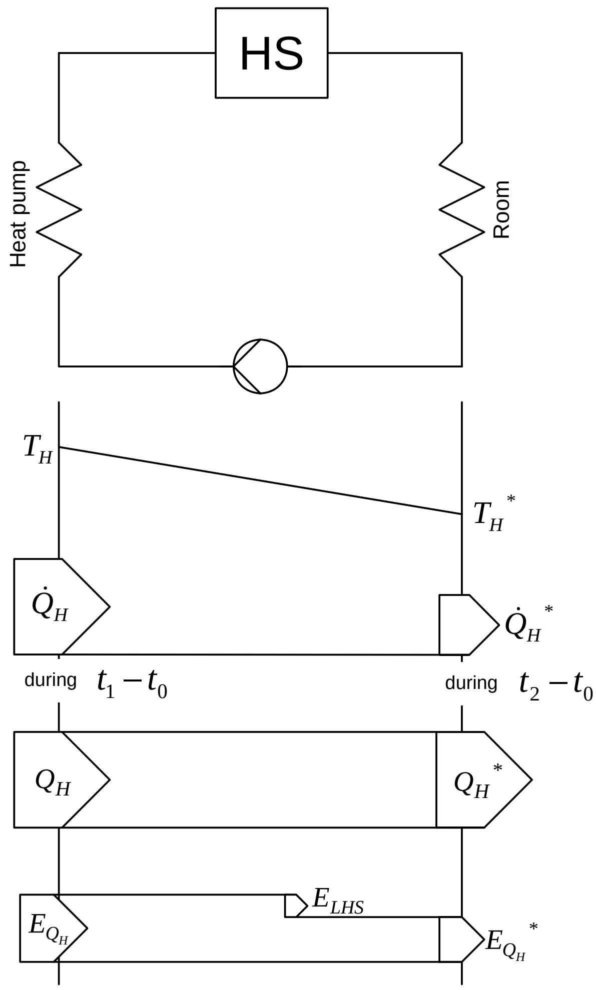

The following applies for the heat *flows*

$$\dot{Q}_H^* = \frac{1}{\upsilon} \cdot \dot{Q}_H \qquad (90)$$

and for the *amount* of heat during a heating cycle

$$Q_H = f \cdot (t_2 - t_0) \cdot \dot{Q}_H = \dot{Q}_H \frac{t_2 - t_0}{\upsilon} \qquad (91)$$

Fig. 3-17: Derivation of the exergy losses in the heat distribution system

From Fig. 3-17, the following is valid for E_{LHS}, the *amount* of exergy lost during a heating cycle:

$$E_{LHS} = E_{Q_H} - E_{Q_H}^{\ *} = f \cdot (t_2 - t_0) \cdot \dot{Q}_H \left(1 - \frac{T}{T_H}\right) - f \cdot (t_2 - t_0) \cdot \dot{Q}_H \left(1 - \frac{T}{T_H^{\ *}}\right) \tag{92}$$

$$E_{LHS} = \dot{Q}_H \cdot \frac{t_2 - t_0}{\upsilon} \cdot T_A \cdot \left(\frac{1}{T_H^{\ *}} - \frac{1}{T_H}\right) \tag{93}$$

If Eq. (93) is divided by $(t_2 - t_0)$, the *continuous exergy loss flow* in the heat distribution system resulting during the heating cycle can be calculated.

$$\dot{E}_{LHS}^{\ *} = \dot{Q}_H^{\ *} \cdot T_A \cdot \frac{T_H - T_H^{\ *}}{T_H \cdot T_H^{\ *}} = \dot{Q}_H^{\ *} \cdot T_A \cdot \frac{\Delta T_H}{T_H \cdot T_H^{\ *}} \tag{94}$$

Finally, we divide Eq. (94) with $(t_1 - t_0)$, in order to obtain a *suitable exergy loss flow* for the heat distribution system for heat pump evaluation purposes:

$$\dot{E}_{LHS} = \dot{Q}_H \cdot T_A \cdot \frac{T_H - T_H^{\ *}}{T_H \cdot T_H^{\ *}} = \dot{Q}_H \cdot T_A \cdot \frac{\Delta T_H}{T_H \cdot T_H^{\ *}} = \upsilon \cdot \dot{E}_{LHS}^{\ *} \tag{95}$$

The *external exergetic efficiency of the required heating temperature* can now appropriately be calculated using Eq. (45):

$$\eta_{exe}^{\ *} = \frac{1}{1 + \dfrac{\dot{E}_{LCp} + \dot{E}_{LEx} + \dot{E}_{LE} + \dot{E}_{LK} + \upsilon \cdot \dot{E}_{LHS}^{\ *}}{\dot{E}_{Q_H}}} = 1 - \frac{\dot{E}_{LCp} + \dot{E}_{LEx} + \dot{E}_{LE} + \dot{E}_{LC} + \upsilon \cdot \dot{E}_{LHS}^{\ *}}{P_i} \tag{96}$$

or correspondingly with

$$\eta_{exe}^{\ *} = \frac{1}{1 + \dfrac{\dot{E}_{LCp} + \dot{E}_{LEx} + \dot{E}_{LE} + \dot{E}_{LC} + \dot{E}_{LHS}}{\dot{E}_{Q_H}}} = 1 - \frac{\dot{E}_{LCp} + \dot{E}_{LEx} + \dot{E}_{LE} + \dot{E}_{LC} + \dot{E}_{LHS}}{P_i} \tag{97}$$

3.3.2 Exergy loss in the heat delivery system

For this heat transfer with an average temperature gradient of $\Delta T_R = T_H^{\ *} - T_R$, a *continuous exergy loss flow* of $\dot{E}_{LR}^{\ *}$ results during the heating cycle.

$$\dot{E}_{LR}^{\ *} = \dot{Q}_H^{\ *} \cdot T_A \cdot \frac{T_H^{\ *} - T_R}{T_H^{\ *} \cdot T_R} \tag{98}$$

And, as far as the intermittent heat flow $\dot{Q}_H$ during the operating time $(t_1 - t_0)$ is concerned:

$$\dot{E}_{LR} = \dot{Q}_H \cdot T_A \cdot \frac{T_H^{\ *} - T_R}{T_H^{\ *} \cdot T_R} = \upsilon \cdot \dot{E}_{LR}^{\ *} \tag{99}$$

For the *external exergetic efficiency of heating systems with heat pumps* (exergetic efficiency of the heated building), the following applies according to (46):

$$\eta_{exHS} = \frac{1}{1+\frac{\dot{E}_{LCp}+\dot{E}_{LEx}+\dot{E}_{LE}+\dot{E}_{LC}+\upsilon\cdot\dot{E}_{LHS}{}^{*}+\upsilon\cdot\dot{E}_{LR}{}^{*}}{\dot{E}_{Q_H}}}$$

$$= 1-\frac{\dot{E}_{LCp}+\dot{E}_{LEx}+\dot{E}_{LE}+\dot{E}_{LC}+\upsilon\cdot\dot{E}_{LHS}{}^{*}+\upsilon\cdot\dot{E}_{LR}{}^{*}}{P_i} \qquad (100)$$

or:

$$\eta_{exHS} = \frac{1}{1+\frac{\dot{E}_{LCp}+\dot{E}_{LEx}+\dot{E}_{LE}+\dot{E}_{LC}+\dot{E}_{LHS}+\dot{E}_{LR}}{\dot{E}_{Q_H}}}$$

$$= 1-\frac{\dot{E}_{LCp}+\dot{E}_{LEx}+\dot{E}_{LE}+\dot{E}_{LC}+\dot{E}_{LHS}+\dot{E}_{LR}}{P_i} \qquad (101)$$

3.4 Energy and exergy flow diagram for the heat pump and its sub-processes

A comparison of the energy and exergy flow diagrams for the heat pump including its sub-processes underlines the benefits and the importance of an exergy analysis for the thermodynamically correct assessment of the air/water heat pump.

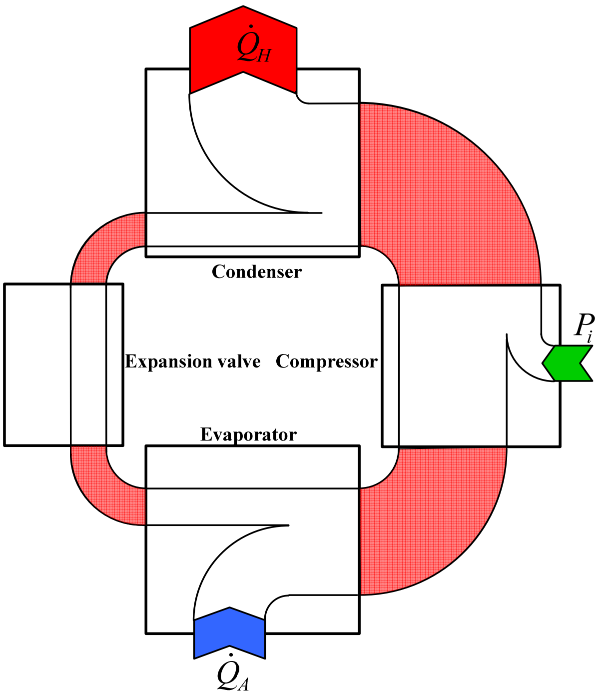

Fig. 3-18: Energy flow diagram for the heat pump including sub-processes

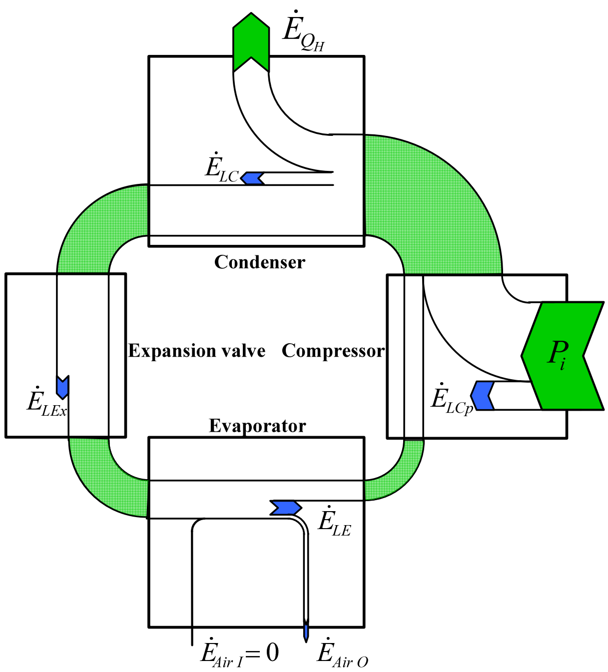

Fig. 3-19: Exergy flow diagram for the heat pump including sub-processes

In order to represent the individual exergy flows and especially the exergy loss flows, the exergy flow diagram has been enlarged by a factor of three in comparison to the energy flow diagram.

In the *energy flow diagram* of the heat pump, just three energy flows (heating capacity, compressor power and heat flow in the evaporator) occur. There are no *energy losses* in the heat pump process.

The *exergy flow diagram* on the other hand, gives information on the sources of loss: i.e. *exergy losses* that occur in the compressor, in the expansion valve, in the condenser and in the evaporator.

For a given exergy flow of the *generated* heating capacity $\dot{E}_{Q_H}$, the internal compressor power P_i needed is increased by the sum of the individual exergy losses as compared to the theoretical minimum (reversible) drive power $P_{rev} = \dot{E}_{Q_H}$ (cf. Eq. (47)).

The largest exergy losses can be found in the compressor and the evaporator. The exergy flow $\dot{E}_{Air\,O} = \dot{E}_A$ of the cooled-down outside air given off to the environment is small and will no longer be separately quantified but will be added to the exergy loss in the evaporator $\dot{E}_{LE}$.

To complete the pictures, Fig. 3-20 and Fig. 3-21 shows a comparison of the exergy and energy flow diagrams for the entire heating system with a heat pump. Here, the exergy losses that occur in the heat delivery and distribution system are also shown.

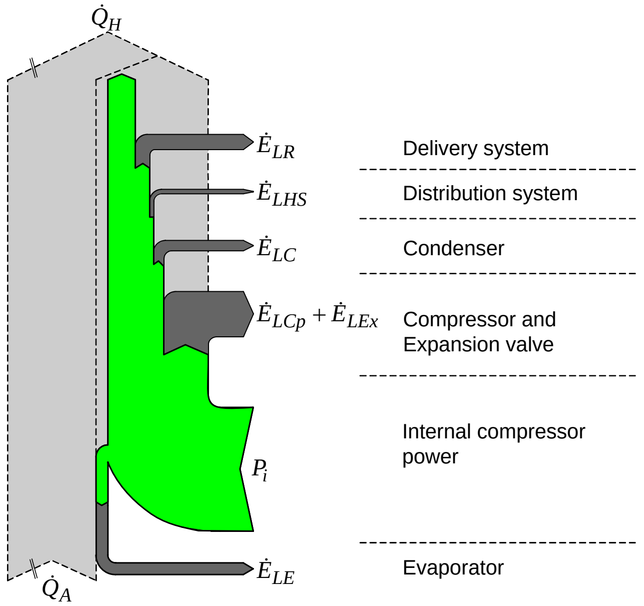

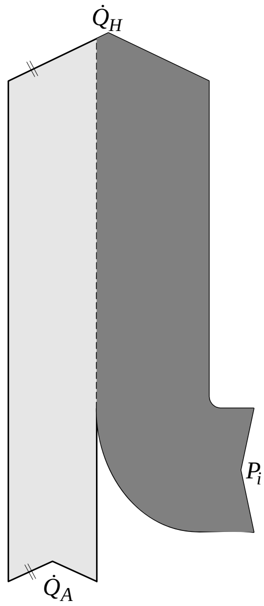

Fig. 3-20: Exergy flow diagram for the entire heating system with a heat pump

Fig. 3-21: Energy flow diagram for the entire heating system with a heat pump

4 Exergy losses of the sub-processes and their determining factors

The basic factors influencing the exergy losses of the four sub-processes of the heat pump are the temperature gradients for heat transfer in the evaporator, ΔT_E, and condenser, ΔT_C, as well as the isentropic compressor efficiency, η_s. These mutually affect each other and so reduce the exergetic efficiency of the heat pump. Moreover, all exergy losses are dependent on the temperature lift. Additionally, the temperature lift is increased by the discrepancy between the *required* and the *generated* heating temperature $\Delta T_H = T_H - T_H^*$. The temperature lift ΔT_{Lift} ist given by:

$$\Delta T_{Lift} = T_C - T_E = \left(T_H^* - T_A\right) + \Delta T_H + \Delta T_E + \Delta T_C = \Delta T_{Lift\ ideal} + \Delta T_H + \Delta T_E + \Delta T_C \qquad (102)$$

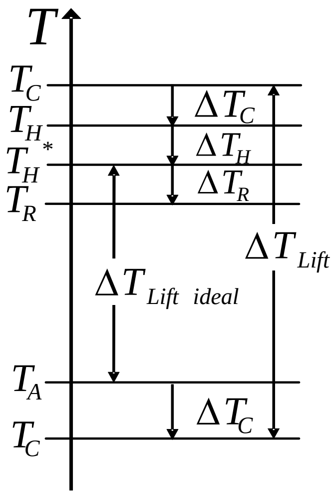

Fig. 4-1 provides an overview of the temperatures and the temperature gradients in a heating system that uses a heat pump.

Physical equations will now be developed in order to show the quantitative effect of these relevant determining factors on exergy losses and exergetic efficiency. By making some approximations, relatively clear equations can be established that can easily be discussed without significant losses in accuracy. These results will be useful to the development engineer working to improve future heat pumps. By using these innovative measures one can make heat pumps that are energetically and economically better.

The heat pump process considered in this study is shown in Fig. 3-5 in a T,s-diagram and briefly explained.

Fig. 4-1: Temperatures and temperature gradients in the heat pump process

4.1 Exergy losses in the compressor

We refer once again to the adiabatic compressor. The *isentropic compressor efficiency* η_s *is* particularly important for the exergy loss in the compressor.

The function of the compressor is to increase the pressure of the working fluid from p_E (evaporation pressure) to p_C (condensation pressure) in accordance with the required temperature lift from T_E to T_C. In a single-stage adiabatic compressor, however, a higher output temperature T_2 is generated than the condensation temperature T_C (cf. representation in the $\log p, h$-diagram, Fig. 4-2, and in the T,s-diagram, Fig. 4-3). This means that the working fluid passes into the condenser overheated by around $\Delta T_{hGsh} = T_2 - T_C$ and contains an appropriate amount of *superheating exergy* that, however, usually hardly ever gets used except if hot water is additionally generated. Is the exergy of the overheated vapour to be taken as being a loss in the compressor or in the condenser? - This depends on the point of view! Here, we add these exergy losses to the balance of the condenser, but, however, identify them separately. In this way, a clear interpretation can be made.

Consequently, the following is valid for the specific exergy loss in the compressor according to Eq. (56):

$$e_{LCp} = T_A \cdot \left(s_2 - s_1\right) \qquad (103)$$

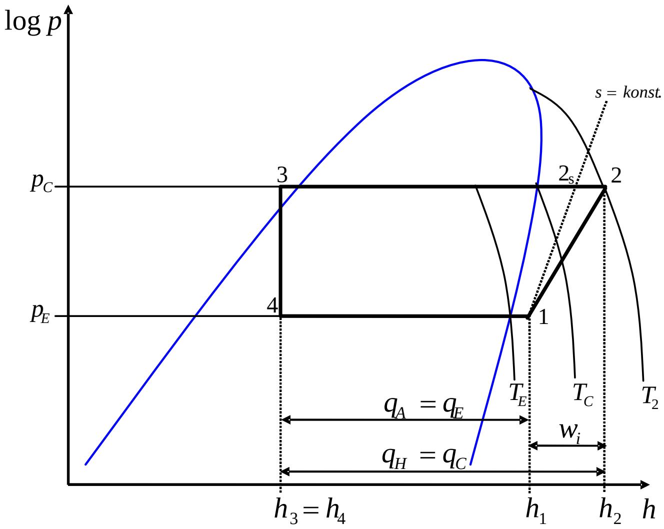

Fig. 4-2: log p,h-diagram for the heat pump process

We now treat the vapour in the compressor as a *perfect gas* with the corresponding *averaged gas properties* c_p, R and κ. Thus, the following is valid for the increase in specific entropy in the compressor

$$s_2 - s_1 = \left[c_{pg} \cdot \ln\left(\frac{T_2}{T_1}\right) - R \cdot \ln\left(\frac{p_2}{p_1}\right)\right] \tag{104}$$

and the consequent specific exergy loss in the compressor is:

$$e_{LCp} = T_A \cdot \left[c_{pg} \cdot \ln\left(\frac{T_2}{T_1}\right) - R \cdot \ln\left(\frac{p_2}{p_1}\right)\right] \tag{105}$$

The compressor exit temperature T_2 is dependent both on the pressure ratio $\varphi = p_2 / p_1$ as well as on the *isentropic efficiency* η_s of the compressor (Appendix A1):

$$T_2 = T_1 \cdot \left[\frac{1}{\eta_s} \cdot \left(\varphi^K - 1\right) + 1 \right] \tag{106}$$

whereby K is defined as:

$$K = \frac{\kappa - 1}{\kappa} \tag{107}$$

Here, $p_1 = p_E$ and $p_2 = p_C$. This means that the pressure ratio is:

$$\varphi = \frac{p_2}{p_1} = \frac{p_C}{p_E} \tag{108}$$

As, primarily, the temperatures T_E and T_C and not the pressures p_E and p_C are the decisive factors in the dimensioning of the heat pump process, is it sensible that our analysis should the vapour pressures express by their boiling point temperatures. In order to be able to discuss the results analytically, we will mathematise the vapour pressure curve using the *Clausius-Clapeyron* relation. In this way, we obtain the pressure ratio (Appendix A2):

$$\varphi = \frac{p_C}{p_E} = e^{\frac{r}{R}\cdot\left(\frac{1}{T_E}-\frac{1}{T_C}\right)} = e^{\frac{r}{R}\cdot\left(\frac{T_C-T_E}{T_E\cdot T_C}\right)} \approx e^{\frac{r}{R}\cdot\frac{\Delta T_{Lift}}{T_A{}^2}} \tag{109}$$

Using Eq. (106) and (109) in (105), the following is valid for the specific exergy loss in the compressor:

$$e_{LCp} = T_A \cdot \left(c_{pg} \cdot \ln\left[\frac{1}{\eta_s} \cdot e^{\frac{K\cdot r}{R}\cdot\frac{T_C-T_E}{T_C\cdot T_E}} - \frac{1}{\eta_s} + 1 \right] - r \cdot \frac{T_C - T_E}{T_C \cdot T_E} \right) \tag{110}$$

Making a simplification concerning the working fluid in the compressor by treating it as a *perfect gas* and with the idealisation of the vapour pressure curve according to *Clausius-Clapeyron,* reliable results can be obtained. For a clear interpretation we approximate the logarithmic and the exponential functions with series expansions (Appendix A3). Moreover, the following identity is employed:

$$\frac{c_p}{R} = \frac{\kappa}{\kappa - 1} = \frac{1}{K} \quad \Rightarrow \quad \frac{c_p \cdot K}{R} = 1 \tag{111}$$

Using this, the essential interrelationship with respect to specific exergy loss in an (adiabatic, single-stage) compressor can be clearly shown.

$$e_{LCp} = T_A \cdot r \cdot \frac{\Delta T_{Lift}}{T_E \cdot (T_E + \Delta T_{Lift})} \cdot \left[\frac{1}{\eta_s} - 1 \right] \tag{112}$$

The exergy loss in the compressor is approximately proportional to the temperature lift ΔT_{Lift}. In wich ΔT_E, ΔT_C and ΔT_H are included (cf. Eq. (102)).

Also, the effect of η_s is immediately clear - see the square brackets in Eq. (112). – Finally, using $T_E \approx T_A$, it follows that:

$$\boxed{e_{LCp} \approx r \cdot \frac{\Delta T_{Lift}}{T_E + \Delta T_{Lift}} \cdot \left(\frac{1}{\eta_s} - 1 \right) \approx r \cdot \frac{1}{COP_{revi}} \cdot \left(\frac{1}{\eta_s} - 1 \right)} \tag{113}$$

The errors resulting from the simplifications are small. At around 50 K temperature lift, the relative error in Eq. (113), when compared with Eq. (110), is only 4% (Appendix A3).

If, for a simple interpretation, the exergy loss flow in the compressor $\dot{E}_{LCp}$ is now referred to the heat flow $\dot{Q}_E$ transferred in the evaporator and the following approximation is made (vapour quality of the working fluid on entry into the evaporator is neglected):

$$\dot{Q}_E \approx \dot{m}_f \cdot r \tag{114}$$

We obtain:

$$\boxed{\frac{\dot{E}_{LCp}}{\dot{Q}_E} \approx \frac{\Delta T_{Lift}}{T_E + \Delta T_{Lift}} \cdot \left(\frac{1}{\eta_s} - 1 \right) \approx \frac{1}{COP_{revi}} \cdot \left(\frac{1}{\eta_s} - 1 \right)} \tag{115}$$

Consequently, the exergy loss in the compressor is primarily dependent on η_s and, in addition to the ideal temperature lift, by ΔT_E, ΔT_C and ΔT_H (cf. Eq. (102)).

4.2 Exergy losses in the expansion valve

The pressure reduction occurs from state point 3 to state point 4 where the pressure is reduced from p_C to p_E, the temperature of the working fluid falls from T_3 to T_4 and the entropy increases from s_3 to s_4. Fig. 4-3 contains the notation employed for this derivation. Again, the exergy loss is to be formulated analytically with the aid of the relevant temperatures and temperature differences. The condensate (point 3) is subcooled by around ΔT_{Csc}.

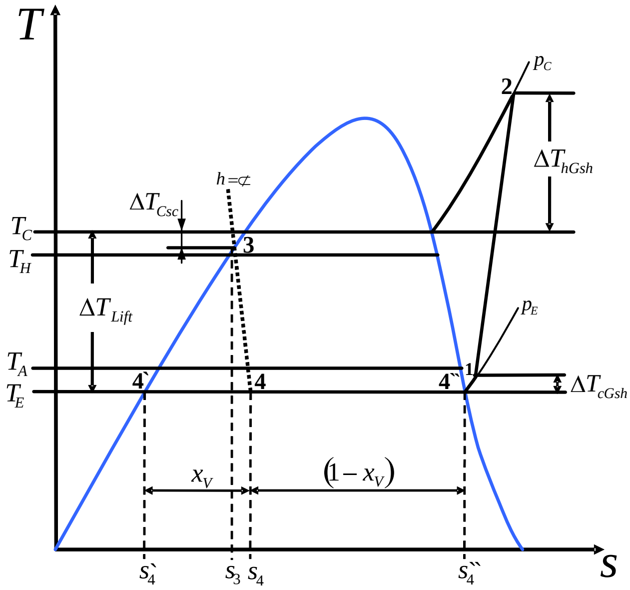

Fig. 4-3: T,s-diagram with specific entropies

As a result of the pressure reduction in the subcooled condensate (point 3) *wet steam* (point 4) is produced with a vapour quality of $x_4 = x_V$. In this way, the *specific enthalpy* h_4 (Appendix A4) can be calculated

$$h_4 = h_4' + x_V \cdot (h_4'' - h_4') = h_4' + x_V \cdot r_E \tag{116}$$

along with the specific entropy (Appendix A4):

$$s_4 = s_4' + x_V \cdot (s_4'' - s_4') = s_4' + x_V \cdot \frac{r_E}{T_E} \tag{117}$$

The pressure reduction is *isenthalpic*:

$$h_4 = h_3 \tag{118}$$

Using Eq. (116), the vapour quality after the expansion valve can be calculated:

$$x_V = x_4 = \frac{h_3 - h_4'}{r_E} \tag{119}$$

For the specific enthalpy difference (along the boiling curve) the following serves:

$$h_3 - h_4' \approx c_{pl} \cdot (T_3 - T_4) \tag{120}$$

Here, c_{pl} is the specific heat capacity of the boiling, liquid working fluid (averaged between the Temperatures T_3 and T_4).

Now, for the vapour quality after the expansion valve is obtained:

$$x_V = x_4 \approx \frac{c_{pl} \cdot (T_3 - T_4)}{r_E} \approx \frac{c_{pl} \cdot (\Delta T_{Lift} - \Delta T_{Csc})}{r_E} \tag{121}$$

From Eq. (121) it can be seen that the condensate subcooling ΔT_{Csc} reduces the formation of vapour in the expansion valve and, therefore, the increase in entropy and the exergy loss also become smaller.

According to Eq. (72), the following is valid for the *specific exergy loss in the expansion valve*:

$$e_{LEx} = T_A \cdot (s_4 - s_3) \tag{72}$$

and, using Eq. (117), it follows that:

$$e_{LEx} = T_A \cdot \left[(s_4' - s_3) + x_V \cdot \frac{r_E}{T_E} \right] \tag{122}$$

Since the specific entropy difference between 3 and $4'$ refers to the liquid state, the specific entropy differential can be approximated:

$$ds = \frac{dh - v \cdot dp}{T} \approx \frac{c_{pl} \cdot dT}{T} \tag{123}$$

and it follows that:

$$s_4' - s_3 = c_{pl} \int_{T_3}^{T_4'} \frac{dT}{T} = c_{pl} \cdot \ln \frac{T_E}{T_E + \Delta T_{Lift} - \Delta T_{Csc}} \tag{124}$$

Using Eq. (121) and (123) in (72), we obtain the following for the *specific exergy loss in the expansion valve*:

$$e_{LEx} = T_A \cdot c_{pl} \cdot \left[\ln\left(\frac{T_E}{T_E + \Delta T_{Lift} - \Delta T_{Csc}} \right) + \frac{\Delta T_{Lift} - \Delta T_{Csc}}{T_E} \right] \tag{125}$$

Here, too, the logarithm will be further approximated by a series expansion in order to obtain a clear interpretation (Appendix A5):

$$e_{LEx} \approx T_A \cdot c_{pl} \cdot \frac{1}{2} \cdot \left(\frac{\Delta T_{Lift}{}^2}{T_E{}^2 + T_E \cdot \Delta T_{Lift}} \right) \tag{126}$$

$$\dot{E}_{LEx} \approx \dot{m}_f \cdot T_A \cdot c_{pl} \cdot \frac{1}{2} \cdot \left(\frac{\Delta T_{Lift}{}^2}{T_E{}^2 + T_E \cdot \Delta T_{Lift}} \right) \tag{127}$$

With $T_E \approx T_A$ it finally follows that:

$$\boxed{\dot{E}_{LEx} \approx \dot{m}_f \cdot c_{pl} \cdot \frac{1}{2} \cdot \left(\frac{\Delta T_{Lift}{}^2}{T_E + \Delta T_{Lift}} \right) \approx \dot{m}_f \cdot c_{pl} \cdot \frac{\Delta T_{Lift}}{2 \cdot COP_{rev\,i}}} \tag{128}$$

Consequently, the exergy loss in the expansion valve is proportional to c_{pl} and to the temperature lift. In practice, ΔT_{Lift} can be influenced by ΔT_E, ΔT_C and ΔT_H. For comparison: the exergy loss in the compressor (according to Eq. (113)) is proportional to specific enthalpy of evaporation r of the working fluid and to the first power of the temperature lift.

In general:

$$\dot{E}_{LEx} << \dot{E}_{LCp} \tag{129}$$

The exergy loss ratio compressor to expansion valve is therefore:

$$\frac{e_{LCp}}{e_{LEx}} = \frac{\dot{E}_{LCp}}{\dot{E}_{LEx}} \approx \frac{2 \cdot r \cdot \left(\frac{1}{\eta_s} - 1\right)}{c_{pl} \cdot \Delta T_{Lift}} \tag{130}$$

4.3 Exergy losses in the evaporator

The exergy loss in the evaporator can be roughly calculated using the equations in section 3.2.4. Here, this will be dealt with in more detail, in particular as far as the need for vapour superheating in the evaporator is concerned and its consequences. Also, the occurrence of temperature glide ΔT_{GE} for multi-component working fluids (such as R407C) is considered in the $T,\dot{Q}$-diagram in Fig. 4-4. The fluid providing the heat, here for example outdoor air with T_A, is cooled down by ΔT_{Air}.

In the $T,\dot{Q}$-diagram in Fig. 4-4, the process in the evaporator is subdivided into two sections.

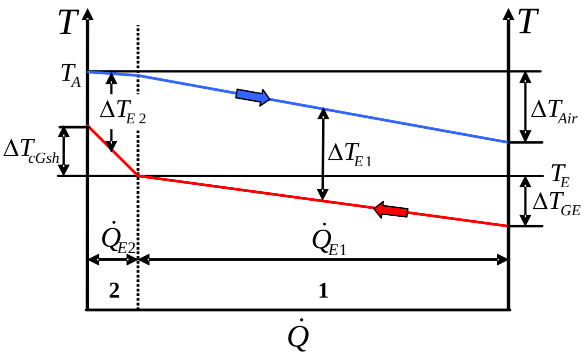

Fig. 4-4: $T,\dot{Q}$-diagram for the evaporator

In section 1, the working fluid, which on entry into the evaporator is in the wet steam area, is evaporated completely. If, in addition, the working fluid exhibits a temperature glide ΔT_{GE} during evaporation, the evaporation temperature T_E is referred to the dew point temperature of the mixture (cf. Appendix A8).

In the second section, the now gaseous working fluid is superheated, whereby the degree of superheating is significantly determined by the setting of the expansion valve. Superheating the vapour assures that the compressor draws in no liquid droplets and thus suffers no damage.

The primary determining factor as far as exergy losses in the evaporator is concerned is the *temperature gradient for heat transfer.* For a given operating point of the air/water heat pump, the exergy losses in the evaporator equipment can be calculated as described in the following procedure.

The total heat flow taken up by the working fluid in the evaporator is

$$\dot{Q}_E = \dot{m}_f \cdot (h_1 - h_4) \tag{131}$$

of which

$$\dot{Q}_{E1} = \dot{m}_f \cdot r_E \cdot (1 - x_V) \tag{132}$$

will be transferred solely for evaporation, and

$$\dot{Q}_{E2} = \dot{m}_f \cdot c_{pg} \cdot \Delta T_{cGsh} \tag{133}$$

for vapour superheating. Here:

$$\dot{Q}_E = \dot{Q}_{E1} + \dot{Q}_{E2} \tag{134}$$

Exergy losses of pure evaporation

For the section 1 (pure evaporation), the exergy loss flow is calculated as in Eq. (23):

$$\dot{E}_{LE1} = T_A \cdot \dot{Q}_{E1} \cdot \frac{\Delta T_{E1}}{T_{E1}^{\ 2}} \tag{135}$$

The average temperature gradient is approximated using Fig. 4-4:

$$\Delta T_{E1} = T_A - \frac{1}{2} \cdot \Delta T_{Air} - \left(T_E - \frac{1}{2} \Delta T_{GE} \right) \tag{136}$$

For the average temperature level of the heat transfer:

$$T_{E1} = \left(T_A - \frac{1}{2} \cdot \Delta T_{Air} \right) - \frac{1}{2} \cdot \Delta T_{E1} \tag{137}$$

Exergy losses during the superheating of vapour in the evaporator

The difference between the evaporator exit temperature and the evaporation temperature T_E will be designated as *vapour superheating in the evaporator* ΔT_{cGsh}. As the temperature drop in the ambient air for the generation of vapour superheating is low, the exergy loss flow occurring in this case can also be calculated using the Eq. (23).

$$\dot{E}_{LE2} = T_A \cdot \dot{Q}_{E2} \cdot \frac{\Delta T_{E2}}{T_{E2}^{\ 2}} \tag{138}$$

using the average temperature gradient for heat transfer

$$\Delta T_{E2} = T_A - \left(T_E + \frac{1}{2} \cdot \Delta T_{cGsh} \right) \tag{139}$$

and the average temperature level of heat transfer

$$T_{E2} = T_A - \frac{1}{2} \cdot \Delta T_{E2} \tag{140}$$

It should be noted here that, in this study, most exergy losses in the transfer of heat can be determined with a sufficient precision for this analysis using Eq. (23). This applies both to a global analysis of the evaporator and condenser as well as to the analysis of their sections for a more exact appraisal. For higher demands on accuracy, the differential exergy loss according to Eq. (79) must be used and integrated.

Total exergy losses in the evaporator

The total exergy loss flow in the evaporator is:

$$\dot{E}_{LE} = \dot{E}_{LE1} + \dot{E}_{LE2} \tag{141}$$

In certain situations, vapour superheating ΔT_{cGsh} has a large negative influence on the exergy losses in the evaporator and therefore also on the exergetic efficiency of the heat pump. This case occurs if a vapour superheating of about 7 K or even 10 K is necessary when reducing pressure with thermostatic expansion valves and, therefore, no lower temperature gradients ΔT_E are possible. Only electronically controlled expansion valves permit lower temperature gradients in the evaporator unit. This problem must be dealt with later.

At an ambient temperature of $\vartheta_A = 0°C$ and a vapour superheating in the evaporator of $\Delta T_{cGsh} = 5K$, the following exergy loss components result in the evaporator.

$$\frac{\dot{E}_{LE2}}{\dot{E}_{LE}} = \frac{3.9W}{154.9W} = 0.025 = 2.5\% \tag{142}$$

and

$$\frac{\dot{E}_{LE1}}{\dot{E}_{LE}} = \frac{151W}{154.9W} = 0.975 = 97.5\% \tag{143}$$

This shows that approximation using Eq. (78) is normally sufficient.

4.4 Exergy losses in the condenser

A simple assessment of the exergy losses in the condenser can already be made using Eq. (68) with an average temperature gradient of ΔT_C. This view can now be refined according to the $T, \dot{Q}$-diagram shown in Fig. 4-5, where three sections can be distinguished for the heat transfer.

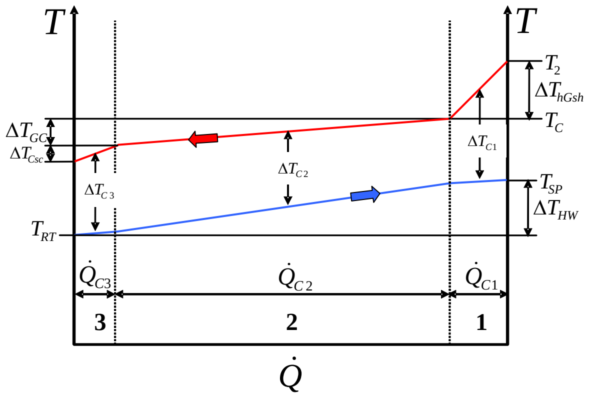

Fig. 4-5: $T, \dot{Q}$-diagram for the condenser

In the first section, the superheated vapour is cooled from the compressor output temperature T_2 down to the condensation temperature T_C, followed by the actual condensation. In the case of working fluids consisting of refrigerant mixtures, a temperature glide ΔT_{GC} occurs (cf. Appendix A8). In the third section, condensate subcooling also occurs. This contribution to exergy losses is negligibly small. Whether vapour saturation occurs on the outer side of the condensate film or, separately, on a "dry" heat exchanger surface, has no influence on $\dot{E}_{LC}$.

In the condenser, the heat flow

$$\dot{Q}_C = \dot{m}_f \cdot (h_2 - h_3) \tag{144}$$

will be transferred in total. This consists of the vapour saturation

$$\dot{Q}_{C1} = \dot{m}_f \cdot c_{pg} \cdot \Delta T_{hGsh} \tag{145}$$

But mainly on the actual condensation

$$\dot{Q}_{C2} = \dot{m}_f \cdot r_C \tag{146}$$

and also condensate subcooling

$$\dot{Q}_{C3} = \dot{m}_f \cdot c_{pl} \cdot \Delta T_{Csc} \tag{147}$$

This means that:

$$\dot{Q}_C = \dot{Q}_{C1} + \dot{Q}_{C2} + \dot{Q}_{C3} \tag{148}$$

The characteristic for the heating water temperature in the $T, \dot{Q}$ -diagram is linear from T_{RT} to T_{SP} .

For the calculation of vapour superheating

$$\Delta T_{hGsh} = T_2 - T_C \tag{149}$$

an algebraically interpretable expression for the compressor output temperature T_2 is developed. Using Eq. (106) and (109) it follows that (Appendix A2):

$$T_2 = \left[\frac{1}{\eta_s} \cdot \frac{1}{c_{pg}} \cdot r \cdot \left(\frac{\Delta T_{Lift}}{T_C \cdot (T_C + \Delta T_{Lift})} \right) + 1 \right] \cdot (T_C + \Delta T_{cGsh}) \tag{150}$$

From this it can be seen that ΔT_{hGsh} is small if η_s is high and ΔT_{Lift} small. Hence, a small isentropic exponent is also beneficial here.

Exergy losses of vapour superheating in the condenser

We continue to calculate the exergy loss flow in section 1 with the Eq. (23) and, in addition, with the heat flow according to Eq. (145).

$$\dot{E}_{LC1} = T_A \cdot \dot{m}_f \cdot c_{pg} \cdot \Delta T_{hGsh} \cdot \frac{\Delta T_{C1}}{T_{C1}^{\;2}} \tag{151}$$

with an average temperature gradient

$$\Delta T_{C1} = \frac{T_2 + T_C}{2} - T_{SP} \tag{152}$$

and the average temperature level for heat transfer

$$T_{C1} = \frac{T_2 + T_C}{2} - \frac{\Delta T_{C1}}{2} \tag{153}$$

This means that the *exergy loss of vapour superheating* is directly proportional to the amount of vapour superheating ΔT_{hGsh}. This is determined significantly by the isentropic efficiency of the compressor, the operating state and the thermal properties of the working fluid.

Exergy losses in condensation

The *exergy loss flow during the condensation* (section 2), i.e. the aggregate state-change from saturated vapour to a boiling fluid, is also calculated using Eq. (23) and, in addition, with the heat flow according to Eq. (146):

$$\dot{E}_{LC2} = \dot{m}_f \cdot T_A \cdot r_C \cdot \frac{\Delta T_{C2}}{{T_{C2}}^2} \tag{154}$$

with an average temperature gradient

$$\Delta T_{C2} = T_C - \frac{\Delta T_{GC}}{2} - \frac{T_{SP} + T_{RT}}{2} \tag{155}$$

and an average temperature level for heat transfer

$$T_{C2} = T_C - \frac{1}{2} \cdot \Delta T_{GC} - \frac{1}{2} \cdot \Delta T_{C2} \tag{156}$$

Exergy losses in condensate subcooling

The exergy loss flow in the third section is noted in a similar manner to the 1st section:

$$\dot{E}_{LC3} = T_A \cdot \dot{m}_f \cdot c_{pl} \cdot \Delta T_{Csc} \cdot \frac{\Delta T_{C3}}{{T_{C3}}^2} \tag{157}$$

with an average temperature gradient

$$\Delta T_{C3} = T_C - \Delta T_{GC} - \frac{\Delta T_{Csc}}{2} - T_{RT} \tag{158}$$

and an average temperature level for heat transfer

$$T_{C3} = T_{RT} + \frac{1}{2} \cdot \Delta T_{C3} \tag{159}$$

Similarly to the vapour superheating in the condenser, the exergy loss for condensate subcooling is directly proportionally to the amount of condensate subcooling ΔT_{Csc}.

Total exergy losses in the condenser

The entire exergy loss flow in the condenser sums up from the following exergy loss flows: vapour superheating in the condenser (Eq. (151)), condensation (Eq. (154)) and condensate subcooling (Eq. (157)).

$$\dot{E}_{LC} = \dot{E}_{LC1} + \dot{E}_{LC2} + \dot{E}_{LC3} \tag{160}$$

For an ambient temperature of $\vartheta_A = 0°C$, a resultant temperature lift $\Delta T_{Lift} = 50K$ and a condensate subcooling of $\Delta T_{Csc} = 5K$, the following exergy loss components result in the condenser:

$$\frac{\dot{E}_{LC1}}{\dot{E}_{LC}} = \frac{14.56W}{141.34W} = 0.103 = 10.3\% \tag{161}$$

and

$$\frac{\dot{E}_{LC2}}{\dot{E}_{LC}} = \frac{124.36W}{141.34W} = 0.88 = 88\% \tag{162}$$

and

$$\frac{\dot{E}_{LC3}}{\dot{E}_{LC}} = \frac{2.41W}{141.34W} = 0.017 = 1.7\% \qquad (163)$$

The share of exergy loss for condensate subcooling is small, but not however, that of the vapour superheating. Here, some potential exists: Use for hot water preparation or diabatic compressors.

5 Operating characteristic of air/water heat pumps with on/off control

If the outdoor temperature rises, the *required heating capacity* of the building drops. Conventional air/water heat pumps, however, increase the *generated heating capacity*. The heating capacities are then matched by using on/off control. A consequence of these two diverging heating capacities is a decrease in thermal efficiency: coefficient of performance, seasonal performance factor and, correspondingly, the exergetic efficiency are not optimal. This will be analysed in the next chapter.

First, the *operating characteristic* of air/water heat pumps with on/off-control will be determined, i.e. the dependence of important physical parameters which (automatically) adjust themselves to ambient temperature during operation. These are:

$$T_E(T_A);\quad T_C(T_A);\quad T_H(T_A);\quad \Delta T_E(T_A);\quad \Delta T_C(T_A);\quad \Delta T_H(T_A)$$

$$\dot{m}_f = \dot{m}_f(T_A)$$

$$\dot{Q}_E = \dot{Q}_E(T_A);\quad \dot{Q}_C = \dot{Q}_H = \dot{Q}_H(T_A);\quad P_i = P_i(T_A)$$

In order to determine the heat pump’s operating characteristic, the process equations required are first compiled.

5.1 Process equations

The self-adjusting operating point at a given ambient temperature can be calculated using the following process equations. The calculations have to be carried out numerically and require several iterations.

The following process equations are also valid if partial condensation or partial de-sublimation occurs in the fin tube evaporator, wich is most frequently used. Only the time-variable aspects of the operating characteristic due to frost formation are not considered here.

5.1.1 Working fluid mass flow

The working fluid mass flow supplied by the compressor is dependent on the type of compressor employed (standard volume flow $\dot{V}_S$, volumetric efficiency λ: see Appendix A1) and on the thermal state of the working fluid on the intake and pressure sides of the compressor:

$$\dot{m}_f(T_E, T_C) = \frac{p_E(T_E)\cdot \dot{V}_S \cdot \lambda(T_E, T_C)}{R \cdot Z \cdot T_1} \tag{164}$$

with:

$$T_1 = T_E(T_A) + \Delta T_{cGsh} \tag{165}$$

5.1.2 Heat flow in the evaporator

The heat flow $\dot{Q}_E$ absorbed by the working fluid in the evaporator with the vapour quality x_V upon entry into the evaporator (i.e. after the expansion valve) is:

$$\dot{Q}_E(T_E, T_C) = \dot{Q}_A = \dot{m}_f(T_E, T_C)\cdot \left[r_E(T_E)\cdot(1 - x_V(T_E, T_C)) + c_{pg}\cdot \Delta T_{cGsh}\right] \tag{166}$$

With a vapour quality x_V according to Eq. (121), it follows that:

$$\dot{Q}_E(T_E,T_C)=\dot{m}_f(T_E,T_C)\cdot\left[r_E(T_E)\cdot\left(1-\frac{c_{pl}\cdot(T_C-T_E-\Delta T_{Csc})}{r_E(T_E)}\right)+c_{pg}\cdot\Delta T_{cGsh}\right] \tag{167}$$

The last term for vapour superheating is negligibly small in comparison to the first, wich contains the evaporation.

5.1.3 Cooling of ambient air in the evaporator

The air taken in from the ambient is cooled down in the (fin tube) evaporator by ΔT_{Air}. If no water vapour condenses or is desublimated, this is determined by:

$$\Delta T_{Air}(T_E,T_C)=\frac{\dot{Q}_E(T_E,T_C)}{\dot{V}_{Air}\cdot\rho_{Air}\cdot c_{pAir}} \tag{168}$$

If, however, *heat and mass transfer* (with condensate or frost formation) occurs on the air side of the evaporator, the cooling of the air by ΔT_{Air} considers only the *sensible heat flow* $\dot{Q}_{As}$ (cf. section 3.2.4):

$$\Delta T_{Air}(T_E,T_C)=\frac{\dot{Q}_{As}}{\dot{V}_{Air}\cdot\rho_{Air}\cdot c_{pAir}} \tag{169}$$

A relationship is now required for the ratio of *total heat flow* $\dot{Q}_A$ to *sensible heat flow* $\dot{Q}_{As}$ in the evaporator:

$$\xi=\frac{\dot{Q}_A}{\dot{Q}_{As}}=\frac{(h_{AirI}-h_{AirO})}{c_{pAir}\cdot(T_{AirI}-T_{AirO})} \tag{170}$$

In the following, we follow an approach that was successfully used in the research project LOREF [5]. It will be assumed that the decrease in enthalpy of the moist ambient air is proportional to the temperature drop (between the input and output sides of the (fin tube) evaporator), even when moisture is deposited as condensate or frost:

$$h_{AirI}-h_{AirO}=b_0\cdot(T_{AirI}-T_{AirO}) \tag{171}$$

Here, the factor b_0 is calculated as a function of the dew point temperature of moist air. For air/water heat pump applications, regression analysis provides the following result:

$$\frac{b_0}{[J/kgK]}=0.039\cdot\frac{\vartheta_{DpI}}{[°C]}+1.6368 \tag{172}$$

Here, ϑ_{DpI} stands for the dew point temperature of the moist air on entry into the (fine tube) evaporator.

Using Eq. (169), (170) and (171), the cooling of the moist ambient air with simultaneous heat and mass transfer in the (fine tube) evaporator can now be calculated directly from the total heat flow $\dot{Q}_E$ with the aid of the factor b_0:

$$\Delta T_{Air}(T_E,T_C)=\frac{\dot{Q}_E(T_E,T_C)}{\dot{V}_{Air}\cdot\rho_{Air}\cdot b_0} \tag{173}$$

The air volume flow $\dot{V}_{Air}$ results from the fan characteristic and the geometry of the (fine tube) evaporator (see also LOREF [5]).

5.1.4 Temperature gradient and evaporation temperature

Two different methods of calculation are shown. The first method is suitable for making estimates.

a) For rough calculations

The average temperature gradient in the evaporator ΔT_E for the transfer of heat is determined using:

$$\Delta T_E(T_E, T_C) = \frac{\dot{Q}_E(T_E, T_C)}{k_E \cdot A_E} \tag{174}$$

Here, the overall heat transfer coefficient k_E is a general value for the whole (fin tube) evaporator, i.e. for evaporation with vapour superheating. If possible, it is determined from measurements made on test heat pumps. If non-steady-state frost formation is neglected, the overall heat transfer coefficient can be used as a constant; this has been confirmed by experimental analysis (LOREF [5]).

The evaporation temperature T_E is calculated on the basis of the average temperature gradient (Eq. (174)) as well as the cooling-down of the air in the evaporator (Eq. (168) and (173)):

$$T_E = \left(T_A - \frac{1}{2} \cdot \Delta T_{Air}\right) - \Delta T_E + \frac{1}{2} \cdot \Delta T_{GE} \tag{175}$$

And for the average evaporation temperature $\overline{T}_E$:

$$\overline{T}_E = T_E - \frac{1}{2} \cdot \Delta T_{GE} \tag{176}$$

Fig. 5-1 shows the simplified $T,\dot{Q}$-diagram, whereby a temperature glide ΔT_{GE} is considered.

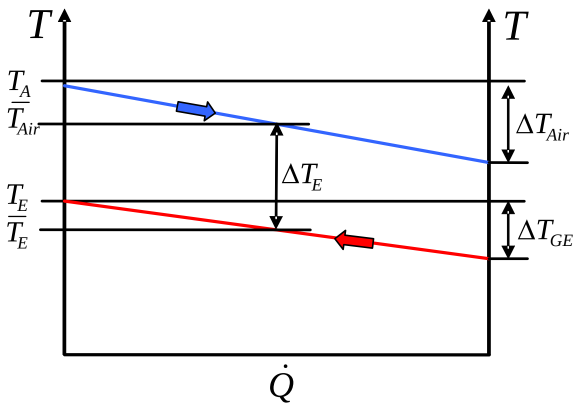

Fig. 5-1: $T,\dot{Q}$-diagram for the evaporator

b) For detailed calculations

Here, the vapour superheating in the evaporator unit is taken into account. As in section 4.3, the $T,\dot{Q}$-diagram is also subdivided into two sections in Fig. 5-2.

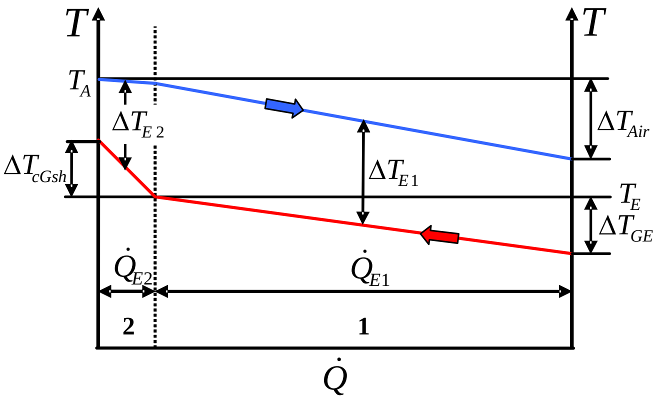

Fig. 5-2: $T,\dot{Q}$-diagram for the evaporator

In the first section, the working fluid is evaporated. In this case, a temperature glide ΔT_{GE} is assumed to occur. In the second section, the gaseous working fluid is superheated by ΔT_{cGsh}, depending on the setting of the expansion valve.

From section 4.3 the Eq. (131) to (134) are used:

$$\dot{Q}_E = \dot{m}_f \cdot (h_1 - h_4) \tag{131}$$

$$\dot{Q}_{E1} = \dot{m}_f \cdot r_E \cdot (1 - x_V) \tag{132}$$

$$\dot{Q}_{E2} = \dot{m}_f \cdot c_{pg} \cdot \Delta T_{cGsh} \tag{133}$$

$$\dot{Q}_E = \dot{Q}_{E1} + \dot{Q}_{E2} \tag{134}$$

The temperature gradients ΔT_{E1} and ΔT_{E2} adjust themselves such that the heat transfer equations for the two partial heat flows $\dot{Q}_{E1}$ and $\dot{Q}_{E2}$ are fulfilled in each section:

$$\dot{Q}_{E1} = k_{E1} \cdot A_{E1} \cdot \Delta T_{E1} \Rightarrow \Delta T_{E1} = \frac{\dot{Q}_{E1}}{k_{E1} \cdot A_{E1}} \tag{177}$$

$$\dot{Q}_{E2} = k_{E2} \cdot A_{E2} \cdot \Delta T_{E2} \Rightarrow \Delta T_{E2} = \frac{\dot{Q}_{E2}}{k_{E2} \cdot A_{E2}} \tag{178}$$

Here, the overall heat transfer coefficients are now to be appropriately determined according to geometry, configuration, fluid properties, flow velocities and phase change. For this, we refer to specialist literature [9].

For (fine tube) evaporators, the heat exchanger surface area A_E and the overall heat transfer coefficient k_E are, for example, *both referred to the outer side*. The total area of the evaporator is taken as A_E and thus the following is defined as an additional condition:

$$A_{E1} + A_{E2} = A_E \tag{179}$$

In most cases A_{E1} and A_{E2} are designed for the minimum ambient temperature $T_{A\,min}$ and the corresponding maximum *required* heating capacity $\dot{Q}_{max}^{*}$. At other ambient temperatures, the states regulate themselves so that the Eq. (131) to (134) and (177), (178) with the overall heat transfer coefficients k_{E1} and k_{E2} in each section are fulfilled. Further, the characteristics of the complete heat pump have an effect, in particular those associated with the working fluid mass flow provided by the compressor and the heat transmission properties of the condenser and injection system. Here it must be distinguished between whether the *generated* heating capacity is adjusted to meet the *required* heating capacity by switching on and off or by continuous power control. Carrying out such an operating analysis does not appear to be particularly worthwhile because quite a number of iterations are required. However, valuable insights result. It makes the analysis easier if one has good measurement results for different ambient and heating temperatures for typical heat pumps.

5.1.5 Compressor power

The compressor power provided to the fluid (internal compressor power) can be calculated using the working fluid mass flow according to Eq. (164):

$$P_i(T_E, T_C) = \dot{m}_f(T_E, T_C) \cdot (T_E + \Delta T_{cGsh}) \cdot c_{pg} \cdot \frac{1}{\eta_s(T_E, T_C)} \cdot \left(\left(\frac{p_C(T_C)}{p_E(T_E)} \right)^{\kappa} - 1 \right) \tag{180}$$

If a high level of accuracy is needed, the Eq. (180) should not be simplified further.

5.1.6 Generated heating capacity

The *generated* heating capacity $\dot{Q}_H$ is, under the assumption of negligible heat losses in the heat pump, the sum of the heat flow transferred in the evaporator (Eq. (167)) and the internal compressor power according to Eq. (180):

$$\dot{Q}_H(T_E, T_C) = \dot{Q}_E(T_E, T_C) + P_i(T_E, T_C) \tag{181}$$

5.1.7 Heating up the water for heating and resultant supply temperature

According to Eq. (181) for the intermittently *generated* heating capacity of heat pumps with on/off control, the heating-up of the heating-circuit water is given by:

$$\Delta T_{HW}(T_E, T_C) = \frac{\dot{Q}_H(T_E, T_C)}{\dot{m}_{HW} \cdot c_{pHW}} \tag{182}$$

Within the framework of this study, it is assumed that the return temperature of the heating water always corresponds to the return temperature defined by the heating curve of the building (cf. Fig. 1-9). Consequently, the return temperature T_{RT} is defined by the heating curve as a function of outdoor temperature. With the *generated* heating water temperature rise ΔT_{HW} as defined in Eq. (182), the *generated* supply temperature T_{SP} of the heating water is obtained:

$$T_{SP}(T_E, T_C, T_A) = T_{RT}(T_A) + \Delta T_{HW}(T_E, T_C) \tag{183}$$

The *generated* heating temperature T_H is thus:

$$T_H(T_E, T_C, T_A) = \frac{1}{2} \cdot \left(T_{RT}(T_A) + T_{SP}(T_E, T_C, T_A) \right) \tag{184}$$

5.1.8 Temperature gradients and condensation temperature

a) For rough calculations

For ascertaining the condensation temperature, the vapour superheating and the condensate subcooling are neglected. The temperature gradient in the condenser ΔT_C is calculated using:

$$\Delta T_C(T_E, T_C) = \frac{\dot{Q}_H(T_E, T_C)}{A_C \cdot k_C} \tag{185}$$

For the overall heat transfer coefficient k_C a standard value is used; if available, one determined from a series of experiments. It includes vapour saturation, condensation and subcooling.

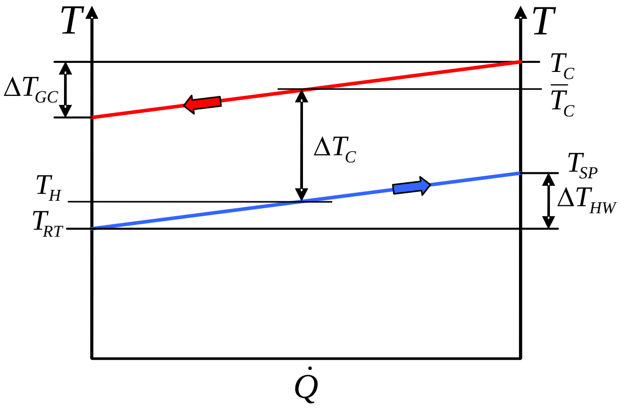

Fig. 5-3: $T,\dot{Q}$ -diagram for the condenser

The condensation temperature T_C is determined using the $T,\dot{Q}$ -diagram in Fig. 5-3:

$$T_C = \left(T_{RT} + \frac{1}{2} \cdot \Delta T_{HW}\right) + \Delta T_C + \frac{1}{2} \cdot \Delta T_{GC} \tag{186}$$

Further, the following applies for the average condensation temperature $\overline{T}_C$:

$$\overline{T}_C = T_C - \frac{1}{2} \Delta T_{GC} \tag{187}$$

If the working fluid has a temperature glide during condensation, the condensation temperature always refers to the dew-point temperature of the mixture, as for evaporation (cf. Appendix A8).

b) For detailed calculations

In order to take vapour superheating and condensate subcooling into consideration, the $T,\dot{Q}$-diagram (Fig. 5-4) is divided into three sections: Saturation of superheated steam (section 1), condensation (section 2) and subcooling of the condensate (section 3).

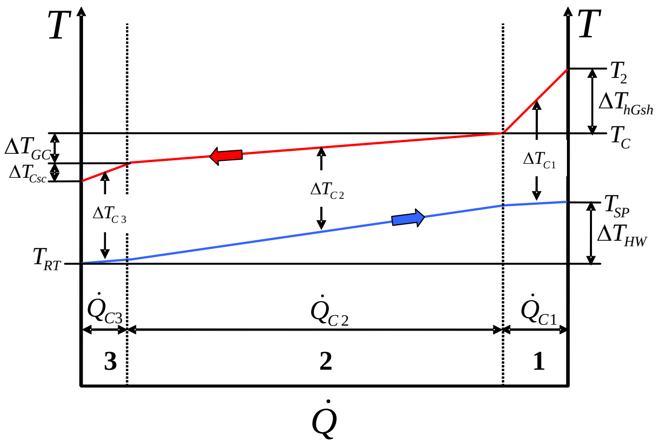

Fig. 5-4: $T,\dot{Q}$-diagram for the condenser

From section 4.4, the Eq. (144) to (148) are used:

$$\dot{Q}_C = \dot{m}_f \cdot (h_2 - h_3) \tag{144}$$

$$\dot{Q}_{C1} = \dot{m}_f \cdot c_{pg} \cdot \Delta T_{hGsh} \tag{145}$$

$$\dot{Q}_{C2} = \dot{m}_f \cdot r_C \tag{146}$$

$$\dot{Q}_{C3} = \dot{m}_f \cdot c_{pl} \cdot \Delta T_{Csc} \tag{147}$$

$$\dot{Q}_C = \dot{Q}_{C1} + \dot{Q}_{C2} + \dot{Q}_{C3} \tag{148}$$

As for the evaporator, heat flow equations for the three heat flows $\dot{Q}_{C1}$, $\dot{Q}_{C2}$ and $\dot{Q}_{C3}$ must be fulfilled:

$$\dot{Q}_{C1} = k_{C1} \cdot A_{C1} \cdot \Delta T_{C1} \Rightarrow \Delta T_{C1} = \frac{\dot{Q}_{C1}}{k_{C1} \cdot A_{C1}} \tag{188}$$

$$\dot{Q}_{C2} = k_{C2} \cdot A_{C2} \cdot \Delta T_{C2} \Rightarrow \Delta T_{C2} = \frac{\dot{Q}_{C2}}{k_{C2} \cdot A_{C2}} \tag{189}$$

$$\dot{Q}_{C3} = k_{C3} \cdot A_{C3} \cdot \Delta T_{C3} \Rightarrow \Delta T_{C3} = \frac{\dot{Q}_{C3}}{k_{C3} \cdot A_{C3}} \tag{190}$$

Here, once more, overall heat transfer coefficients are also to be determined according to geometry, configuration, fluid properties and flow velocities including possible phase changes. For this, we refer to specialist literature [9].

For the transfer of the three partial heat flows, the total heat exchanger surface-area A_C in the condenser is available:

$$A_{C1} + A_{C2} + A_{C3} = A_C \tag{191}$$

The calculation of the self-regulating condensation temperature proves to be difficult here. In the case of part-load, the variables $\dot{Q}_{Ci}$, T_{Ci} and ΔT_{Ci} for the sections i=1, 2 and 3 in the condenser modify themselves as a result of the working fluid flow $\dot{m}_f$ and the overall heat transfer coefficient k_{Ci}. The analysis can be a little more extensive here than in the case of the evaporator as the heat flows $\dot{Q}_{C1}$ and $\dot{Q}_{C3}$ are not or possibly only partially transmitted to separate heat exchanger surfaces. In older publications, it is said that superheat is removed on "dry surfaces" and condensation occurs afterwards. Today, however, it is known that a large part of vapour superheat or even the whole superheat is removed on the outer surface of the condensate film, depending on the particular heat transfer coefficient of the vapour, which can be influenced by geometrically guiding the flow. Fig. 5-5 shows the temperature profile in the condenser at right angles to the flow of the condensate and supereated vapour. Condensate subcooling mostly occurs only within the condensate film and is, therefore, low.

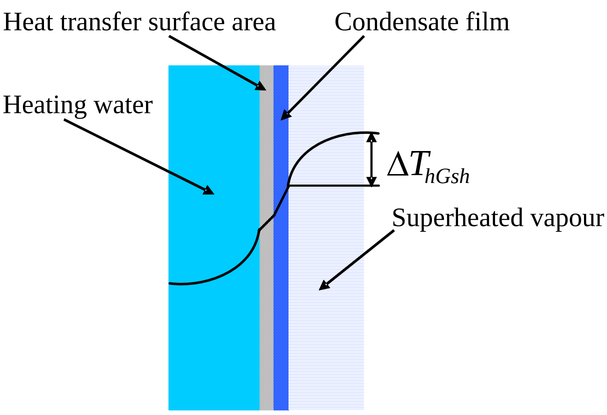

Fig. 5-5: Temperature profile in the condenser at right angles to flow of the condensate and the superheated vapour (shown schematically)

5.2 Required and generated heating capacity

5.2.1 Required heating capacity

The heating capacity *required* by the building is dependent on the ambient temperature T_A, the average *required* room temperature T_R and the thermal insulation. The difference between these temperatures $T_R - T_A$ represents the driving temperature gradient across the building envelope. In this way, the heat flows out to the environment. The *required* heating capacity $\dot{Q}_H^*$ is thus proportional (when fixed temperature differences prevail) to this temperature gradient (cf. section 1.4 also):

$$\dot{Q}_H^* = A_R \cdot k_R \cdot (T_R - T_A) \tag{192}$$

Dependent on thermal insulation of the building and the heat delivery system, the *heating curve* for the building can now be calculated. The heating curve determines the *required* supply and return temperatures of the heating water, i.e. the *required* heating temperature, as a function of the ambient temperature for a heating water mass flow $\dot{m}_{HW}$, so that the *required* heating capacity is always guaranteed as a function of the ambient temperature (cf. Fig. 5-6):

$$\dot{Q}_H^*(T_A) = \dot{m}_{HW} \cdot c_{pHW} \cdot \left(T_{SP}^*(T_A) - T_{RT}^*(T_A)\right) \tag{193}$$

In this case, the following applies for the heating temperature T_H^* continuously *required* by the building:

$$T_H^*(T_A) = \frac{1}{2} \cdot \left(T_{RT}^*(T_A) + T_{SP}^*(T_A)\right) \tag{194}$$

The resultant *generated* supply and heating temperatures T_{SP} and T_H adjust themselves correspondingly in accordance with the operating point.

Fig. 5-6 shows the heating curve of a single-family house in the Swiss central plain. The *required* heating capacity resulting from the following heating curve is shown in Fig. 5-9. At ambient temperatures above a pre-set *heating limit temperature,* the heat pump is switched off.

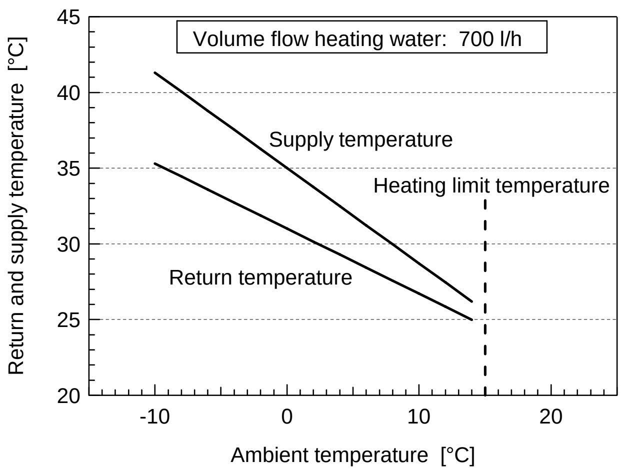

Fig. 5-6: Heating curve of a single-family house in the Swiss central plain

The simulations of operating characteristics presented below are valid for an air/water heat pump with 5.4 kW nominal heating capacity at $\vartheta_{A\,min} = -10°C$ with on/off control. Detailed specifications of this heat pump can be found in appendix A7. The simulations can be carried out in a simplified manner in accordance with the program shown in appendix A6. The simulations presented in this study were carried out, however, in great detail using a simulation program for air/water heat pumps which was developed and documented in LOREF [5].

5.2.2 Generated heating capacity

Using the process equations quoted in section 5.1, the *generated* heating capacity by the air/water heat pump specified above is calculated as a function of the ambient temperature and shown in Fig. 5-7.

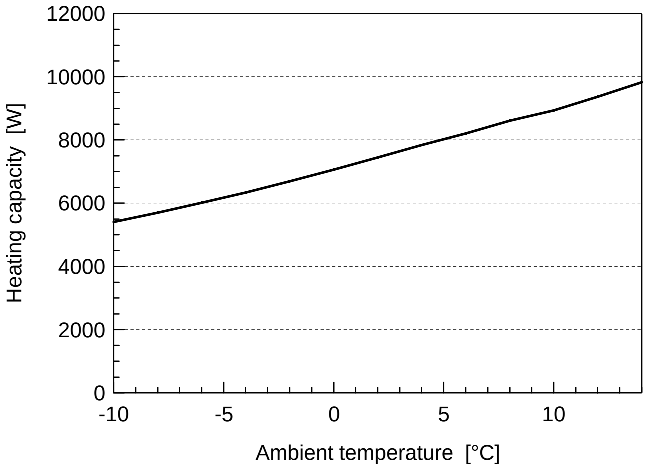

Fig. 5-7: Generated heating capacity as a function of ambient temperature

First of all, it should be pointed out once more that the *generated* heating capacity increases with higher ambient temperatures. The reason for this is the unfavourable characteristic of the constant rotation speed compressor: The *working fluid mass flow* (Eq. (164)) increases with increasing ambient temperature and, therefore, the *generated* heating capacity increases too. Fig. 5-8 shows the curve for the *working fluid mass flow* against ambient temperature.

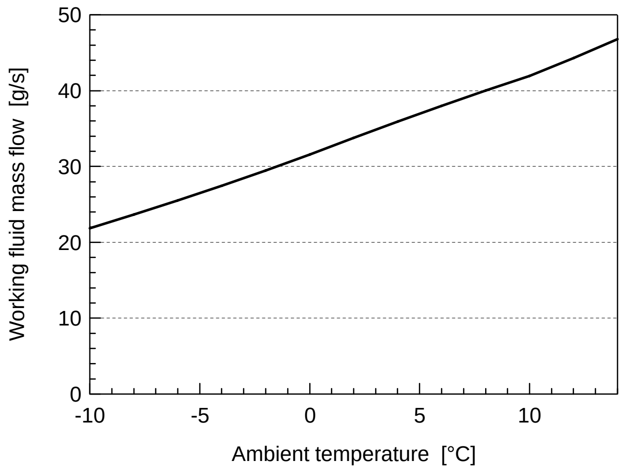

Fig. 5-8: Working fluid mass flow as a function of the ambient temperature

This means that the *generated* heating capacity is approximately proportional to the *working fluid mass flow*.

5.2.3 Discrepancy between required and generated heating capacities

Fig. 5-9 shows the curves for of the *generated* and the *required* heating capacity as a function of ambient temperature.

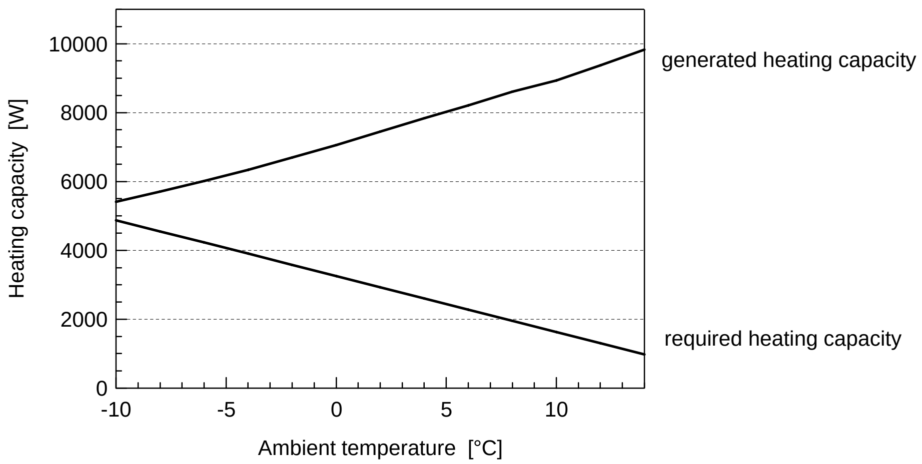

Fig. 5-9: Generated and required heating capacities as a function of ambient temperature

The discrepancy between the two curves means that, as a consequence, traditional air/water heat pumps operate in a cyclic (on/off) manner, which leads to bad part-load efficiencies, seasonal performance factors and low annual average exergetic efficiencies.

With increasing outside temperature, moreover, the *generated* heating temperatures are, as a result of this discrepancy, higher than those *required.* This results in additional exergy losses. The temperature lift is also influenced in an adverse way due to the *generated* heating temperatures which are too high - cf. Eq. (102). Fig. 5-10 shows the continuously *required* and the heating temperatures intermittently *generated* by the air/water heat pump specified in appendix A7 as a function of ambient temperature, which is operated in on/off mode.

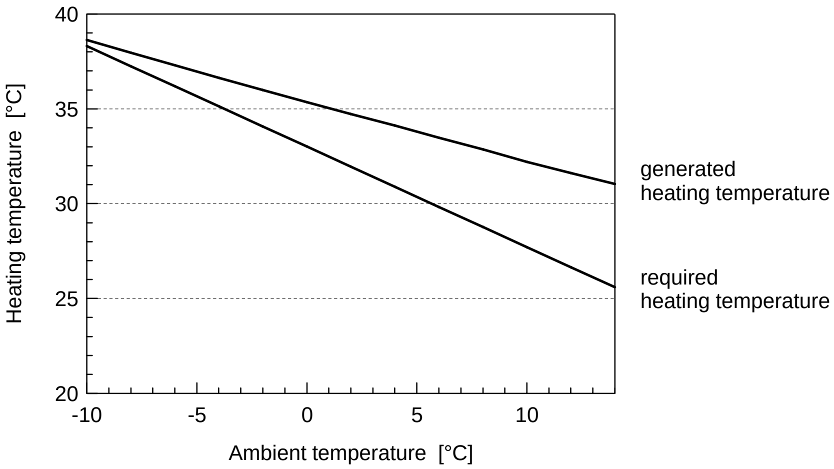

Fig. 5-10: Generated and required heating temperature for an air/water heat pump with on/off control

5.3 Resulting operating characteristic

As a result of the *generated* heating capacity of the air/water heat pump with on/off-control shown in Fig. 5-9, permanently increasing temperature gradients can be noted in the heat exchangers for increasing ambient temperatures - cf. Fig. 5-11.

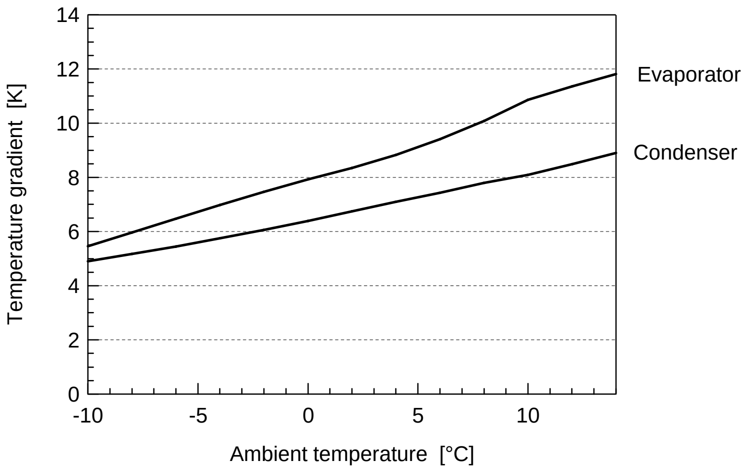

Fig. 5-11: Resulting average temperature gradients in the evaporator and condenser of the air/water heat pump with on/off control

The increasing temperature gradients in the evaporator and condenser lead to an increase of temperature lift ΔT_{Lift} (cf. Eq. (102)). This has further negative influences on the heat pump process.

The temperature lift produced by the heat pump (from which the pressure relationship p_K / p_V is calculated that must be overcome) is shown in Fig. 5-12 as a function of the ambient temperature.

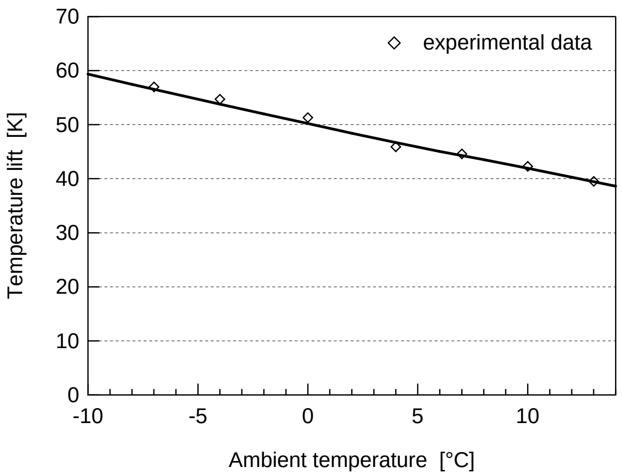

Fig. 5-12: Temperature lift of a heat pump with on/off control

The evaporation and condensation temperatures that arise dependent on ambient temperature are shown in Fig. 5-13. In addition to the simulated temperatures, the condensation and evaporation temperatures measured on the experimental heat pump are shown in Fig. 5-13.

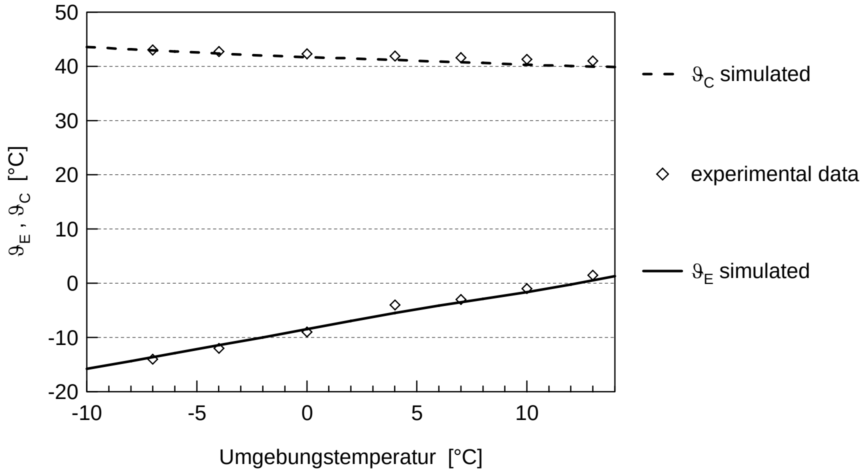

Fig. 5-13: Evaporation and condensation temperature of an air/water heat pump with on/off control

The difference between the condensation and evaporation temperatures represents the temperature lift to be provided by the heat pump (cf. Fig. Fig. 5-12).

6 Results of the exergy analysis for air/water heat pumps with on/off control - without drive losses

In the previous chapters, a basis for exergy assessments has been developed and analytical interpretations have been made concerning the exergy losses in the various sub-processes. There now follows the representation and discussion of numerically determined results. These are valid for an air/water heat pump with 5.4 kW nominal heating capacity at ambient temperature of -10°C as specified in appendix A7. Further, this heat pump was analysed experimentally. The influence of frost formation on the operating characteristic over time and the corresponding effects on exergetic efficiency will not be dealt with. In this way important findings can already be obtained.

6.1 Interpretation of exergy losses in the sub-processes

In the following, the exergy losses of the sub-processes which were derived in chapter 4 are in each case represented graphically and interpreted. The most important findings will be clearly summarised in section 6.4.

The exergy losses in the compressor and the expansion valve are caused by dissipative drops of pressure in the flow of the working fluid. On the other hand, the exergy losses during heat transfer in evaporator and condenser do not originate in the working fluid but on account of the temperature gradients ΔT_E and ΔT_C required for heat transfer. Pressure losses due to flow in piping and fittings as well as in the evaporator and condenser on the working fluid side are not considered. Also, the drive losses of the compressor as well as the fan power to be provided in the case of forced convection in the evaporator are not considered here.

6.1.1 Exergy loss flow and exergy loss ratios

The development engineer is interested both in the magnitude of the individual exergy loss flows as well as in comparisons made between them. The *amount of exergy loss flow* in relation to ambient temperature is calculated from simulations for the four sub-processes of the specified air/water heat pump and shown in separate diagrams. Further, an *exergy loss ratio* (i.e. exergy loss flow in reference to the *internal compressor power* P_i) is also shown in the same diagram for each case. The reason for this is so that one can directly follow the subtractive effect on *exergetic efficiency*. This can indeed be calculated from the following exergy loss ratios:

$$\eta_{exe} = 1 - \frac{\dot{E}_{LCp}}{P_i} - \frac{\dot{E}_{LC}}{P_i} - \frac{\dot{E}_{LEx}}{P_i} - \frac{\dot{E}_{LE}}{P_i} \tag{195}$$

6.1.2 Exergy loss in the compressor

The influence on exergy loss flow in an adiabatic, single-stage compressor can be calculated using Eq. (115):

$$\dot{E}_{LCp} \approx \dot{Q}_E \cdot \frac{\Delta T_{Lift}}{T_E + \Delta T_{Lift}} \cdot \left(\frac{1}{\eta_s} - 1 \right) \approx \dot{Q}_E \cdot \frac{1}{COP_{rev\,i}} \cdot \left(\frac{1}{\eta_s} - 1 \right) \tag{115}$$

It is, of course, proportional to the heat flow $\dot{Q}_E$ that is transferred from the environment to the working fluid in the evaporator. This increases with increasing ambient temperature as does the *generated* heating capacity, too (cf. Fig. 5-7). Further, the exergy loss flow in the compressor is approximately proportional to the temperature lift of the heat pump.

The following applies to the temperature lift according to Eq. (102):

$$\Delta T_{Lift} = T_C - T_E = \left(T_H^* - T_A\right) + \Delta T_H + \Delta T_E + \Delta T_C = \Delta T_{Lift\,ideal} + \Delta T_H + \Delta T_E + \Delta T_C \tag{102}$$

In Fig. 6-1 a) the curves for the *exergy loss flow* are shown for scroll compressors and reciprocating compressors. As opposed to the scroll compressor, the reciprocating compressor becomes increasingly more unfavourable with increasing ambient temperature. This has to do with η_s and λ. The comparison of the *exergy loss ratio* in Fig. 6-1 b) is interesting: That of the reciprocating compressor sinks with increasing ambient temperature from 0.28 to 0.27 slightly. For the scroll compressor, it is higher at low air temperatures but, however, sinks from 0.38 to 0.21.

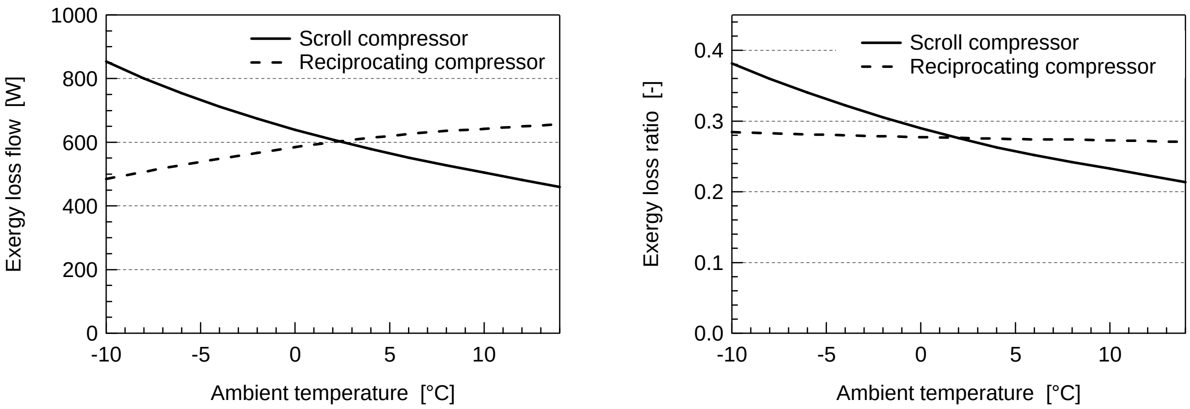

a): Exergy loss flow in the compressor *b): Exergy loss ratio in the compressor*

Fig. 6-1: Exergy loss flow and exergy loss ratio in the compressor with scroll and reciprocating compressors for an air/water heat pump with on/off control

More precise information on the compressor models employed and their characteristics are given in (Appendix A1).

6.1.3 Exergy loss in the expansion valve

The exergy loss flow in the expansion valve is determined by Eq. (128):

$$\dot{E}_{LEx} \approx \dot{m}_f \cdot c_{pl} \cdot \frac{1}{2} \cdot \left(\frac{\Delta T_{Lift}^{\,2}}{T_E + \Delta T_{Lift}} \right) \approx \dot{m}_f \cdot c_{pl} \cdot \frac{\Delta T_{Lift}}{2 \cdot COP_{rev\,i}} \tag{128}$$

It is approximately proportional to the temperature lift. The more exact equation (Eq. (125)) shows that by increasing condensate subcooling ΔT_{Csc} the exergy losses in the expansion valve can be reduced:

$$e_{LEx} = T_A \cdot c_{pl} \cdot \left[\ln\left(\frac{T_E}{T_E + \Delta T_{Lift} - \Delta T_{Csc}} \right) + \frac{\Delta T_{Lift} - \Delta T_{Csc}}{T_E} \right] \tag{125}$$

Also, when reducing pressure by throttling, the temperature gradients ΔT_E, ΔT_C and ΔT_H for heat transfer increase the temperature lift (cf. Eq. (102)) and, therefore, the exergy loss in the expansion valve too.

Fig. 6-2 shows the curves for the *exergy loss flow* and the *exergy loss ratio* in the expansion valve.

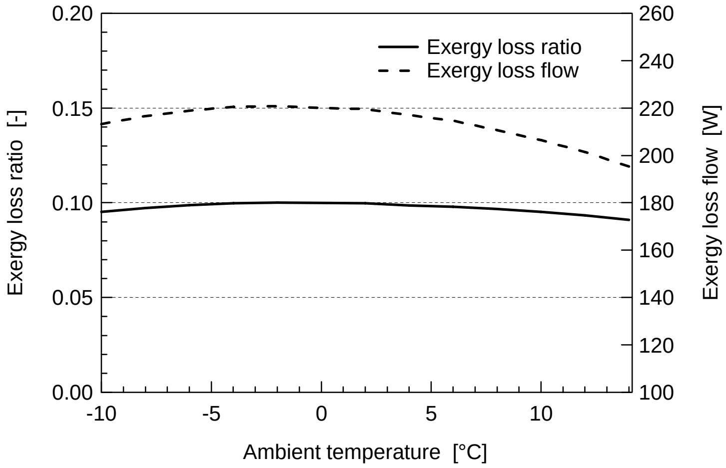

Fig. 6-2: Exergy loss flow and exergy loss ratio in the expansion valve of an air/water heat pump with on/off control

The exergy loss flow increases from -15°C to 0°C slightly and, afterwards, drops more rapidly until 15°C is reached. This can be explained by the combination of falling temperature lift (cf. Fig. 5-12) and increasing working fluid mass flow as atmospheric temperatures increase (cf. Fig. 5-8).

Here and in the following analyses the exergy loss ratio referrs to the scroll compressor only. It is almost constant over the whole temperature range and, at around 10% within relevant bounds.

6.1.4 Exergy loss in the evaporator

Two exergy loss components in the evaporator are presented in chapter 4 and, by means of a numeric example, it is shown that the part due to vapour superheating is small. It is sufficient by far to analyse the exergy loss flow in the evaporator with Eq. (77):

$$\dot{E}_{LE} = \dot{Q}_E \cdot T_A \cdot \frac{\Delta T_E}{\overline{T}_E \cdot \left(\overline{T}_E + \Delta T_E\right)} \approx \dot{Q}_E \cdot T_A \cdot \frac{\Delta T_E}{\overline{T}_E^{\,2}} \approx \dot{Q}_E \cdot \frac{\Delta T_E}{T_A} \tag{77}$$

The result is clear; the exergy loss flow in the evaporator is proportional to the heat flow as well as approximately proportional to the temperature gradient ΔT_E for heat transfer.

The curves for the *exergy loss flow* and *exergy loss ratio* are shown in Fig. 6-3 against ambient temperature. Both increase quite progressively with increasing ambient temperature. While the *internal exergy losses* (compressor and expansion valve) clearly declines with increasing outside temperature, the exergy loss caused by heat transfer in the evaporator increase strongly. The consequences of this are looked at in section 6.3. The cause of this behaviour is, once more, the unfavourable characteristic of the heat pump's constant speed compressor with on/of control (cf. section 5.2). Since the exergy loss of vapour superheating is very low, it is not shown separately.

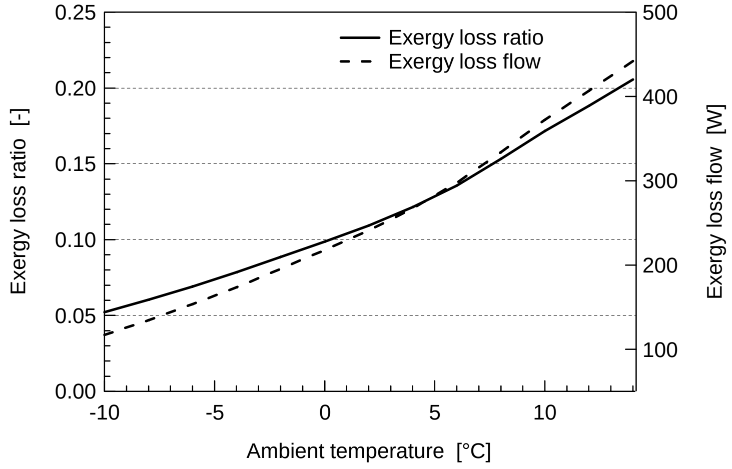

Fig. 6-3: Exergy loss flow and exergy loss ratio in the evaporator of an air/water heat pump with on/off control

6.1.5 Exergy loss in the condenser

For the discussion of the exergy loss in the condenser, the simple Eq. (67) suffices here too; i.e. without subdivision into vapour saturation, condensation and condensate subcooling:

$$\dot{E}_{LC} = \dot{Q}_H \cdot T_A \cdot \frac{\Delta T_C}{T_H \cdot \overline{T}_C} = \dot{Q}_H \cdot T_A \cdot \frac{\Delta T_C}{T_H \cdot \left(T_H + \Delta T_C\right)} \approx \dot{Q}_H \cdot T_A \cdot \frac{\Delta T_C}{T_H^{\ 2}} \tag{67}$$

$\dot{E}_{LC}$ is proportional to the *generated* heating capacity $\dot{Q}_H$ (including vapour saturation and condensate subcooling) as well as being proportional to the temperature gradient ΔT_C for heat transfer. It is further approximately inversely proportional to the square of the *generated* heating temperature T_H. ΔT_C is calculated using Eq. (155). The curves for the *exergy loss flow* and *exergy loss ratio* in the condenser are shown in Fig. 6-4 once more against ambient temperature. Both curves are similar to those of the evaporator (cf. Fig. 6-3); They are, however, smaller, this because of lower temperature gradients ΔT_C (cf. Fig. 5-11).

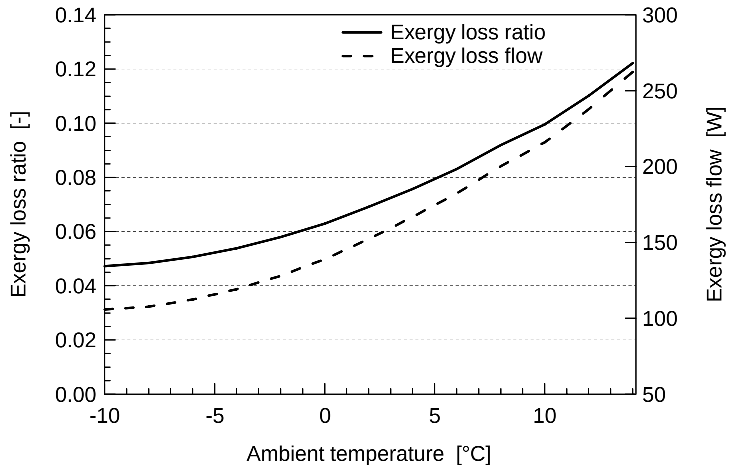

Fig. 6-4: Exergy loss flow and exergy loss ratio in the condenser of an air/water heat pump with on/off control

6.1.6 Exergy loss in the heat distribution system

The exergy loss caused by the non-steady-state characteristics of on/off controlled heat pumps for *required* and *generated* heating temperature T_H and T_H^* is modelled in section 3.3.1. This loss is calculated using Eq. (95) as an average exergy loss flow $\dot{E}_{LHS}$ during heat pump operation $(t_1 - t_0)$ and, as far as the *continuously required* heating capacity is concerned, calculated as $\dot{E}_{LHS}^*$ using Eq. (94). The *exergy loss flows* $\dot{E}_{LHS}^*$ and $\dot{E}_{LHS}$ are shown in Fig. 6-5 along with the *exergy loss ratio* $\dot{E}_{LHS} / P_i$ as a function of ambient temperature.

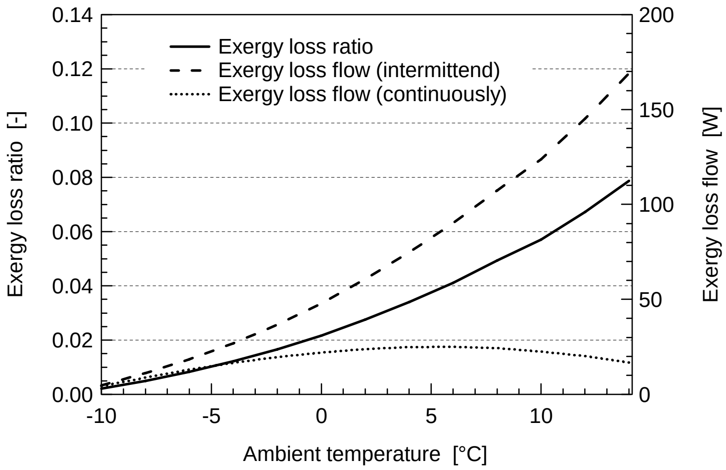

Fig. 6-5: Exergy loss flow and exergy loss ratio for the heat distribution system of an on/off controlled air/water heat pump

The continuously resulting exergy loss flow $\dot{E}_{LHS}^*$ increases from around 5 W at -10°C to 25 W at 5°C and it subsequently falls again to around 16 W. The exergy loss ratio, however, increases quite progressively with increasing outside temperature: From almost zero at the design point to around 8% at 15°C. The effect on the *external exergetic efficiency* of the heat pump as far as *the required heating temperature* is *concerned* is therefore also noticeable (cf. section 6.3).

6.1.7 Exergy loss in the heat delivery system

The exergy loss flow continuously resulting in the heat delivery system (heat transfer to the room) $\dot{E}_{LR}^{*}$ is calculated using Eq. (98) and the intermittently resulting $\dot{E}_{LR}$ as far as heat pump operation is concerned $(t_1 - t_0)$ is calculated using Eq. (99). Curves for the *exergy loss flows* $\dot{E}_{LR}^{*}$ and $\dot{E}_{LR}$ are shown in Fig. 6-6 along with the *exergy loss ratio* $\dot{E}_{LR} / P_i$ as a function of ambient temperature.

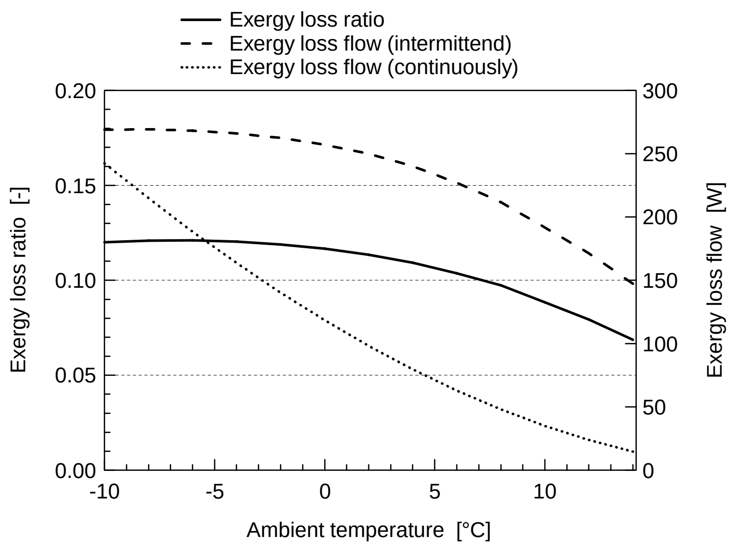

Fig. 6-6: Exergy loss flow and exergy loss ratio in the heat delivery system of an air/water heat pump with on/off control

The continuously exergy loss flow in the heat delivery system decreases with increasing outdoor temperature from around 240 W at -10°C to 20 W at 14°C. This is caused by the *required* heating temperature T_H^{*} decreasing with increasing ambient temperature (cf. Fig. 5-10) as well as the decreasing *required* heat flow $\dot{Q}_H^{*}$ (cf. Fig. 5-9). The exergy loss ratio decreases with increasing outside temperature from around 12% at -10°C to 7% at 14°C.

6.1.8 Comparison of the exergy loss ratios

In Fig. 6-7, the curves of the *exergy loss ratios* are compared. They are referred to the internal compressor power P_i of a heat pump with a scroll compressor (in accordance with the specification in appendix A7).

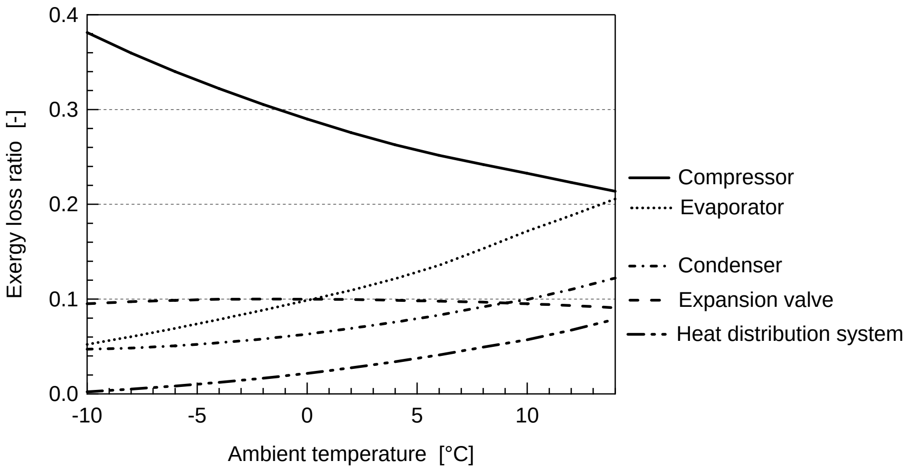

Fig. 6-7: Overview of the exergy loss ratios of an air/water heat pump with on/off control

The exergy loss ratio of the compressor is quite predominant. At outdoor temperatures below 0°C it is even four to eight times as high as the other three sub-processes. The exergy loss ratio is 38% at -10°C and then decreases to 22% at 15°C - but is still much higher than the other losses. Here, an important potential for making improvements in the co-operation between manufacturers of heat pumps and compressors still exists.

The exergy loss ratios for the heat transfer in the evaporator and condenser at -10°C is only 5%. These could no doubt be halved again by using a larger heat exchanger surface and, in addition, with the use of electronically controlled expansion valves. Decisively dramatic, however, is the increase in the exergy loss ratio: at 14°C it is 13% in the condenser and even 20% in the evaporator – still without frost formation. This situation will be dealt with separately in chapter 7.

Finally, the exergy loss ratio of the expansion valve remains: it is always around 10% and is thus comparatively high. For heat pumps that are designed for low temperature lift, the exergy loss flow and exergy loss ratio must become more favourable as $\dot{E}_{LEx} \sim \Delta T_{Lift}$.

Also, the exergy loss ratio in the heat distribution system increases quasi progressively with increasing outdoor temperature: from 0% at -10°C to 8% at 14°C.

6.2 Internal exergetic efficiency

The *internal exergetic efficiency* is defined in section 3.2. It is used to judge the thermal efficiency of the heat pump's working fluid circuit. It considers the total temperature lift and therefore includes the temperature gradients in the evaporator and condenser but not, however, their exergy losses. Consequently, the *internal exergetic efficiency* is influenced by the exergy losses in the expansion valve and compressor only in accordance with the pressure ratio corresponding to the total temperature lift. Pressure losses in piping and fittings are not considered here. The electrical and mechanical efficiencies of the compressor as well as the fan power are not considered in this section. Thus, from Eq. (50):

$$\eta_{exi} = 1 - \frac{\dot{E}_{LCp} + \dot{E}_{LEx}}{P_i} \tag{50}$$

In Fig. 6-8 a comparison is made between the internal exergetic efficiency of an air/water heat pump (as specified in appendix A7) when operated with scroll or reciprocating compressors. The curves show that the *internal exergetic efficiency* increases somewhat with increasing ambient temperature. The reason for this is the decrease of temperature lift (cf. Fig. 5-12). With a scroll compressor, it increases from 52% at -10°C to 70% at 14°C; in the case of the reciprocating compressor, it increases from 60% to 64%.

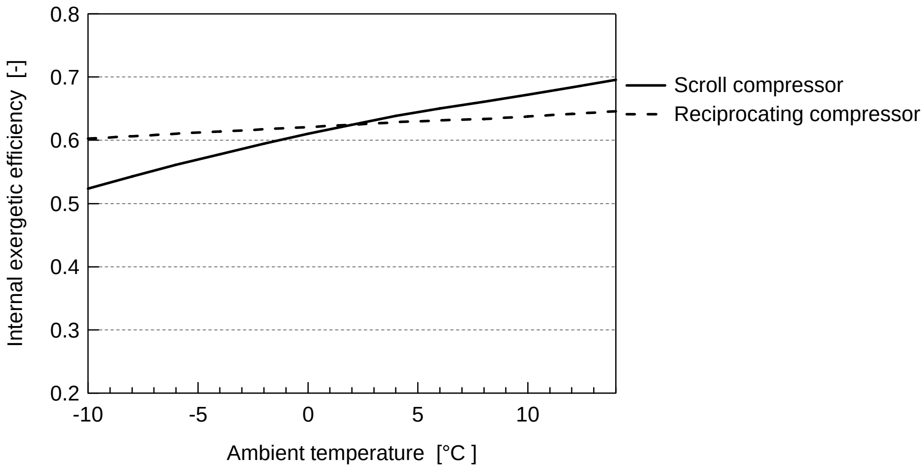

Fig. 6-8: Internal exergetic efficiency of an air/water heat pump with on/off control when using scroll or reciprocating compressors

6.3 External exergetic efficiency and coefficient of performance

In section 3.1, three *external exergetic efficiencies* are defined for heat pumps with on/off control. These consider the exergy losses caused by heat transfer in addition to the *internal exergetic efficiency.*

In this section, the mechanical and electrical efficiencies of the compressor, the fan power and the pressure losses in fittings and piping will also not yet be included. The following was derived for the *external exergetic efficiency of the generated heating temperature of the heat pump*:

$$\eta_{exe} = 1 - \frac{\dot{E}_{LCp} + \dot{E}_{LEx} + \dot{E}_{LE} + \dot{E}_{LC}}{P_i} \qquad (51)$$

Fig. 6-3 and Fig. 6-4, show that the exergy losses in the evaporator and condenser increase quasi-progressively with increasing ambient temperature. As can be seen in Fig. 6-9, this results in the curves for *external exergetic efficiency of the generated heating temperature* dropping with increasing ambient temperature. The difference between scroll and reciprocating compressors already dwindles away.

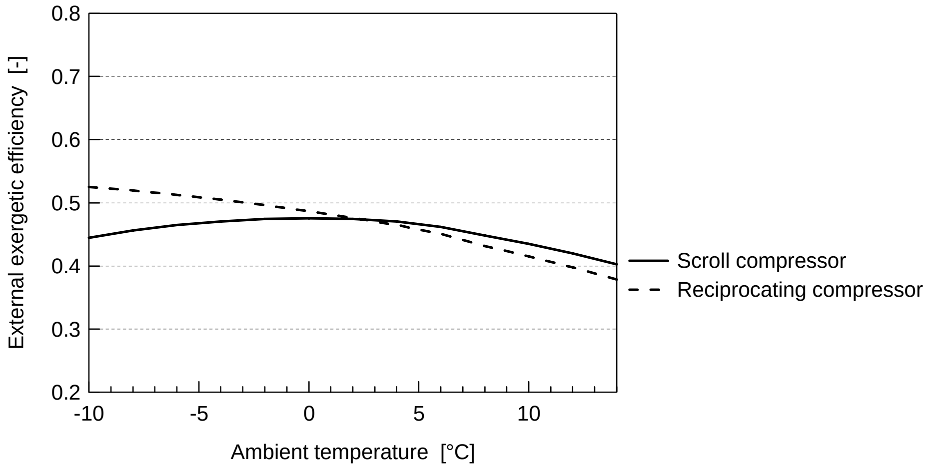

Fig. 6-9: External exergetic efficiency of the generated heating temperature of an air/water heat pump with on/off control for scroll and reciprocating compressors

Next, the exergy loss in the heat distribution system, which increases with increasing outdoor temperature, is added on. For this purpose, the *external exergetic efficiency of the required heating temperature was* defined. It is calculated using:

$$\eta_{exe}^{*} = \frac{1}{1 + \frac{\dot{E}_{LCp} + \dot{E}_{LEx} + \dot{E}_{LE} + \dot{E}_{LC} + \upsilon \cdot \dot{E}_{LHS}^{*}}{\dot{E}_{Q_H}}} = 1 - \frac{\dot{E}_{LCp} + \dot{E}_{LEx} + \dot{E}_{LE} + \dot{E}_{LC} + \upsilon \cdot \dot{E}_{LHS}^{*}}{P_i} \qquad (96)$$

Fig. 6-10 shows the curves against ambient temperature, once more for scroll and reciprocating compressors.

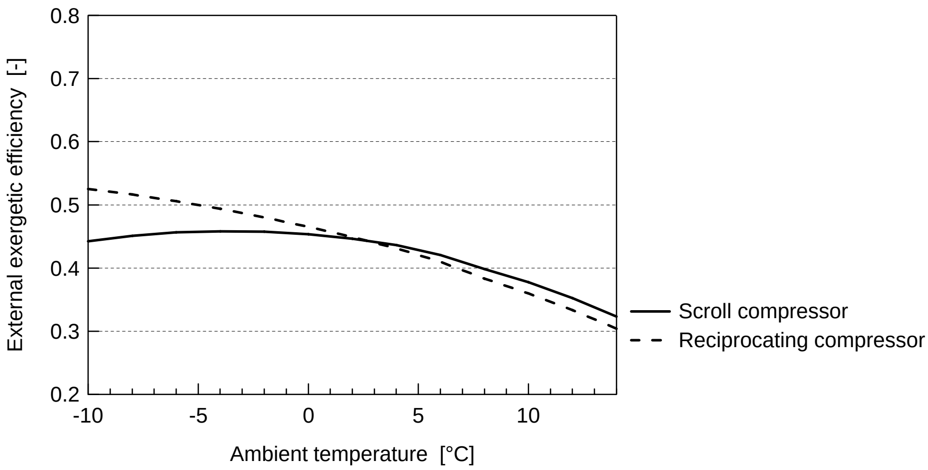

Fig. 6-10: External exergetic efficiency of the required heating temperature of an air/water heat pump with on/off control for scroll and reciprocating compressors

The *external exergetic efficiency of the required heating temperature* falls with increasing outdoor temperature even more strongly than the *external exergetic efficiency of the generated heating temperature*.

Which compressor is more suitable for the air/water heat pump with on/off control specified (in appendix A7) can only be judged on the basis of annual mean values, i.e. the *seasonal performance factor* and the *annual average exergetic efficiency.*

The curves for the *coefficients of performance* of the air/water heat pump are shown in Fig. 6-11 for scroll and reciprocating compressors, plotted against ambient temperature; this without taking the drive losses of the compressor into account and without fan, i.e.:

$$COP = \frac{\dot{Q}_H}{P_i} \tag{196}$$

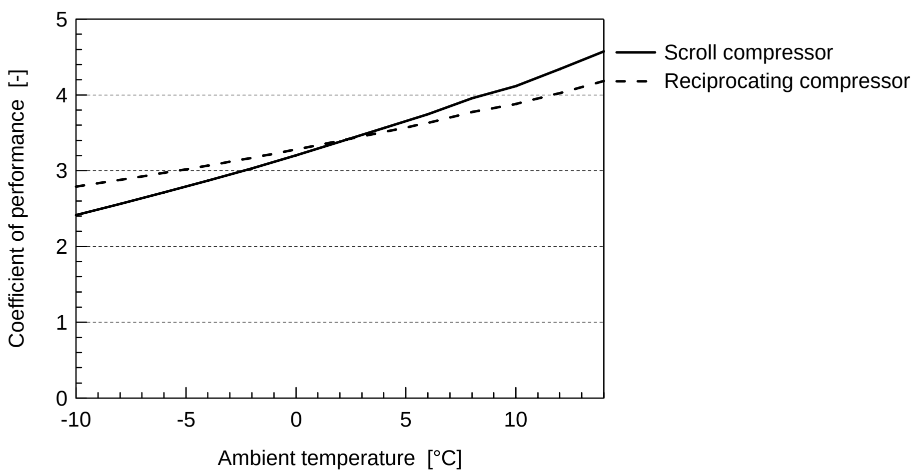

Fig. 6-11: Coefficient of performance of an air/water heat pump with on/off control for scroll and reciprocating compressors

The *coefficient of performance* at low outside temperatures is lower for a scroll compressor than for a reciprocating compressor; when compared with the reciprocating compressor, however, it gets increasingly better with increasing outdoor temperature.

Tab. 6-1 shows the calculated *seasonal performance factor* for an air/water heat pump with on/off control (as specified in appendix A7) for scroll and reciprocating compressors - once more without the drive losses of the compressor and fan power and also without the influence of frost formation and the periodic defrosting necessary. The calculation of the seasonal performance factor as well as the annual average exergetic efficiency is carried out according to the method proposed by v. Boeck [6] by using the cumulative distribution function of ambient temperature represented in Fig. 1-3 along with the heat pump operation ratio according to Eq. (17). Here, the scroll compressor has slightly better values. For somewhat warmer climatic conditions, it is superior for use in air/water heat pumps.

Compressor model	Scroll compressor	Reciprocating compressor
Seasonal performance factor [-]	3.49	3.45

Tab. 6-1: Seasonal performance factor of an air/water heat pump with on/off control for scroll and reciprocating compressors without drive losses of compressor and without fan power

6.4 Findings

The most important findings from sections 6.1 to 6.3 are briefly summarised below.

- The exergy losses of all four sub-processes of the air/water heat pump with on/off control are adversely influenced by the temperature gradients ΔT_E and ΔT_C required for heat transfer as well as by the discrepancy between *required* and *generated* heating temperatures ΔT_H.
- The temperature gradients ΔT_E and ΔT_C have a direct influence on the exergy losses in evaporator and condenser. They also have an indirect effect on the expansion valve and the compressor.
- The temperature gradients ΔT_E and ΔT_C in the evaporator and condenser that increase with increasing ambient temperature and also ΔT_H in the heat distribution system are caused by the discrepancy between *required* and *generated* heating capacities.
- The unfavourable operating characteristics of on/off controlled air/water heat pumps (which are driven with a constant speed compressor) are the cause for *generated* heating capacities that increase with increasing ambient temperature as well as for *generated* heating temperatures that are too high.
- The air/water heat pump process can be clearly improved by the *reduction of the temperature gradients* in the evaporator and condenser as well as by adaptation of the *generated* heating temperature to the *required* heating temperature.
- By reducing the *required* supply temperature, the temperature gradient ΔT_R, the *required* heating temperature, the temperature lift and, therefore, the exergy losses in the compressor, expansion valve and the heat delivery system can be reduced. As a result, the *internal exergetic efficiency* as well as the *external exergetic efficiency of heating systems using heat pumps* can be improved.
- The further development of compressors will be worthwhile because the exergy loss ratio in the compressor is high.

7 The air/water heat pump with continuous power control

In the previous chapter, it is often mentioned that the efficiency of the heat pump can be especially increased by using *continuous power control*: For it, the rotational speed of the compressor should correlate to outdoor temperature. The various changes in heating requirements and in the state of the outdoor air occur slowly (in most cases), so the heat pump process can at least be considered as being quasi steady state. During ice and frost formation on the fins of the evaporator, process changes occur more rapidly, but it is still satisfactory to analyse the behaviour as being steady-state. Corrections will no doubt be required for defrosting time and defrosting energy.

7.1 Adapt generated heating capacity continuously

In chapter 6 it became clear that improvements in the exergetic efficiency of the air/water heat pump can be achieved by a reduction of the temperature gradients for heat transfer in evaporator and condenser in accordance with avoiding any discrepancy between *required* and *generated* heating temperatures. The cause for these increasingly large temperature gradients is the unfavourable operating characteristic of compressors with constant speed. Discrepancies between *required* and *generated heating capacities* and *heating temperatures* result with increasing ambient temperature.

Our aim is to avoid this discrepancy between *required* and *generated* heating capacity and heating temperature and, as a result, effectively reduce the temperature gradients for heat transfer in evaporator and condenser. The air/water heat pump should no longer operate in intermittent on/off mode but continuously so that

$$\dot{Q}_H(T_A) \approx \dot{Q}_H^*(T_A) \tag{197}$$

The above equation must be supplemented if periodic defrosting is required when frost formation occurs in order to compensate for the increased energy needs resulting from interruptions in operation.

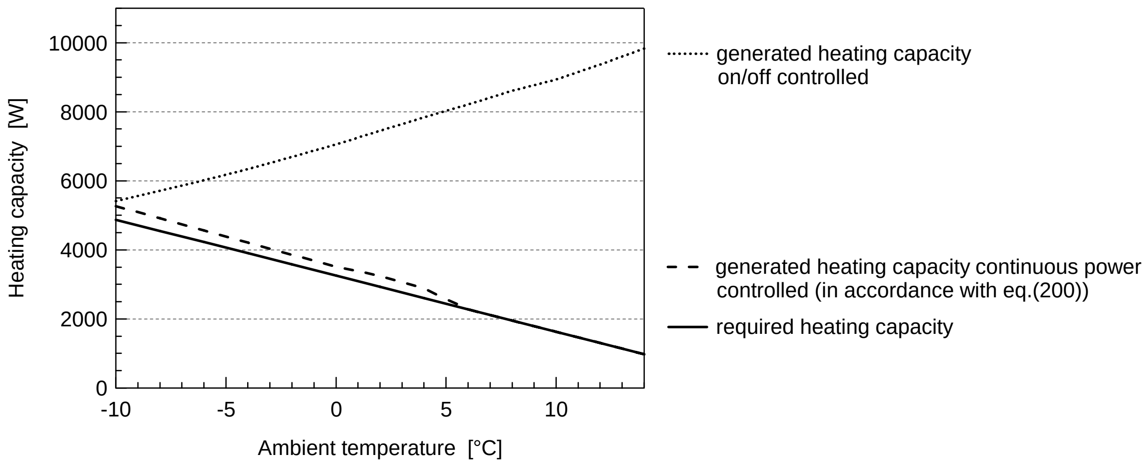

Fig. 7-1: Required heating capacity and two different delivered heating capacities as a function of ambient temperature (generated heating capacity of a continuous power controlled air/water heat pump in accordance with Eq. (200))

Fig. 7-1 presents three curves showing heating capacity as a function of outdoor temperature: the heating capacities *generated* by the air/water heat pump with on/off control and of the continuously power controlled air/water heat pump as well as the heating capacity *required* by the building.

The compressor should be equipped with continuous power control in order to adapt the *generated* heating capacity to the heating capacity *required* (e.g. its rotational speed could be adjusted using a variable-frequency drive). A good option could be the installation of several compressors, as often found in refrigeration installations, so that heating requirements can be met by switching compressors or individually pistons of a compressor on and off.

7.2 Operating characteristic of air/water heat pumps with continuous power control

In order to evaluate the air/water heat pump with *continuous power control* from the exergetic point of view, its self-adjusting operating characteristic is needed - as it was for the on/off-controlled air/water heat pump. The relevant temperatures and temperature gradients must once more be iteratively found as a function of ambient temperature:

$$T_E(T_A);\quad T_C(T_A);\quad T_H(T_A);\quad \Delta T_E(T_A);\quad \Delta T_C(T_A);\quad \Delta T_H(T_A)$$

$$\dot{m}_f = \dot{m}_f(T_A)$$

$$\dot{Q}_E = \dot{Q}_E(T_A);\quad \dot{Q}_C = \dot{Q}_H = \dot{Q}_H(T_A);\quad P_i = P_i(T_A)$$

For the determination of these relevant data, the process equations following below are used.

7.2.1 Required and generated heating capacity

Once more, the heating capacity *continuously required* by the building

$$\dot{Q}_H^* = \dot{Q}_H^*(T_A) \tag{198}$$

is known for a given average room temperature T_R. The average *required* heating temperature T_H^* is determined by the heating surface in the building (i.e. by the heat delivery system). This means that the relationship between *required* supply and return temperatures of the heating water as well as the heating water mass flow must be fulfilled:

$$\dot{Q}_H^*(T_A) = \dot{m}_{HW} \cdot c_{pHW} \cdot \left(T_{SP}^*(T_A) - T_{RT}^*(T_A)\right) \tag{199}$$

Usually T_{RT} is controlled via the settings of the heating curve as a function of T_A. The *generated* supply temperature T_{SP} adjusts itself correspondingly.

During frost formation in the (fin tube) evaporator, the (instantaneous) heating capacity *generated* must be increased by a *compensation factor* C because of the (periodically required) defrosting.

$$\dot{Q}_H(T_A) = C \cdot \dot{Q}_H^*(T_A) \tag{200}$$

The compensation factor C depends on the amount of frost deposited which itself depends on the state of the ambient air as well as the design of the (fin tube) evaporator and its fan (LOREF [5]). The following serve as guiding values:

$$\vartheta_A < 0°C \quad \Rightarrow \quad C \approx 1.08 \tag{201}$$

$$0°C < \vartheta_A < 5°C \quad \Rightarrow \quad C \approx 1.11 \tag{202}$$

$$\vartheta_A > 5°C \quad \Rightarrow \quad C \approx 1 \tag{203}$$

At ambient temperatures above 4°C or 5°C, hardly any frost formation occurs with continuously power controlled air/water heat pumps and, below this temperature, less than in the case of air/water heat pumps with on/off control.

Using the factor C, the *generated* heating water supply temperature T_{SP} is calculated - including compensation for defrosting - using:

$$T_{SP}(T_A) = T_{RT}(T_A) + \Delta T_{HW}(T_A) = T_{RT}(T_A) + C \cdot \left(T_{SP}^{*}(T_A) - T_{RT}^{*}(T_A)\right) \tag{204}$$

Therefore, the supply temperature T_{SP} *generated* during heat pump operation is slightly higher than that (continuously) *required* by the heating system T_{SP}^{*}. The *generated* heating temperature T_H, however, corresponds almost to that *required*. This already means that a striking improvement is made compared with the air/water heat pump with on/off control, as the exergy losses in the heat distribution system resulting from the *generated* heating temperatures being too high almost cease to exist.

7.2.2 Working fluid mass flow

Working fluid mass flow $\dot{m}_f$ is continuously controlled via the rotational speed of the compressor in such a way as to meet heating capacity requirements. The working fluid mass flow is determined for the following calculations by the next three equations.

Total energy balance:

$$\dot{Q}_H(T_A) = \dot{Q}_E(T_E, T_A) + P_i(T_E, T_A) \tag{205}$$

The heat flow $\dot{Q}_E$ transferred in the evaporator without vapour superheating according to Eq. (167):

$$\dot{Q}_E(T_E, T_A) = \dot{m}_f(T_E, T_A) \cdot r_E(T_E) \cdot \left(1 - \frac{c_{pl} \cdot (T_C(T_A) - T_E - \Delta T_{Csc})}{r_E(T_E)}\right) \tag{167}$$

Internal compressor power P_i according to Eq. (180):

$$P_i(T_E, T_A) = \dot{m}_f(T_E, T_A) \cdot (T_E + \Delta T_{cGsh}) \cdot c_{pg} \cdot \frac{1}{\eta_s(T_E, T_A)} \cdot \left(\left(\frac{p_C(T_A)}{p_E(T_E)}\right)^{\kappa} - 1\right) \tag{180}$$

This yields:

$$\dot{m}_f(T_E, T_A) = \frac{\dot{Q}_H(T_A)}{r_E(T_E) \cdot \left[1 - \left(\frac{c_{pl} \cdot (T_C(T_A) - T_E - \Delta T_{Csc})}{r_E}\right)\right] + (T_E + \Delta T_{cGsh}) \cdot c_{pg} \cdot \frac{1}{\eta_s(T_E, T_A)} \cdot \left[\left(\frac{p_C(T_A)}{p_E(T_E)}\right)^{\kappa} - 1\right]} \tag{206}$$

Working fluid mass flow can thus be calculated iteratively as a function of ambient and evaporation temperatures.

7.2.3 Cooling of ambient air in the evaporator

The calculation of air cooling ΔT_{Air} in the (fin tube) evaporator is performed using Eq. (168) or (173). In the case of the continuous power controlled air/water heat pump, the heat flow in the evaporator $\dot{Q}_E$ is dependent merely on the ambient and evaporation temperatures: $\dot{Q}_E = \dot{Q}_E(T_E, T_A)$.

7.2.4 Temperature gradients and evaporation temperature

The self-adjusting average temperature gradient for heat transfer in the evaporator results from the heat transfer equation:

$$\Delta T_E(T_E, T_C) = \frac{\dot{Q}_E(T_E, T_A)}{k_E \cdot A_E} \tag{207}$$

Here, the overall heat transfer coefficient k_E is a value for the entire (fin tube) evaporator. It also covers the effects of vapour superheating and the formation of condensate and/or frost on the air side if these occur. It is advantageous if k_E is determined from measurements made on a heat pump test rig. Changing air velocity in the fin tube evaporator by controlling the rotational speed of the fan changes the overall heat transfer coefficient. For it we apply the relation (LOREF [5]):

$$\frac{k_E}{[W/m^2 K]} = a + b \cdot \left(\frac{w_{Air}}{[m/s]} \right)^{0.8} \tag{208}$$

The values for a and b can be determined from simulations or by experiment.

The evaporation temperature is determined using Eq. (175):

$$T_E = \left(T_A - \frac{1}{2} \cdot \Delta T_{Air} \right) - \Delta T_E + \frac{1}{2} \cdot \Delta T_{GE} \tag{175}$$

It should be remembered that, in the case of working fluids with a temperature glide, the dew point temperature T_E is to be used (cf. appendix A8).

7.2.5 Temperature gradient and condensation temperature

The temperature gradient for heat transfer in the condenser is determined by:

$$\Delta T_C(T_A) = \frac{\dot{Q}_H(T_A)}{A_C \cdot k_C} \tag{209}$$

The condenser surface area A_C is known. The overall heat transfer coefficient k_C should be determined for the respective operating state either by calculation or experimentally and should consider vapour superheating, condensation and condensate subcooling. This varies only a little, so that an average value suffices for this analysis. Once more, the following is valid for the calculation of the condensation temperature:

$$T_C = \left(T_{RT} + \frac{1}{2} \cdot \Delta T_{HW} \right) + \Delta T_C + \frac{1}{2} \cdot \Delta T_{GC} \tag{186}$$

For working fluids with temperature glide, the dew point temperature is to be used for T_K (cf. appendix A8).

7.3 Results achievable with continuous power control - without drive losses

In order to identify the improvements to be made with continuously power controlled heat pumps, the exergetic efficiencies and the coefficients of performance will be compared to those of the on/off controlled heat pump. The results will be represented as a function of ambient temperatures and, further, as annual averages according to the cumulative distribution function of atmospheric temperature as shown in Fig. 1-3.

Heat transfer in the evaporator of air/water heat pumps mostly occurs through forced convection. Fans are used to provide a flow of air through the fin tube evaporator. The following evaluations are made:

- without consideration of the fan
- with consideration of the fan

The product of overall heat transfer coefficient and heat exchanger surface area ($k_E \cdot A_E$) in the evaporator may be considered in each case as being of the same magnitude, so that the same operating characteristics (evaporation and condensation temperatures etc.) can be found. The mechanical and electrical drive losses of the compressor and the fan will once more not be included in the calculations in this section in order to, at first, examine the heat pump process in more detail and thus avoid complicating the results any further.

7.3.1 Without consideration of the fan

Continuously power controlled air/water heat pumps will be compared with those using on/off control, whereby in each case the fan power will not be considered. In Fig. 7-2 the average temperature gradients for heat transfer in evaporator and condenser with on/off control and continuous power control are compared.

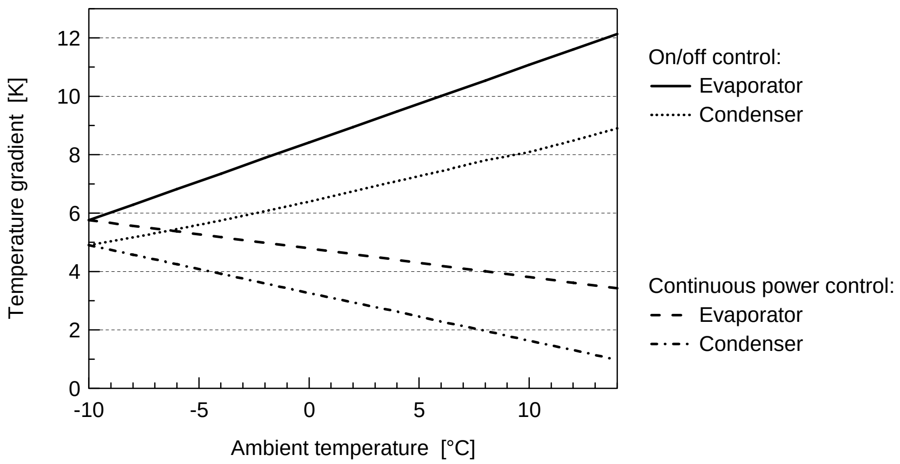

Fig. 7-2: Temperature gradient in evaporator and condenser with and without continuous power control

Because continuous power control is used for the compressor, the temperature gradients for heat transfer decrease: With increasing ambient temperature, they are reduced for both evaporator and condenser. This means that the temperature lift to be overcome by the heat pump becomes smaller (cf. Eq. (102)).

In the evaporator, however, such small temperature differences can not be handled with common thermostatic expansion valves. For the stable functioning of an injection control system, a certain minimum amount of vapour superheating is required. The minimum temperature gradient in the evaporator is limited by these facts. On the other hand, low temperature gradients can be achieved today using electronic expansion valves.

The resultant temperature lift ΔT_{Lift} is shown in Fig. 7-3 for a continuously power controlled and for an on/off controlled air/water heat pump as a function of ambient temperature.

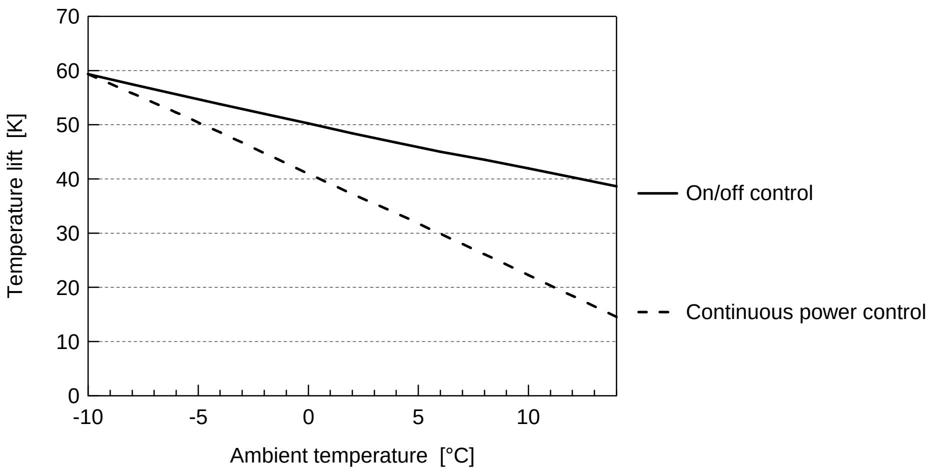

Fig. 7-3: Temperature lift with and without continuous power control

Here, the essential advantages of continuous power control are shown: the temperature lift to be overcome is reduced considerably. It also follows from Fig. 7-4 that the evaporation and condensation temperatures are more favourable when continuous power control is used as compared with on/off control.

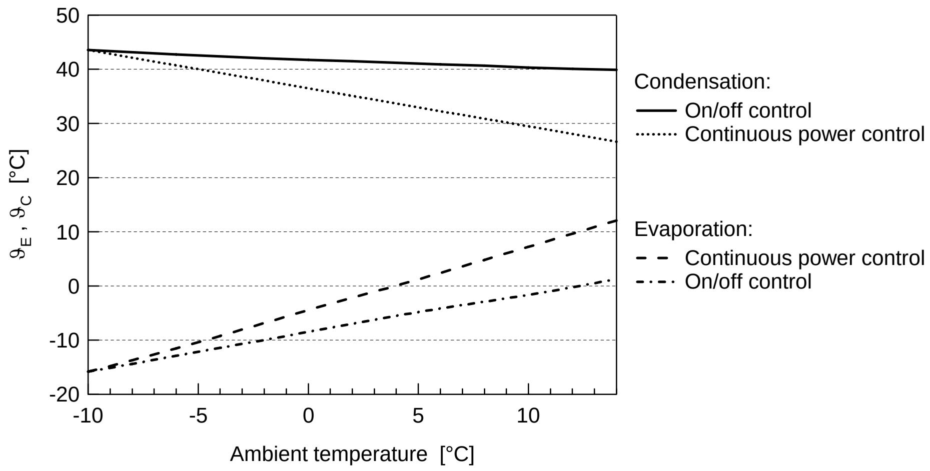

Fig. 7-4: Evaporation and condensation temperatures with and without continuous power control

The change for the evaporation temperature is also of great importance for air/water heat pumps. For continuously power controlled heat pumps it is closer to ambient temperature and, therefore, less frost formation on the fins and tubes of the fin tube evaporator occurs. In the so-called critical range between 4°C and 7°C (LOREF [5]), frost formation is at its highest for on/off controlled heat pumps. After only a short heating phase, the heating process has to be interrupted for defrosting. On the other hand, it seems possible with continuous power control that defrosting may no longer required at all in this temperature range. This is an important increase in efficiency especially as such conditions in this critical range are common during the heating season in the Central European climate.

The evaluation of the continuously power controlled heat pump can now be performed using the two *external exergetic efficiencies* defined. The one concerning the *generated heating temperature* is calculated without consideration of the fan using:

$$\eta_{exe} = 1 - \frac{\dot{E}_{LCp} + \dot{E}_{LEx} + \dot{E}_{LE} + \dot{E}_{LC}}{P_i} \tag{51}$$

And the one concerning the *required heating temperature* using:

$$\eta_{exe}^{*} = 1 - \frac{\dot{E}_{LCp} + \dot{E}_{LEx} + \dot{E}_{LE} + \dot{E}_{LC} + \upsilon \cdot \dot{E}_{LHS}^{*}}{P_i} \tag{96}$$

Fig. 7-5 shows the appropriate curves in relation to ambient temperature. For comparison, the curves for the air/water heat pump with on/off control are also shown.

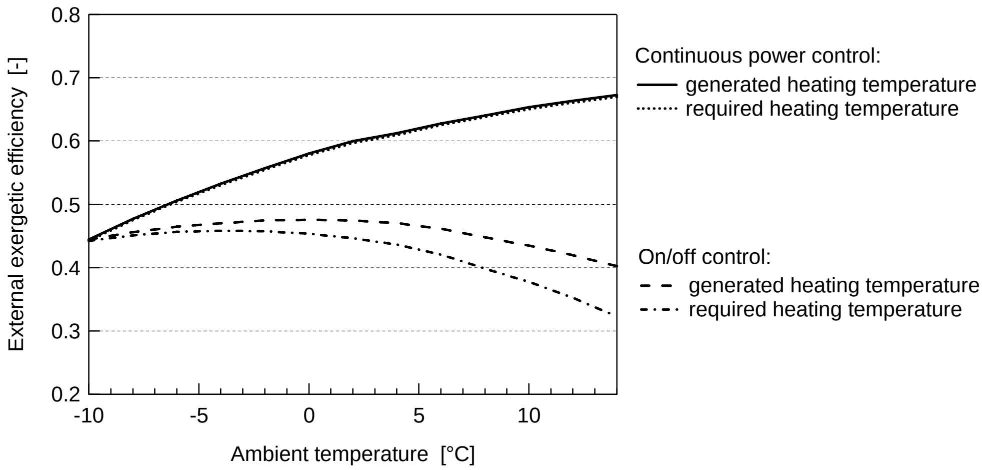

Fig. 7-5: External exergetic efficiency of the generated and required heating temperatures with and without continuous power control of the compressor (without consideration of the fan power)

Much higher exergetic efficiencies are achieved using continuous power control of the compressor. η_{exe} and η_{exe}^{*} are almost the same and rise from 44% at -10°C to 68% at 14°C. The resulting benefits are high compared with the on/off controlled heat pump. For the latter: $\eta_{exe} = 40\%$ and $\eta_{exe}^{*} = 32\%$, which is about half of the performance of the continuously power controlled machine. With the on/off controlled heat pump, a loss of 8% in exergetic efficiency at 14°C results from non-steady-state heat distribution (in the heat distribution system).

Without consideration of the fan, the increase in efficiency is high due to the continuous power control of the compressor. Not only is the *exergetic efficiency* considerably improved, but frost formation is also clearly reduced as the evaporation temperature increasingly adjusts itself to a value above the freezing-point of water.

The *coefficient of performance* is shown in Fig. 7-6 for the two control strategies against ambient temperature and is calculated here using:

$$COP = \frac{\dot{Q}_H}{P_i} \tag{196}$$

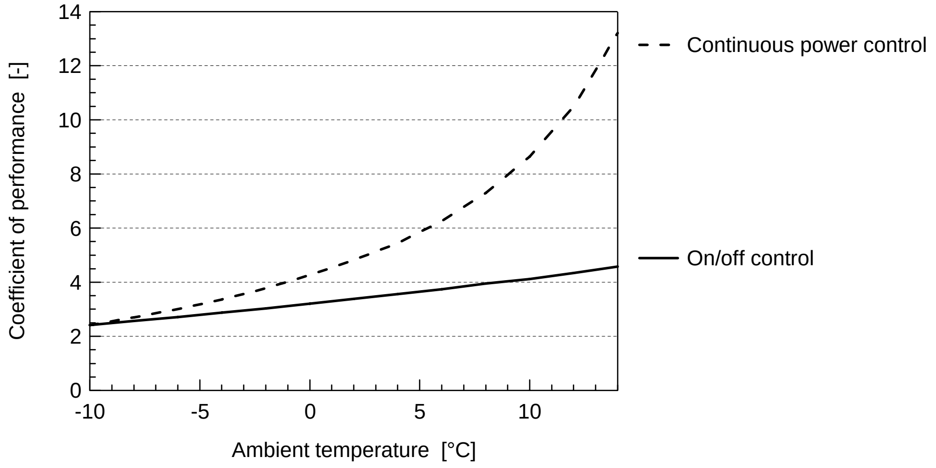

Fig. 7-6: Coefficient of performance with and without continuous power control of the compressor (without consideration of the fan)

At -10°C the *coefficients of performance* for the different control strategies are both 2.2, at 0°C they are 4.2 and 3.2 and at 12°C they are 12 and 4.2. The improvement obtained using continuous power control is considerable.

Tab. 7-1 presents an overview of the resultant seasonal performance factor and the annual average exergetic efficiency of the two control strategies for the air/water heat pump. Periodic defrosting due to frost formation is not considered. With on/off control, more defrosting is required in general.

Control strategy	On/off control	Continuous power control of the compressor
Seasonal performance factor [-]	3.49	7.57
Annual average exergetic efficiency of the generated heating temperature [-]	0.46	0.62
Annual average exergetic efficiency of the of the required heating temperature [-]	0.43	0.62

Tab. 7-1: Seasonal performance factor and annual average exergetic efficiency for on/off and continuous power control (without consideration of the fan)

7.3.2 *With consideration of the fan*

a) Fan without speed control

Without taking mechanical and electrical drive losses into account, the following applies for the drive power of an air/water heat pump using the theoretical fan power according to (211) under consideration of the fan:

$$P \approx P_i + P_{Fi} \tag{210}$$

P_{Fi} it is the internal fan power necessary. It is calculated using:

$$P_{Fi} = \frac{1}{\eta_{Fi}} \cdot \dot{V}_{Air} \cdot \Delta p_{Air} \tag{211}$$

The air volume flow to be produced $\dot{V}_{Air}$ is determined in order to achieve favourable flow velocities in the fin tube evaporator; in this case, a pressure loss Δp_{Air} occurs. For the air/water heat pump specified in appendix A7, the air volume flow in the fin tube evaporator in an unfrosted state is approximately 2400 m^3/h and the resultant air-side pressure drop is approximately 30 Pa. The internal fan efficiency varies in practice over an enormously large range. In this subsection we choose $\eta_{Fi} = 1$. In the next chapter we will investigate using real values. The internal fan power is dissipated and must be evaluated as an exergy loss.

$$\dot{E}_{LF} = P_{Fi} \tag{212}$$

Consequently, the *external exergetic efficiency of the generated heating temperature*, without taking drive losses into account, is given by:

$$\eta_{exe} = 1 - \frac{\dot{E}_{LCp} + \dot{E}_{LEx} + \dot{E}_{LE} + \dot{E}_{LC} + \dot{E}_{LF}}{P_i + P_{Fi}} \tag{213}$$

And for the *external exergetic efficiency of the required heating temperature* without taking drive losses into account:

$$\eta_{exe}^{*} = 1 - \frac{\dot{E}_{LCp} + \dot{E}_{LEx} + \dot{E}_{LE} + \dot{E}_{LC} + \upsilon \cdot \dot{E}_{LHS}^{*} + \dot{E}_{LF}}{P_i + P_{Fi}} \tag{214}$$

P_{Fi} is also to be taken into account in the coefficient of performance:

$$COP = \frac{\dot{Q}_H}{P_i + P_{Fi}} \tag{215}$$

It is presupposed here, too, that the product ($k_E \cdot A_E$) remains unchanged compared to section 7.3.1 and thus the resultant operating characteristic also remains identical in order to be able to make comparisons between the results with and without consideration of the fan. The fan is assumed to be working at a constant rotational speed and delivering a constant air volume flow over the entire range of ambient temperatures, so that the fan power P_{Fi} (independent of the ambient temperature) is also constant.

The effect on the *external exergetic efficiency of the required heating temperature* and the *coefficient of performance* are shown in Fig. 7-7 and Fig. 7-8.

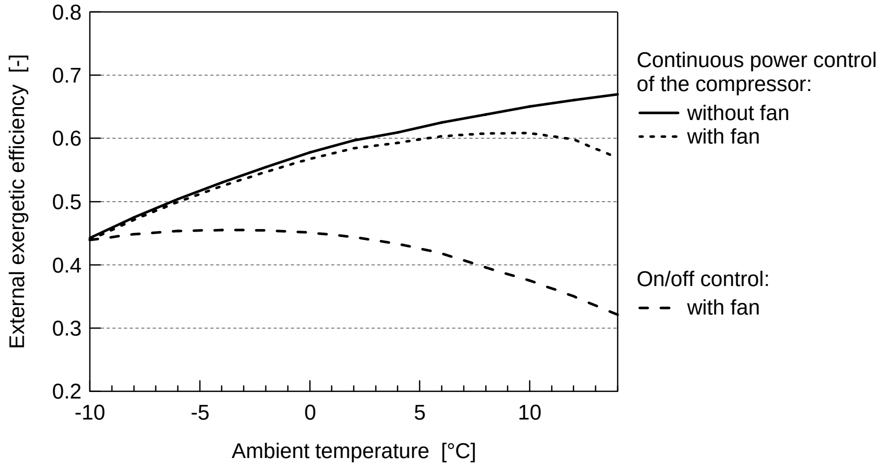

Fig. 7-7: External exergetic efficiency of the required heating temperature with and without continuous power control of the compressor (with and without consideration of the fan)

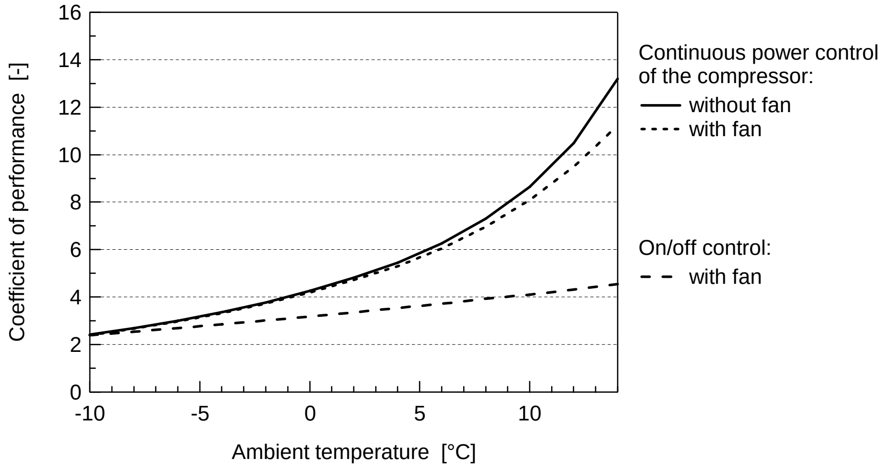

Fig. 7-8: Coefficient of performance with and without continuous power control of the compressor (with and without consideration of the fan)

The new curve with consideration of the fan is slightly below that for the continuously power controlled heat pump without consideration of the fan. However, it can be seen (with $\eta_{Fi} = 1$) that the exergetic efficiency decreases still more at ambient temperatures above 10°C for constant fan speed and continuously power controlled compressor. The cause of this behaviour is the constant fan power P_{Fi} resulting over the entire range of ambient temperatures. In comparison, the internal compressor power P_i decreases considerably with increasing ambient temperature.

Tab. 7-2 presents an overview of the *seasonal performance factor* and the *annual average exergetic efficiency* for on/off and continuous power control of the compressor with and without fan. Mechanical and electrical drive losses as well as periodic defrosting are, once more, not taken into consideration.

Control strategy	On/off control		Continuous power control of the compressor	
	with fan	without fan	with fan	without fan
Seasonal performance factor [-]	3.47	3.49	6.94	7.57
Annual average exergetic efficiency of the required heating temperature [-]	0.42	0.43	0.58	0.62

Tab. 7-2: Seasonal performance factor and annual average exergetic efficiency with and without continuous power control of the compressor with and without consideration of the fan

b) Fan with speed control

Can the curves for coefficient of performance and exergetic efficiency and thus also the values of the seasonal performance factor and the annual average exergetic efficiency be further improved when not only the compressor but also the fan is continuously power controlled? In order to answer this question, the operating characteristic of the air/water heat pump with continuous power control of the compressor and the fan is determined once more and evaluated exergetically.

For the investigation of this, the air volume flow is reduced linearly by adjusting the fan speed depending on decreasing ambient air temperature in accordance with Fig. 7-9. The optimal dependence should be analysed further in an additional study. This is mathematically rather complex to determine.

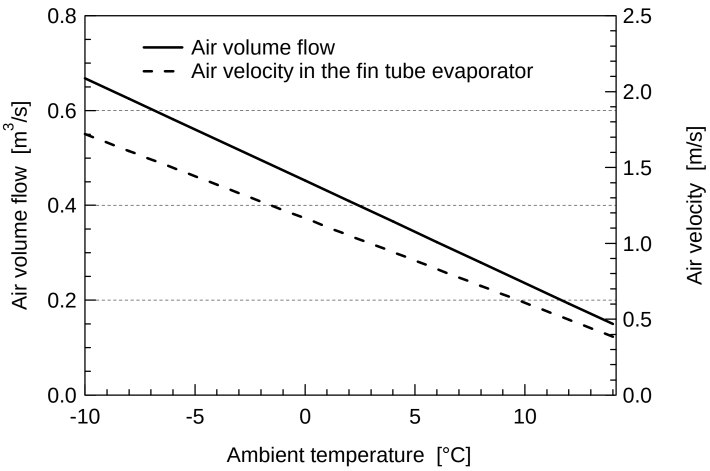

Fig. 7-9: Air volume flow and air velocity in the fin tube evaporator as a function of ambient temperature

In Fig. 7-10, the average *temperature gradients* for heat transfer in the evaporator and condenser for air/water heat pumps with on/off control and continuous power control are compared. In each case both a constant-speed and variable speed fan are compared according to Fig. 7-9. It can be shown that with the simultaneous regulation of compressor and fan speed the temperature gradient in the evaporator is reduced less strongly than when only the compressor speed is regulated.

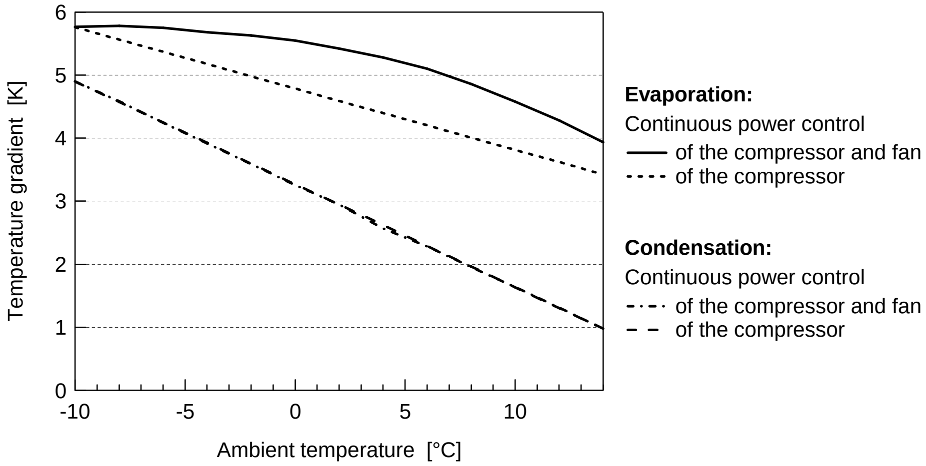

Fig. 7-10: Temperature gradient in evaporator and condenser with continuous power control of the compressor and continuous power control of the compressor and fan

Three curves for the *external exergetic efficiency of the required heating temperature* and of the *coefficient of performance* as a function of ambient temperature (without taking the mechanical and electrical drive losses into account) are shown in Fig. 7-11 for speed control of the compressor: without consideration of the fan and with consideration of the fan (constant-speed and controlled speed).

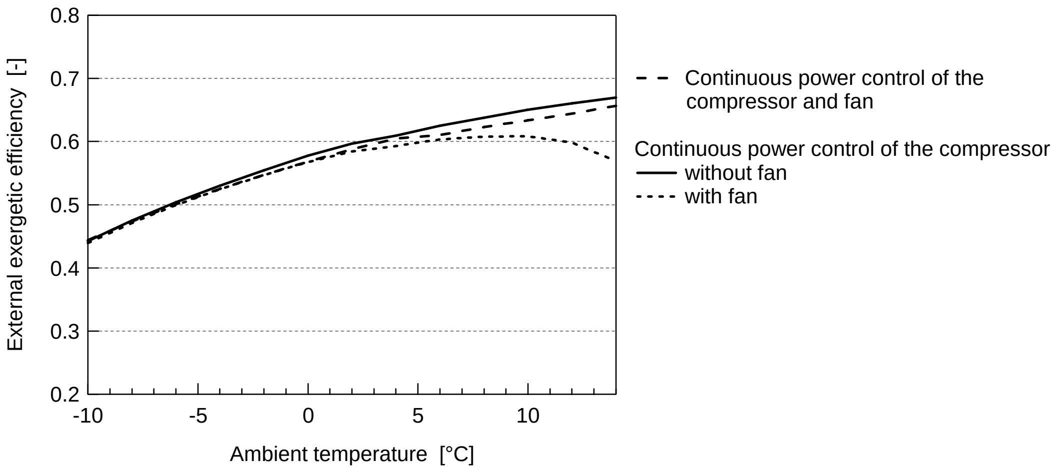

Fig. 7-11: External exergetic efficiency of the required heating temperature with continuous power control of the compressor with and without consideration of the fan as well as with continuous power control of the compressor and fan

If the compressor and fan of an air/water heat pump (without taking drive losses into account) are continuously power controlled, the characteristics of an air/water heat pump with continuous power control of the compressor without consideration of the fan are almost reached (cf. Fig. 7-5).

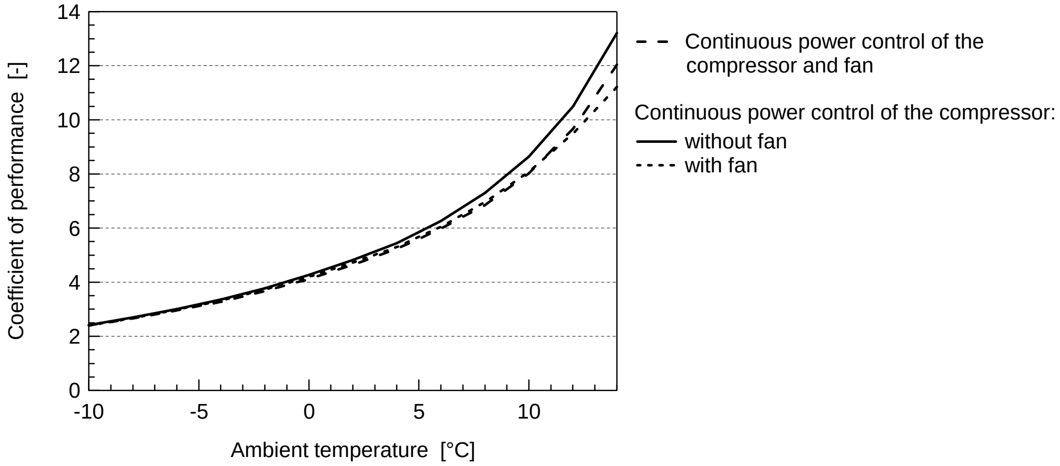

Fig. 7-12: Coefficient of performance with continuous power control of the compressor with and without consideration of the fan as well as with continuous power control of the compressor and of the fan

Tab. 7-3 provides an overview of the *seasonal performance factor* and *annual average exergetic efficiency* for different control strategies with consideration of the fan (without taking mechanical and electrical drive losses as well as defrosting into account).

Control strategy	On/off	Continuous power control of compressor only	Continuous power control of compressor and fan
Seasonal performance factor [-]	3.47	6.94	7.12
Annual average exergetic efficiency of the required heating temperature [-]	0.42	0.58	0.61

Tab. 7-3: Seasonal performance factor and annual average exergetic efficiency with and without continuous power control of the compressor and fan (with consideration of the fan)

When compared with air/water heat pump using on/off control, the efficiency of an air/water heat pump can be clearly increased by using continuous power control of the compressor and fan.

8 Effects of drive losses on the heat pump process

In previous analyses, the drive losses have not been included in order to show the direct exergy losses of the heat pump process clearly and dependant on only thermal data. Now the effect of drive losses on the exergetic efficiency and the coefficient of performance of on/off and continuously power controlled air/water heat pumps will be looked at. In each case the fan is considered here.

8.1 Drive losses of compressor and fan

As a first step the orders of magnitude of the various drive losses for compressor and fan are looked at and the effect of these losses on the calculation of exergetic efficiency and coefficient of performance demonstrated.

8.1.1 Drive losses of the compressor

The electrical drive power of the compressor is calculated using:

$$P_{Cp} = P_i \cdot \frac{1}{\eta_{Cpm}} \cdot \frac{1}{\eta_{Cpel}} \tag{216}$$

η_{Cpm} is the mechanical efficiency of the compressor and η_{Cpel} is the efficiency of the electric motor for compressors with constant speed. For compressors with variable speed η_{Cpel} is the efficiency of the electric motor including the frequency converter. For present-day heat pumps with constant compressor speed:

$$\eta_{CpD} = \eta_{Cpm} \cdot \eta_{Cpel} = 0.75...0.90 \tag{217}$$

Measurements made on the air/water heat pump specified in appendix A7, show that η_{CpD} increases from 81% at -10°C ambient temperature up to 88% at 14°C. The drive efficiency of the compressor η_{CpD} as a function of pressure ratio φ can (for constant compressor speed) be approximated as a straight line (cf. Fig. 8-1).

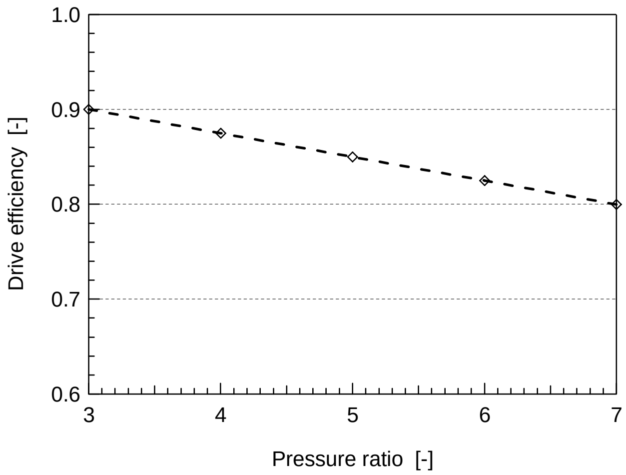

Fig. 8-1: Drive efficiency of the compressor (valid for constant compressor speed) as a function of pressure ratio (determined from measurements on the air/water heat pump specified in appendix A7)

If the speed of the compressor is controlled by means of a *frequency converter*, drive efficiency is additionally dependent on the set speed of the compressor.

From measurements made on the "Pioneer" continuously power controlled air/water heat pump of Eggenberger [6], the curve shown in Fig. 8-2 for the drive efficiency of the compressor including the electric motor as well as the frequency converter can be calculated.

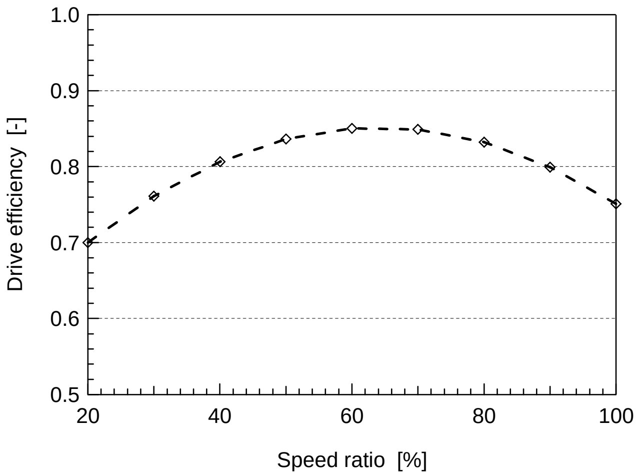

Fig. 8-2: Electrical drive efficiency in the case of variable speed as a function of the speed ratio (from measurements made on Eggenberger's Pioneer heat pump)

For full speed (100%) the compressor is driven with approximately 110 Hertz. If the compressor speed is reduced, the drive efficiency decreases for frequencies down to approximately 50 Hertz slightly, and then, for frequencies below 50 Hertz, quite distinctively.

The development of more efficient induction motors and frequency converters is at the present time being worked on intensely. In the future the total efficiency of the compressor is expected to be almost independent of rotational speed.

The drive loss in the compressor is:

$$\Delta P_{Cp} = P_{Cp} - P_i = P_i \cdot \left(\frac{1}{\eta_{Cpm}} \cdot \frac{1}{\eta_{Cpel}} - 1 \right) \qquad (218)$$

This must be considered as being completely an exergy loss for the entire heat pump.

8.1.2 Drive losses of the fan

The electrical drive power for the fan P_F is calculated using:

$$P_F = P_{Fi} \cdot \frac{1}{\eta_{Fm}} \cdot \frac{1}{\eta_{Fel}} \qquad (219)$$

where η_{Fm} is the mechanical efficiency of the fan and η_{Fel} the efficiency of the electric motor and, where appropriate, of the frequency converter.

The combination of the individual efficiencies together with the internal fan efficiency η_{Fi} of present-day heat pumps (from Eq. (211)) varies even more than in compressors:

$$\eta_{F0} = \eta_{Fi} \cdot \eta_{Fm} \cdot \eta_{Fel} = 0.03...0.30 \qquad (220)$$

A significant source of this low total efficiency is the internal fan efficiency η_{Fi}.

The above-mentioned efficiency is valid at the rated speed of the fan, i.e. at the design point ($\vartheta_U = -10°C$) of air/water heat pumps. With the reduction of rotational speed (for higher ambient temperatures) the total efficiency of the fan declines further. Ascertaining the amount proves to be difficult. The manufacturer Ziehl-Abegg [10] quotes a curve for electrical driving power consumption as a function of rotational speed ratio for EC motors as shown in Fig. 8-3.

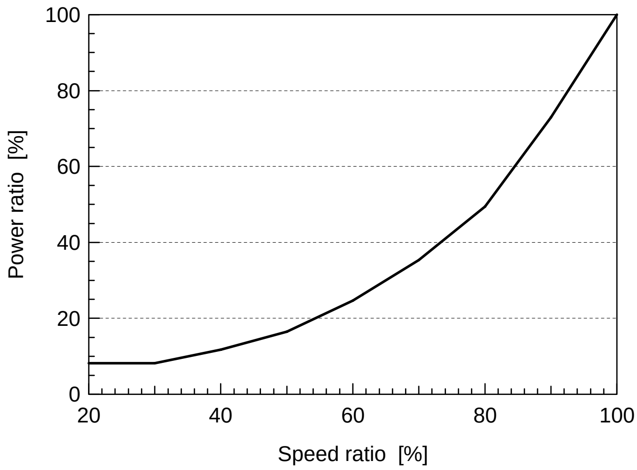

Fig. 8-3: Fan power ratio for speed controlled fan with EC motor (Ziehl-Abegg)

Below 30% of the rated speed, the drive power consumed is not further reduced. Above this value, however, the drive power of fans with EC motors can be reduced. In the case of fans, too, it can be expected that, in the future, the dependence of total efficiency on rotational speed will be almost eliminated.

The drive loss of the fan is also evaluated as an exergy loss:

$$\Delta P_F = P_F - P_{Fi} = P_{Fi} \cdot \left(\frac{1}{\eta_{Fm}} \cdot \frac{1}{\eta_{Fel}} - 1 \right) \tag{221}$$

8.1.3 *Effects of the drive losses on exergetic efficiency and coefficient of performance*

Taking the drive losses of the compressor and fan into account, the following applies for the calculation of the *external exergetic efficiency of the generated heating temperature:*

$$\eta_{exe} = 1 - \frac{\left(\dot{E}_{LCp} + \dot{E}_{LEx} + \dot{E}_{LE} + \dot{E}_{LC}\right) + \dot{E}_{LF} + \left(\Delta P_{Cp} + \Delta P_F\right)}{P_{Cp} + P_F} \tag{222}$$

And, for the *external exergetic efficiency of the required heating temperature,* the following applies*:*

$$\eta_{exe}^{\ *} = 1 - \frac{\left(\dot{E}_{LCp} + \dot{E}_{LEx} + \dot{E}_{LE} + \dot{E}_{LC} + \upsilon \cdot \dot{E}_{LHS}^{\ *}\right) + \dot{E}_{LF} + \left(\Delta P_{Cp} + \Delta P_F\right)}{P_{Cp} + P_F} \tag{223}$$

And, finally, the following applies for *the coefficient of performance*:

$$COP = \frac{\dot{Q}_H}{P_{Cp} + P_F} \tag{224}$$

8.2 On/off controlled air/water heat pump with drive losses

The exergy analysis of the air/water heat pump with on/off control performed in chapter 6 is now complemented by considering the drive losses for the compressor and the fan. For this, the operating characteristic determined in chapter 5 can be adopted without change as the drive losses have no influence on it.

In order to demonstrate the influence of the drive losses, the curves for *exergetic efficiency* and *coefficient of performance* with and without taking the drive losses into account are compared. The following assumptions are made:

$$\eta_{F0} = \eta_{Fi} \cdot \eta_{Fm} \cdot \eta_{Fel} = 0.25 \qquad (225)$$

$$\eta_{CpD} = \eta_{Cpm} \cdot \eta_{Cpel} = 0.90 \quad \text{(independent of pressure ratio)} \qquad (226)$$

The efficiency chosen for the compressor is high, but appears, in the light of continuous further development, realistic (please note that the isentropic compressor efficiency η_s is not included here).

In Fig. 8-4, the curves for the *external exergetic efficiency of the required heating temperature* of the air/water heat pump with on/off control are shown with and without the drive losses being taken into consideration.

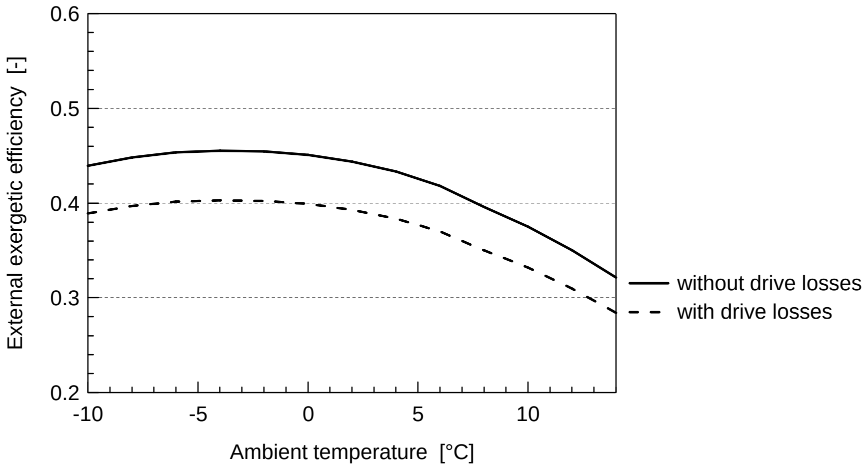

Fig. 8-4: External exergetic efficiency of the required heating temperature of the air/water heat pump with on/off control and with and without drive losses

Fig. 8-5 shows the curve for coefficient of performance with and without the drive losses being taken into consideration.

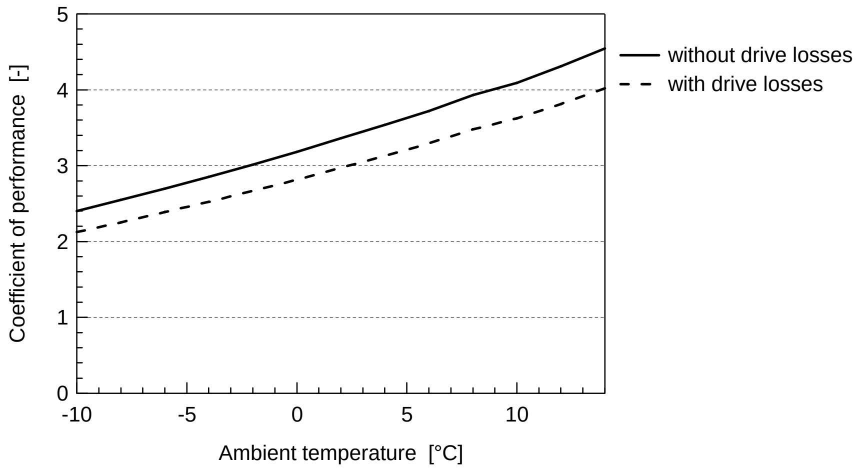

Fig. 8-5: *Coefficient of performance of the air/water heat pump with on/off control with and without drive losses*

The *exergetic efficiency* and the *coefficient of performance* are reduced by the drive losses in compressor and fan. The *coefficient of performance* is reduced by around 12% and the exergetic efficiency by around 14% at 0°C ambient temperature.

Tab. 8-1 provides an overview of the *seasonal performance factor* and *annual average exergetic efficiency* (without occasional defrosting) for an air/water heat pump with and without taking drive losses into account.

	Without drive losses	With drive losses
Seasonal performance factor [-]	3.47	3.07
Annual average exergetic efficiency of the required heating temperature [-]	0.42	0.375

Tab. 8-1: *Seasonal performance factor and annual average exergetic efficiency of the air/water heat pump with on/off control with and without drive losses*

8.3 Drive losses in the case of continuously power controlled compressor and constant fan speed

The operating characteristic discussed in section 7.3 for the continuously power controlled heat pump is still valid even with the drive losses in compressor and fan. Can an improvement now also be made in the *exergetic efficiency* as well as in the *coefficient of performance* by merely *controlling the power of the compressor*?

Since, in contrast to the on/off control situation, the fan runs with constant power, the total efficiency of the fan is now decisive when considering if an increase in the efficiency of the whole heat pump can be made. Its effect is examined using the following parameter values:

$$\eta_{F0} = \eta_{Fi} \cdot \eta_{Fm} \cdot \eta_{Fel} = 0.10,\; 0.25 \text{ and } 0.50 \tag{227}$$

To ease interpretation, the drive efficiency of the compressor is also examined using the following parameter values.

$$\eta_{CpD} = \eta_{Cpm} \cdot \eta_{Cpel} = 0.80,\; 0.90 \text{ and } 0.95 \tag{228}$$

Any dependence on pressure ratios as well as on rotational speed is neglected here.

In Fig. 8-6 the *external exergetic efficiency of the required heating temperature* with continuous power control and on/off control of the compressor are shown against ambient temperature. The total efficiency of the fan is varied in accordance with the above parameter values for a compressor drive efficiency of 90%.

Built-in fans exist with total efficiencies of less than 5%. In such cases a lower exergetic efficiency results than in the case of heat pumps with on/off control. If, however, the total efficiency of the fan is higher than around 10%, an increase of efficiency results with continuous power control of the compressor.

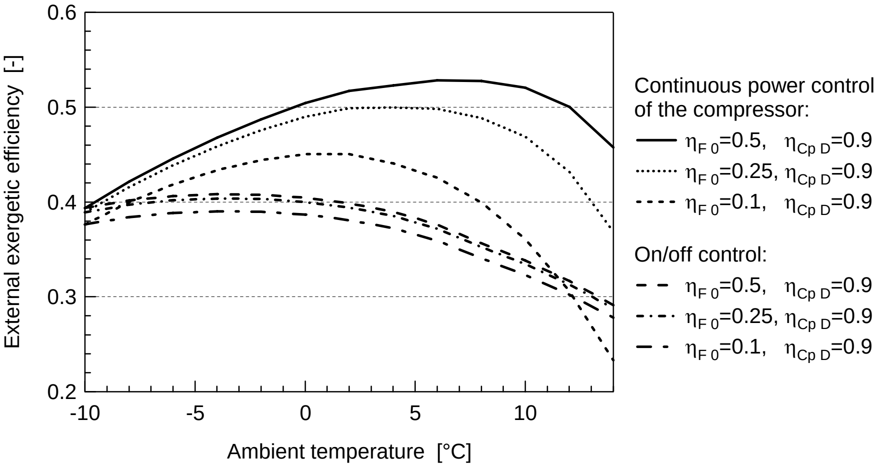

Fig. 8-6: External exergetic efficiency of the required heating temperature of the air/water heat pump with continuous power control and on/off control of the compressor against ambient temperature (total efficiency of the fan as a parameter)

In Fig. 8-7 the *external exergetic efficiency of the required heating temperature* with continuous power control and on/off control of the compressor are once more shown as a function of ambient temperature. This time, however, drive efficiency of the compressor is varied. The total efficiency of the fan is 25%.

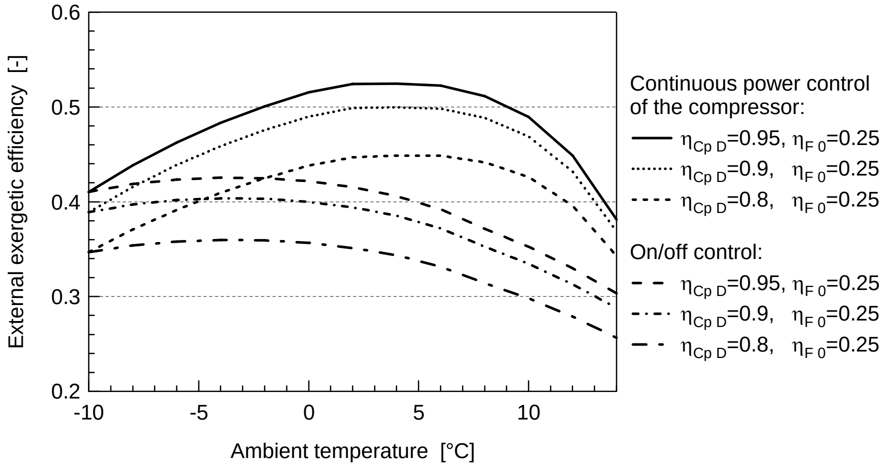

Fig. 8-7: *External exergetic efficiency of the required heating temperature of an air/water heat pump with continuous power control and on/off control of the compressor as a function of ambient temperature (drive efficiency of the compressor as a parameter)*

Fig. 8-6 and Fig. 8-7 show that the total efficiency of the fan has a considerable influence on the curve of exergetic efficiency when continuous power control is used for the compressor. If the total efficiency of the fan is low, the exergetic efficiency at higher ambient temperatures is strongly reduced. On the other hand, the drive efficiency of the compressor has only a small influence on the shape of the curve (even reduction of the curve over the entire range of outdoor temperatures).

The curves of the *coefficient of performance* with continuous power control and on/off control of the compressor as a function of ambient temperature are shown in Fig. 8-8 and Fig. 8-9. In Fig. 8-8, the total efficiency of the fan, and in Fig. 8-9 the drive efficiency of the compressor are the varied parameters.

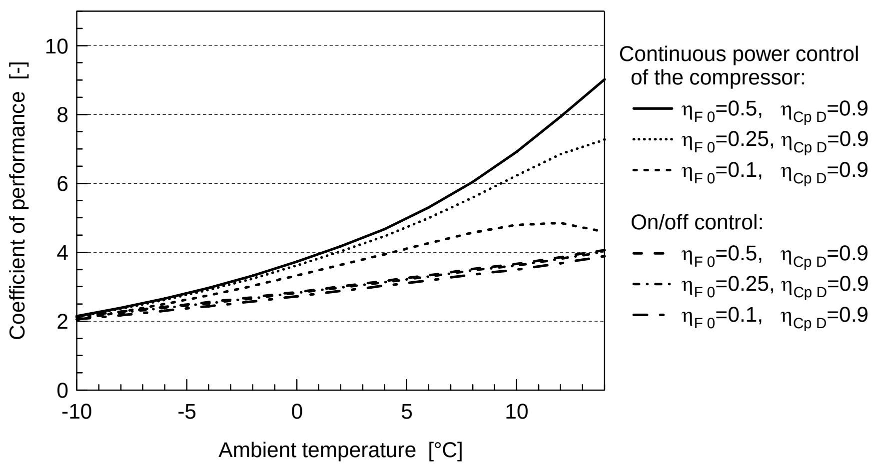

Fig. 8-8: *Coefficient of performance of the air/water heat pump with continuous power control and on/off control of the compressor as a function of ambient temperature (total efficiency of the fan as a parameter)*

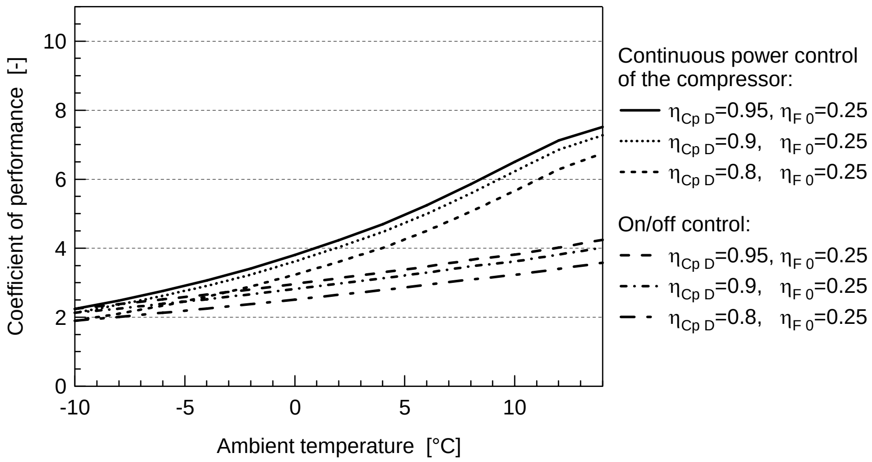

Fig. 8-9: Coefficient of performance of the air/water heat pump with continuous power control and on/off control of the compressor as a function of ambient temperature (drive efficiency of the compressor as a parameter)

Here too, the total efficiency of the fan clearly affects the curves for the coefficient of performance more strongly than the drive efficiency of the compressor.

The influence of the fan efficiency in heat pumps with continuous power control of the compressor and constant fan speed is high at outdoor temperatures above 0°C, quite unlike that for heat pumps with on/off control. The coefficients of performance for heat pumps with continuous power control of the compressor can, at an ambient temperature of 14°C, vary by around 4.6 to 9, depending on the total efficiency of the fan.

The *seasonal performance factors* and *annual average exergetic efficiencies* (without periodic defrosting) of the air/water heat pump with continuous power control and with on/off control of the compressor are shown in Tab. 8-2. Here, the drive efficiency of the compressor used is 90%.

Control strategy	On/off control			Continuous power control of the compressor		
Fan efficiency	0.10	0.25	0.50	0.10	0.25	0.50
Seasonal performance factor [-]	2.97	3.07	3.11	4.09	5.24	5.88
Annual average exergetic efficiency of the required heating temperature [-]	0.36	0.375	0.38	0.38	0.46	0.50

Tab. 8-2: Seasonal performance factor and annual average exergetic efficiency with respect to the required heating temperature of the air/water heat pump with continuous and on/off power control of the compressor (fan efficiencies as parameters)

For fan efficiencies higher than around 10%, the annual average exergetic efficiency and, therefore, the seasonal performance factor for continuous power control of the compressor and constant fan speed too, increase strongly. The efficiency of the air/water heat pump with on/off control is surpassed by far. With this control strategy, the overall efficiency of the fan has a considerable influence on the efficiency of the air/water heat pump.

8.4 Continuous power control of the compressor and the fan with drive losses

The question must further be asked whether the efficiency of the air/water heat pump can be further improved in comparison to section 8.3 if the compressor and the fan were continuously power controlled. Due to the drive losses, the operating characteristic still remains unchanged and is adopted from section 7.3.2. The air volume flow is, once more, controlled in accordance with Fig. 7-9 using the rotational speed of the fan.

In section 8.3, it was shown that the drive efficiency of the compressor has an influence on the figures for exergetic efficiency and coefficient of performance, but, however, that the characteristics are hardly influenced. The drive efficiency of the compressor is consequently no longer varied. Also, the dependence on pressure ratio as well as on rotational speed is no longer included here.

$$\eta_{CpD} = \eta_{Cpm} \cdot \eta_{Cpel} = 0.90 \tag{229}$$

The total efficiency of the fan is examined using the following parameter values:

$$\eta_{F0} = \eta_{Fi} \cdot \eta_{Fm} \cdot \eta_{Fel} = 0.10,\ \ 0.25\ \text{ and }\ 0.50 \tag{230}$$

Considering on-going development in the field of fan engineering, the dependence of the total efficiency of the fan on rotational speed is neglected here.

Fig. 8-10 compares once more the curves for external *exergetic efficiency of the required heating temperature* for continuous power control of the compressor and fan as well as for on/off control with total fan efficiency as parameter.

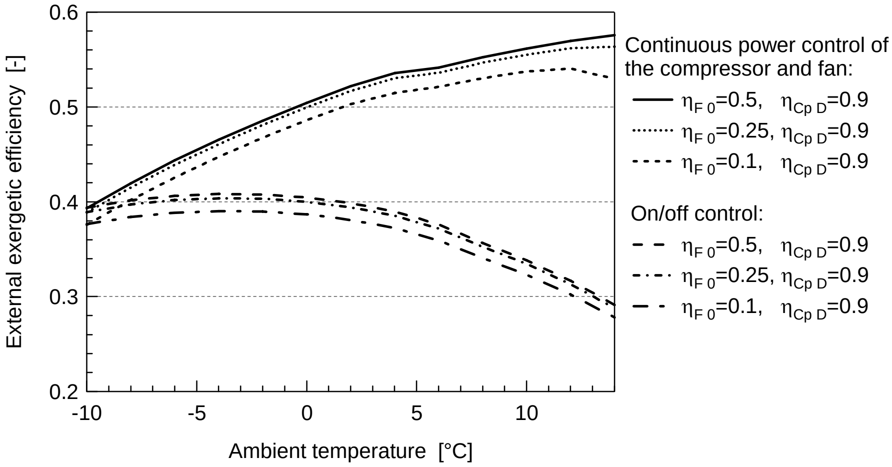

Fig. 8-10: External exergetic efficiency of the required heating temperature of the air/water heat pump with continuous power control of the compressor and fan as well as on/off control as a function of ambient temperature (total efficiency of the fan as a parameter)

This result is also interesting: If the rotational speed of the fan is also controlled in addition to that of the compressor, the efficiency of the fan has a far lower influence on the characteristic of exergetic efficiency than when only the compressor is controlled. The lower the total efficiency of the fan (at the design point) the stronger the reduction of exergetic efficiency near the heating limit temperature ($\vartheta_A = 15°C$).

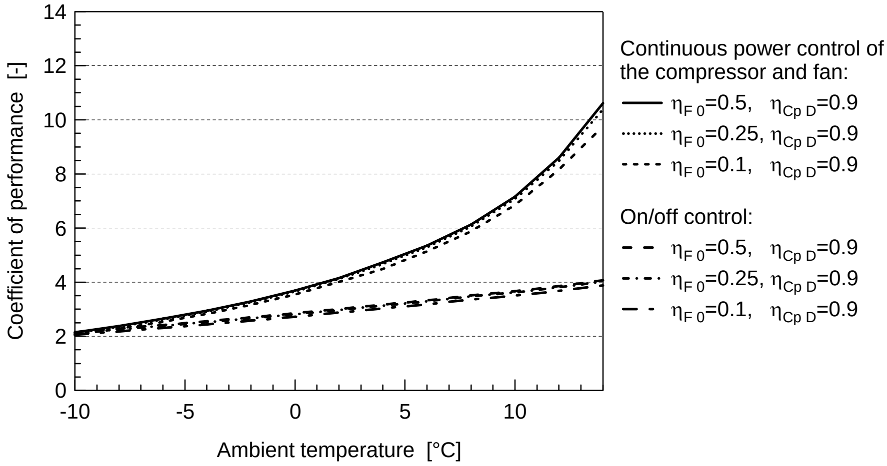

Fig. 8-11: Coefficient of performance of the air/water heat pump with continuous power control of the compressor and fan as well as on/off control as a function of ambient temperature (total efficiency of the fan as a parameter)

The analogous curves for *coefficient of performance* are shown in Fig. 8-11. The fan efficiency only has a small influence on the coefficient of performance for this control strategy. Near the heating limit temperature, the coefficient of performance is only reduced slightly by bad fan efficiencies. It therefore appears that for simultaneous speed control of the compressor and the fan less attention must be paid to fan efficiency as in the case of pure regulation of the compressor.

Finally, the *seasonal performance factor* and *annual average exergetic efficiency of the required heating temperature* (without periodic defrosting) are the decisive results. These are shown in Tab. 8-3.

Control strategy	Continuous power control of the compressor			Continuous power control of the compressor and fan		
Fan efficiency	0.10	0.25	0.50	0.10	0.25	0.50
Seasonal performance factor [-]	4.09	5.24	5.88	5.95	6.21	6.3
Annual average exergetic efficiency of the required heating temperature [-]	0.38	0.46	0.50	0.51	0.53	0.54

Tab. 8-3: Seasonal performance factor and annual average exergetic efficiency of the required heating temperature for an air/water heat pump with continuous power control of the compressor as well as for continuous power control of the compressor and fan (total efficiency of the fan as a parameter)

The additional speed control of the fan provides a further improvement in comparison with the sole control of compressor speed.

8.5 Comparison of the various control strategies

In conclusion, the attainable *seasonal performance factors* and *annual average exergetic efficiencies* whilst taking drive losses into consideration are summarised for the different control strategies for air/water heat pumps. The results presented here are valid for a total fan efficiency of 50% and a drive efficiency of the compressor of 90%. The figures for the efficiencies used here may appear high, but should, however, be attainable in the long term.

Control strategy	On/off control	Continuous power control of the compressor	Continuous power control of the compressor and fan
Seasonal performance factor [-]	3.11	5.88	6.3
Annual average exergetic efficiency of the required heating temperature [-]	0.38	0.50	0.54

Tab. 8-4: Seasonal performance factor and annual average exergetic efficiencies for an air/water heat pump with different control strategies (with drive losses taken into account)

Even just with continuous power control of the compressor, the efficiency of the air/water heat pump can be clearly improved in comparison with on/off control. If, in addition to the compressor, the fan speed is also controlled, the seasonal performance factor is doubled compared with the on/off controlled version.

8.6 Findings

The findings made in chapter 8 are summarised as follows:

- Both the seasonal performance factor and the annual average exergetic efficiency are reduced by around 12% as a result of drive losses in compressor and fan.
- If only the compressor in air/water heat pumps is equipped with continuous power control, the efficiency of the fan has a decisive influence on the seasonal performance factor and the annual average exergetic efficiency to be achieved.
- If, in addition to the compressor, the fan is also continuous power controlled, the influence of the fan efficiency becomes much lower in comparison to the sole control of the compressor.
- If, for an air/water heat pump with continuous power control of the compressor, a fan with a sufficiently high efficiency is used, considerably better seasonal performance factors and annual average exergetic efficiencies can be obtained using this control strategy than with on/off control of the heat pump. The choice of the fan plays, therefore, an important role here.
- The best seasonal performance factors and annual average exergetic efficiencies can be achieved through the simultaneous control of compressor and fan.

9 Conclusions

The topic of exergy is of far-reaching importance. Technical processes require effective work, i.e. exergy, for their execution which is obtained from primary sources of energy. If one aims to save primary energy, one has to make use of low exergy processes. Therefore, exergy is that part of energy "that matters" - it is valuable both technically and economically. There is no conservation law for exergy; on the contrary, it is destroyed and irreversibly converted to anergy. All transformations of energy should, as far as the criterion of efficiency and economics allows, be adapted to be reversible processes.

Energy-balances are necessary for the assessment of the heat pump process (and many other processes too) but is not sufficient. The second law of thermodynamics provides information on the quality of the process. The application of the second law can be advantageously done by using exergy balances instead of abstract entropy balances. Exergy is an extremely practical and descriptive way of evaluating technical processes involving thermodynamic cycles and heat transfer. Using exergy analysis, technical and economical evaluations can be carried out in the best possible way.

With the exergy analysis carried out here, it has been clearly shown that the source of the non impressive efficiency of common air/water heat pumps with on/off control is their unfavourable operating characteristic, which results from the characteristics of compressors running at constant rotational speed. With increasing outdoor temperature, the coefficient of performance of such installations indeed increases. In contrast to this, however, the exergetic efficiency, as a thermodynamically correct evaluation factor, decreases. The thermodynamics of heating would, on the other hand, make an increase of exergetic efficiency possible. With increasing outdoor temperature, the required heating capacity for a building decreases. The behaviour of a heat pump, on the other hand, with its compressor running at constant speed, is the opposite. The lower the heating capacity and the heating temperature required by the building (for increasing outdoor temperature), the higher the heating capacity and temperature generated. This behaviour has the effect of causing temperature gradients for heat transfer in the evaporator and condenser to increase with increasing ambient temperature. This leads to a clear discrepancy between required and generated heating (water) temperature. The actual temperature lift generated decreases less strongly in comparison with the ideal temperature lift, and the exergetic efficiency itself is then considerably reduced.

A distinct increase in the efficiency of air/water heat pumps can be achieved by continuously adapting the heating capacity generated to meet the heating capacity required. This is done using a suitable performance-control system (e.g. speed control of the compressor). Even just by using continuous power control for the compressor, much better coefficients of performance and higher exergetic efficiency are achieved in comparison to the on/off control strategy. In case of using this continuous power control strategy, the efficiency of the fan employed plays an important role and has a significant effect on the seasonal performance factor and the annual average exergetic efficiency. The best coefficients of performance and exergetic efficiencies can be achieved by using continuous power control of the compressor and the fan. Calculations show that, when using this control strategy, the seasonal performance factor can be approximately doubled in comparison to on/off control.

In this study, we have concentrated on the heat pump. In order to attain high energetic and exergetic efficiencies, integral and optimised solutions are needed. A prerequisite for this are, in addition to highly efficient heating systems, well thought out architectural designs and the consideration of the various physical qualities of buildings. Further, the building, its heating system and the heat pump employed must be matched to each other in the best possible way. This calls for the co-operation of architects and designers of building technical services as well as heat pump manufacturers.

The study presented here should provide a stimulus for further discussion on the subject of heat pumps and their efficiency. It should also help to establish the topic of exergy analysis as an increasingly important part of the training of engineers and planners.

10 List of symbols

10.1 Roman symbols

A	Heat exchanger surface area	m^2
A_C	Condenser heat exchanger surface area	m^2
A_{C1}	Required condenser heat exchanger surface area for vapour saturation	m^2
A_{C2}	Required condenser heat exchanger surface area for pure condensation	m^2
A_{C3}	Required condenser heat exchanger surface area for condensate subcooling	m^2
A_R	Building envelope surface area	m^2
A_E	Evaporator heat exchanger surface area	m^2
A_{E1}	Evaporator heat exchanger surface area required for pure evaporation	m^2
A_{E2}	Evaporator heat exchanger surface area required for vapour superheating	m^2
a	Constant for the calculation of the overall heat transfer coefficient in the evaporator	$W/(m^2\ K)$
b	Constant for the calculation of the overall heat transfer coefficient in the evaporator	[-]
b_0	Factor for the calculation of the simultaneous heat and mass transfer in the evaporator	J/(kg K)
C	Compensation factor	[-]
COP	Coefficient of performance	[-]
COP_{rev}	Ideal coefficient of performance of the reversible heat pump	[-]
$COP_{rev\,e}$	Best possible coefficient of performance of the reversible heat pump with reference to the generated heating temperature	[-]
$COP_{rev\,e}^{*}$	Best possible coefficient of performance of the reversible heat pump with reference to the required heating temperature	[-]
$COP_{rev\,HS}$	Best possible coefficient of performance of reversible heating systems with heat pumps	[-]
$COP_{rev\,i}$	Internal coefficient of performance of the reversible heat pump	[-]
c_p	Specific heat capacity (at constant pressure)	J/(kg K)
c_{pSt}	Specific heat capacity of water vapour (steam)	J/(kg K)
c_{pg}	Specific heat capacity of the gaseous working fluid	J/(kg K)
c_{pHW}	Specific heat capacity of the heating water	J/(kg K)
c_{pCd}	Specific heat capacity of the condensate deposited	J/(kg K)
c_{pAir}	Specific heat capacity of air (dry)	J/(kg K)
c_{pl}	Specific heat capacity of the (boiling) liquid working fluid	J/(kg K)
c_{pW}	Specific heat capacity of water	J/(kg K)
dh	Differential change in specific enthalpy	J/kg
dp	Differential change in pressure	Pa
ds	Differential change in specific entropy	J/kg

dT	Differential change in temperature	K
E_{ch}	Chemical Energy	J
E_{el}	Electrical Energy	J
E_{m}	Mechanical Energy	J
E_{Q}	Amount of exergy of the heat	J
E_{LHS}	Amount of exergy loss in the heat distribution system during a heating cycle	J
$\dot{E}$	Exergy flow	W
$\dot{E}_{Air\,O}$	Exergy flow of air at the output of the evaporator	W
$\dot{E}_{Air\,I}$	Exergy flow of air on entry into the evaporator	W
$\dot{E}_{Q}$	Exergy flow of the heat flow	W
$\dot{E}_{Q_H}$	Heating exergy flow of the generated heating capacity at the generated heating temperature	W
$\dot{E}_{Q_H}^{*}$	Heating exergy flow of the required heating capacity at the required heating temperature	W
$\dot{E}_{Q_A}$	Exergy flow from the environment	W
$\dot{E}_{RT}$	Exergy flow of the heating water at return temperature	W
$\dot{E}_{A}$	Exergy flow to environment	W
$\dot{E}_{SP}$	Exergy flow of the heating water at supply temperature	W
$\dot{E}_{L}$	Exergy loss flow	W
$\dot{E}_{LEx}$	Exergy loss flow in the expansion valve	W
$\dot{E}_{LHS}$	Exergy loss flow in the heat distribution system (intermittent)	W
$\dot{E}_{LHS}^{*}$	Exergy loss flow in the heat distribution system (continuous)	W
$\dot{E}_{L\,i}$	Internal exergy loss flow	W
$\dot{E}_{LC}$	Exergy loss flow in the condenser	W
$\dot{E}_{LC1}$	Exergy loss flow in the condenser (vapour saturation)	W
$\dot{E}_{LC2}$	Exergy loss flow in the condenser (pure condensation)	W
$\dot{E}_{LC3}$	Exergy loss flow in the condenser (condensate subcooling)	W
$\dot{E}_{LCp}$	Exergy loss flow in the compressor	W
$\dot{E}_{LR}$	Exergy loss flow in the heat delivery system (intermittent)	W
$\dot{E}_{LR}^{*}$	Exergy loss flow in the heat delivery system (continuous)	W
$\dot{E}_{Ltot}$	Sum of the exergy loss flows in the sub-processes of the heat pump	W
$\dot{E}_{LE}$	Exergy loss flow in the evaporator	W
$\dot{E}_{LE1}$	Exergy loss flow in the evaporator (pure evaporation)	W
$\dot{E}_{LE2}$	Exergy loss flow in the evaporator (vapour superheating)	W
$\dot{E}_{LF}$	Internal exergy loss flow of the fan	W
$\dot{E}_{j}$	Exergy flow in the individual state points of the heat pump process (j=1-4)	W
e	Specific exergy	J/kg
e_{Q_H}	Specific exergy of the generated heat	J/kg
e_{L}	Specific exergy loss	J/kg
e_{LEx}	Specific exergy loss in the expansion valve	J/kg
e_{LC}	Specific exergy loss in the condenser	J/kg
e_{LCp}	Specific exergy loss in the compressor	J/kg

e_{LE}	Specific exergy loss in the evaporator	J/kg
e_j	Specific exergy in the individual state points of the heat pump process (j=1-4)	J/kg
f	Heat pump operation ratio	[-]
$\dot{H}$	Enthalpy flow	W
$\dot{H}_j$	Enthalpy flow in the individual state points of the heat pump process (j=1-4)	W
h	Specific enthalpy	J/kg
$h_{Air\,O}$	Specific enthalpy of air at the output of the evaporator	J/kg
$h_{Air\,I}$	Specific enthalpy of air on entry into the evaporator	J/kg
h_A	Specific enthalpy at ambient temperature and pressure	J/kg
h_j	Specific enthalpy in the individual state points of the heat pump process (j=1-4)	J/kg
h_{2s}	Specific enthalpy after compressor for isentropic compression	J/kg
h'_4	Specific enthalpy at evaporation pressure on the boiling line	J/kg
h''_4	Specific enthalpy at evaporation pressure on the dew line	J/kg
K	Substitution for $(\kappa-1)/\kappa$	[-]
k	Overall heat transfer coefficient	W/(m^2 K)
k_C	Overall heat transfer coefficient condenser	W/(m^2 K)
k_{C1}	Overall heat transfer coefficient condenser (for vapour superheating)	W/(m^2 K)
k_{C2}	Overall heat transfer coefficient condenser (for pure condensation)	W/(m^2 K)
k_{C3}	Overall heat transfer coefficient condenser (for condensate subcooling)	W/(m^2 K)
k_R	Overall heat transfer coefficient of the building envelope	W/(m^2 K)
k_E	Overall heat transfer coefficient evaporator	W/(m^2 K)
k_{E1}	Overall heat transfer coefficient evaporator (for pure evaporation)	W/(m^2 K)
k_{E2}	Overall heat transfer coefficient evaporator (for vapour superheating)	W/(m^2 K)
m	Exponent for the calculation of the required heating temperature	[-]
$\dot{m}$	Mass flow	kg/s
$\dot{m}_f$	Mass flow working fluid	kg/s
$\dot{m}_{HW}$	Mass flow heating water	kg/s
$\dot{m}_{Air}$	Mass flow air	kg/s
P	Mechanical drive power	W
P_{el}	Electrical drive power	W
P_i	Internal compressor power	W
P_{Cp}	Electrical drive power of the compressor	W
P_{rev}	Minimum drive power of the reversible heat pump	W
P_F	Electrical drive power of the fan	W
P_{Fi}	Internal fan power	W
ΔP_{Cp}	Exergy loss flow compressor drive	W
ΔP_F	Exergy loss flow fan drive	W
p	Pressure	Pa

p_C	Condensation pressure	Pa
p_A	Ambient pressure	Pa
p_E	Evaporation pressure	Pa
p_j	Pressure in the individual state points of the heat pump process (j=1-4)	Pa
Δp_{Air}	Air-side pressure loss in the fin tube evaporator	Pa
Q	Heat quantity	J
Q_H	Amount of heat generated during the heating cycle	J
Q_H^*	Amount of heat required during the heating cycle	J
$\dot{Q}$	Heat flow	W
$\dot{Q}_H$	Heating capacity generated	W
$\dot{Q}_{Hnom}$	Nominal heating capacity	W
$\dot{Q}_H^*$	Heating capacity required	W
$\dot{Q}_C$	Heat flow in the condenser	W
$\dot{Q}_{C1}$	Heat flow in the condenser (vapour saturation)	W
$\dot{Q}_{C2}$	Heat flow in the condenser (pure condensation)	W
$\dot{Q}_{C3}$	Heat flow in the condenser (condensate subcooling)	W
$\dot{Q}_{max}^*$	Maximally required heating capacity	W
$\dot{Q}_A$	Heat flow from environment	W
$\dot{Q}_{Al}$	Latent heat flow from environment	W
$\dot{Q}_{As}$	Sensible heat flow from environment	W
$\dot{Q}_{A_{rev}}$	Heat flow from environment for a reversible heat pump	W
$\dot{Q}_E$	Heat flow in the evaporator	W
$\dot{Q}_{El}$	Latent heat flow in the evaporator	W
$\dot{Q}_{Es}$	Sensible heat flow in the evaporator	W
$\dot{Q}_{E1}$	Heat flow in the evaporator (pure evaporation)	W
$\dot{Q}_{E2}$	Heat flow in the evaporator (vapour superheating)	W
q_H	Specific heat for heating purposes	J/kg
q_A	Specific heat from environment	J/kg
q_E	Specific heat in the evaporator	J/kg
R	Individual gas-constant working fluid	J/(kg K)
R_{St}	Individual gas-constant water vapour	J/(kg K)
R_{Air}	Individual gas-constant for air (dry)	J/(kg K)
r	Specific enthalpy of evaporation of the working fluid	J/kg
r_{Sd_w}	Specific enthalpy of solidification of water	J/kg
r_C	Specific enthalpy of condensation of the working fluid at condensation temperature	J/kg
r_{S_w}	Specific enthalpy of sublimation of water	J/kg
r_E	Specific enthalpy of evaporation of the working fluid at evaporation temperature	J/kg
r_{E_w}	Specific enthalpy of evaporation of water	J/kg
s	Specific entropy	J/kg
s_{irr}	Non-reversible-increase in specific entropy	J/kg
s_{rri12}	Non-reversible increase in specific entropy in the compressor	J/kg

s_A	Specific entropy at ambient temperature and ambient pressure	J/kg
s_1	Specific entropy in the individual state points of the heat pump process (j=1-4)	J/kg
s'_4	Specific entropy at evaporation pressure on the boiling line	J/kg
s''_4	Specific entropy at evaporation pressure on the dew line	J/kg
SPF	Seasonal performance factor	[-]
T	Absolute temperature	K
T_H	Generated heating temperature	K
T_H^*	Required heating temperature	K
$\overline{T}_H$	Average over time for the generated heating temperature during the heating cycle	K
$T_{H\,max}^*$	Maximally required heating temperature	K
T_C	Condensation temperature	K
T_{C1}	Average temperature level in the condenser (vapour saturation)	K
T_{C2}	Average temperature level in the condenser (pure condensation)	K
T_{C3}	Average temperature level in the condenser (condensate undercooling)	K
$\overline{T}_C$	Average condensation temperature	K
T_{Cd}	Temperature of the condensate deposited	K
$T_{Air\,O}$	Output air temperature	K
$T_{Air\,I}$	Input air temperature	K
$\overline{T}_{Air}$	Average air temperature in the evaporator	K
T_R	Room temperature	K
T_{RT}	Generated return temperature of heating water	K
T_{RT}^*	Required return temperature of heating water	K
$\overline{T}_{RT}$	Average over time of generated return temperature during the heating cycle	K
T_A	Ambient temperature	K
$T_{A\,min}$	Minimum ambient temperature	K
T_E	Evaporation temperature	K
T_{E1}	Average temperature level in the evaporator (pure evaporation)	K
T_{E2}	Average temperature level in the evaporator (vapour superheating)	K
$\overline{T}_E$	Average evaporation temperature	K
T_{SP}	Generated supply temperature of heating water	K
T_{SP}^*	Required supply temperature of heating water	K
$\overline{T}_{SP}$	Average over time of the generated supply temperature during the heating cycle	K
T_j	Temperature in the individual state points of the heat pump process (j=1-4)	K
ΔT	Temperature gradient	K
ΔT_{hGsh}	Vapour superheating after compressor with reference to the condensation temperature (hot gas superheating)	K

ΔT_{GC}	Temperature glide in the condenser	K
ΔT_{GE}	Temperature glide in the evaporator	K
ΔT_{H}	Temperature gradient in the heat distribution system between generated and required heating temperatures	K
ΔT_{Lift}	Temperature lift	K
$\Delta T_{Lift\,ideal}$	Minimum temperature lift with respect to the required heating temperature	K
$\Delta T_{Lift\,min}$	Minimum temperature lift with respect to the desired room temperature	K
ΔT_{HW}	Heating water warming in the condenser	K
ΔT_{C}	Temperature gradient in the condenser	K
ΔT_{C1}	Average temperature gradient in the condenser (vapour saturation)	K
ΔT_{C2}	Average temperature gradient in the condenser (pure condensation)	K
ΔT_{C3}	Average temperature gradient in the condenser (condensate subcooling)	K
ΔT_{Air}	Cooling of air in the evaporator	K
ΔT_{R}	Temperature gradient from the heat distribution system to the room (Temperature gradient in the heat delivery system)	K
ΔT_{Csc}	Condensate subcooling	K
ΔT_{cGsh}	Vapour superheating in the evaporator	K
ΔT_{E}	Temperature gradient in the evaporator	K
ΔT_{E1}	Average temperature gradient in the evaporator (pure evaporation)	K
ΔT_{E2}	Average temperature gradient in the evaporator (vapour superheating)	K
t_0	Switch-on point in time for the heat pump	s
t_1	Switch-off point in time for the heat pump	s
t_2	End of standstill-time	s
$\dot{V}_{Air}$	Volume flow air	m^3/s
$\dot{V}_{S}$	Standard volume flow compressor	m^3/s
W	Compressor work during a heating cycle	J
w_{Air}	Air velocity in the finned sectional view of the fin tube evaporator	m/s
w_{i}	Specific internal work of the compressor	J/kg
x	Humidity of air	[-]
x_{V}	Vapour quality in the working fluid after expansion valve	[-]
$x_{Air\,O}$	Humidity of air on output from the evaporator	[-]
$x_{Air\,I}$	Humidity of air on entry into the evaporator	[-]
x_{A}	Humidity of air in the ambient state	[-]
Δx_{E}	Average humidity gradient in the evaporator	[-]
Z	Compressibility factor	[-]
z	Number of days per year	[-]

10.2 Greek symbols

ϑ	Temperature	°C
ϑ_H	Generated heating temperature	°C
ϑ_H^*	Required heating temperature	°C
ϑ_{Hmax}^*	Maximally required heating temperature	°C
ϑ_{Dpl}	Dew point of air on entry into the evaporator	°C
ϑ_A	Ambient temperature	°C
η_{ex}	Exergetic efficiency	[-]
η_{exe}	External exergetic efficiency of the generated heating temperature	[-]
η_{exe}^*	External exergetic efficiency with reference to the required heating temperature	[-]
η_{exHS}	External exergetic efficiency of heating systems with heat pumps	[-]
η_{exi}	Internal exergetic efficiency	[-]
η_{exrev}	Exergetic efficiency of the reversible heat pump	[-]
η_C	Carnot factor	[-]
η_{Ce}	Carnot factor with reference to the generated heating temperature	[-]
η_{Ce}^*	Carnot factor with reference to the required heating temperature	[-]
η_{CHS}	Carnot factor with reference to the room temperature	[-]
η_{Ci}	Carnot factor with reference to the internal process temperatures	[-]
η_{CpD}	Drive efficiency of the compressor	[-]
η_{Cpel}	Efficiency of the electric motor (compressor)	[-]
η_{Cpm}	Mechanical efficiency of the compressor	[-]
η_s	Isentropic compressor efficiency	[-]
η_{Fel}	Efficiency of the electric motor (fan)	[-]
η_{Fi}	Internal fan efficiency	[-]
η_{Fm}	Mechanical efficiency of the fan	[-]
η_{F0}	Total efficiency of the fan	[-]
κ	Isentropic exponential of the working fluid	[-]
λ	Volumetric efficiency of the compressor	[-]
λ_{Air}	Thermal conductivity of air (dry)	W/(m K)
λ_W	Thermal conductivity of water	W/(m K)
φ	Pressure ratio	[-]
ν	Kinematic viscosity	m^2/s
ρ_{Air}	Density of air (dry)	kg/m^3
ρ_W	Density of water	kg/m^3
υ	Heat flow ratio	[-]

11 Bibliography

[1] H.D. Baehr: Zur Thermodynamik des Heizens (I. Der zweite Hauptsatz und die konventionellen Heizsysteme), Brennstoff-Wärme-Kraft 32, Nr. 1, S. 9/15, 1980

[2] H.D. Baehr: Zur Thermodynamik des Heizens (II. Primärenergieeinsparung durch Anergienutzung), Brennstoff-Wärme-Kraft 32, Nr. 2, S. 47/57, 1980

[3] W. Raiss: Heiz- und Klimatechnik, 2. Band, 15. Auflage, S. 64/67, Berlin, Heidelberg, New York: Springer Verlag, 1970

[4] O. Albrecht: Verbesserungspotential von Luft/Wasser-Wärmpepumpen durch Exergie-Analyse: Diplomarbeit, Hochschule für Technik und Architektur, Horw, 2005

[5] L. Berlinger, M. Imholz, M. Albert, B. Wellig, K. Hilfiker: LOREF – Lamellenluftkühler-Optimierung mit Reduktion von Eis- und Frostbildung: Optimierung des Lamellenluftkühlers/Verdampfers von Luft/Wasser-Wärmepumpen – Teil 1: Theoretische und experimentelle Untersuchungen. Bundesamt für Energie, 2008

R. Sahinagic, L. Gasser, B. Wellig, K. Hilfiker: LOREF – Lamellenluftkühler-Optimierung mit Reduktion von Eis- und Frostbildung: Optimierung des Lamellenluftkühlers/Verdampfers von Luft/Wasser-Wärmepumpen – Teil 2: Mathematisch-physikalische Simulation des Lamellenluftkühlers mit Kondensat- und Frostbildung. Bundesamt für Energie, 2008

R. Sahinagic, M. Imholz, L. Berlinger, H. Huber, K. Hilfiker: LOREF – Lamellenluftkühler-Optimierung mit Reduktion von Eis- und Frostbildung: Untersuchung der Frostbildung für Lamellenluftkühler von Wärmepumpen. Bundesamt für Energie, 2004

[6] P. von Böckh, H.J. Eggenberger, Marc Borer, Thomas Borer: Geregelte Wärmepumpe Pioneer – Geregelte Luft/Wasser-Wärmepumpe für Sanierungen von Öl- und Elektroheizungen. Bundesamt für Energie, 2005

[7] Z. Rant: Die Heiztechnik und der zweite Hauptsatz der Thermodynamik, Gaswärme International 12, Nr. 1 und 8, S. 1/8 und 297/304, 1963

[8] H.D. Baehr: Thermodynamik, 6 Auflage, Hannover, Springer Verlag, 1988

[9] VDI-Wärmeatlas, 10. bearbeitete und erweiterte Auflage, Berlin, Heidelberg, New York: Springer Verlag, 2006

[10] Ziehl Abegg: Drehzahlregelung von Ventilatoren für die Kälte und Klimatechnik, 2007

[11] Bitzer International: Kältemittel Report, 13. Auflage, 2005

A1 Compressor model and characteristics

The driving force of every compression heat pump is the compressor. This sucks in the cold suction gas at low pressure (evaporation pressure) and compresses it to the higher condensation pressure.

Various models of compressor are available. Within the framework of this research study, various compressor models for use in air/water heat pumps are examined. In the modern air/water heat pumps available on the market, scroll or reciprocating compressors are usually employed.

A1.1 Compressor models employed

A1.1.1 Scroll compressors

The compression concept of the scroll compressor consists of an evolvent spiral which, together with a second, similar spiral, forms a series of sickle-shaped pockets. During compression, one spiral remains fixed (fixed spiral), while the other (orbiting spiral) rolls around it. In the course of this movement, the gas pockets between the two forms are moved slowly towards the centre of the two spirals whereby, at the same time, their volume decreases.

In this way, the scroll compressor works according to the volumetric principle. Since the volume reduction in the spiral is a result of its construction, the pressure conditions in the compressor is also given by the spiral’s design. This means that the scroll compressor needs no valves. If the pressure conditions required by the plant are lower than the pressure conditions resulting in the compressor, a decompression of the compressed gas at the end of the spirals occurs.

Within the framework of this study, a semi-hermetic, suction-gas cooled scroll compressor manufactured by Copeland is employed.

The seal between the faces of the spirals during operation is achieved with the aid of centrifugal forces. For this reason, scroll compressors are suitable for operation at variable speed only for a very small range of rotational speeds.

A1.1.2 Reciprocating compressors

The oldest and probably the most common compressor model is the reciprocating compressor. It is robust, technically mature and relatively cheap to manufacture. Its main drawbacks are the free mass-forces which call for appropriate measures to be taken with regard to the transfer of vibrations.

In this study, a semi-hermetic reciprocating compressor manufactured by Bitzer is employed.

The drive motor is overhung on the compressor axle and, in its suction-gas cooled variant, is cooled by suction-gas flowing through it. Motor cooling, especially at high specific loading, is therefore achieved using the cold suction-gas passing through it.

A1.2 Compressor characteristics

In the following section, the characteristics required from the various compressors employed for the mathematical-physical simulation of the air/water heat pump are derived.

Within the framework of this study, the following two compressor models were employed:

- **Scroll compressor:** Copeland ZR 40 K 3E (semi-hermetic, operation with R407C)
- **Reciprocating compressor:** Bitzer 2EC-3.2Y (semi-hermetic, operation with R407C)

A1.2.1 Standard volume flow

The standard volume flow $\dot{V}_S$ is given by the geometrical volume of the compression chamber as well as by the nominal speed of the compressor. The following applies to the compressors employed:

- **Scroll compressor:** $\dot{V}_S = 9.44\,m^3/h$ at 50Hz mains frequency
- **Reciprocating compressor:** $\dot{V}_S = 11.36\,m^3/h$ at 50Hz mains frequency

A1.2.2 Compressibility factor

The compressibility factor Z of the working fluid is required for the calculation of working fluid mass flow in Eq. (164). This can be determined for each working fluid as a function of pressure and temperature. In Eq. (164) an averaged value is used for the compressibility factor (temperature and pressure averaged during compression). For R407C the following applies:

$$Z = 0.94$$

A1.2.3 Volumetric efficiency

The volumetric efficiency λ is the relation between the effective volume flow $\dot{V}_{eff}$ sucked in and the standard volume flow $\dot{V}_S$, which, for volumetric compressors, is given by the geometry of the compression chamber.

$$\lambda = \frac{\dot{V}_{eff}}{\dot{V}_S} \approx 0.6...0.9$$

The volumetric efficiency is effectively dependent on the pressure ratio $\varphi = p_C / p_E$. With increasing pressure ratio, the volumetric efficiency gets worse. This is valid both for reciprocating as well as for scroll compressors. In the case of scroll compressors, the volumetric efficiency decreases on account of leakage between the faces of the rotating spirals that increases with increasing pressure ratio. For reciprocating compressors, on the other hand, the dead space (for inlet and outlet valves) is responsible for the reduction of volumetric efficiency.

Volumetric efficiency can be determined as a function of the pressure ratio as provided by manufacturer's data on the compressors. Using these data, the working fluid mass flow $\dot{m}_f$ from the compressor can be determined as a function of the pressure ratio φ as well as of the entry temperature T_1. The volumetric efficiency can now be calculated as a function of the pressure ratio and a regression equation can be formulated.

$$\lambda = \lambda(\varphi) = \frac{\dot{m}_f(\varphi, T_1) \cdot Z \cdot R \cdot T_1}{p_E(T_E) \cdot \dot{V}_S}$$

The regression equations for the calculation of the volumetric efficiency of the scroll and reciprocating compressor are shown in Fig. A 1:

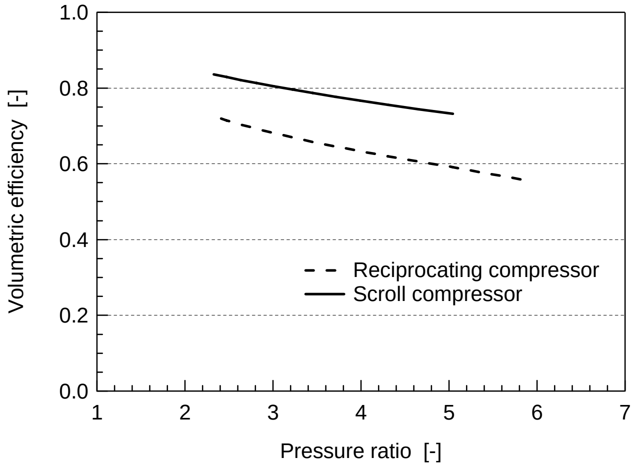

Fig. A 1: Volumetric efficiency of scroll and reciprocating compressors

A1.2.4 Isentropic compressor efficiency

The isentropic compressor efficiency η_s is decisive with respect to the exergy losses occurring in the compressor and therefore can be considered as being an important characteristic. The isentropic compressor efficiency is, in analogy to volumetric efficiency, a function of the pressure ratio φ. Using manufacturer's data, the electrical power P_{el} supplied to the compressor can be calculated as a function of the pressure ratio φ as well as of the compressor entry temperature T_1. The specific internal compressor work w_i can be calculated from the working fluid mass flow $\dot{m}_f$ as well as from the drive efficiency of the compressor η_{CpD}.

$$w_i = \frac{P_{el} \cdot \eta_{CpD}}{\dot{m}_f}$$

If, during compression from p_E to p_C, the gaseous working fluid is considered to be an ideal gas, the following is valid for the specific internal compressor work:

$$w_i = T_1 \cdot c_{pg} \cdot \frac{1}{\eta_s} \cdot \left(\varphi^{\kappa} - 1\right)$$

Consequently, the following applies to the isentropic compressor efficiency as a function of the pressure ratio:

$$\eta_s = \eta_s(\varphi) = T_1 \cdot c_{pg} \cdot \frac{\dot{m}_f(\varphi, T_1)}{P_{el}(\varphi, T_1) \cdot \eta_{CpD}} \cdot \left(\varphi^{\kappa} - 1\right)$$

The resulting isentropic efficiencies of the scroll and reciprocating compressors are shown in Fig. A 2 as a function of the pressure ratio.

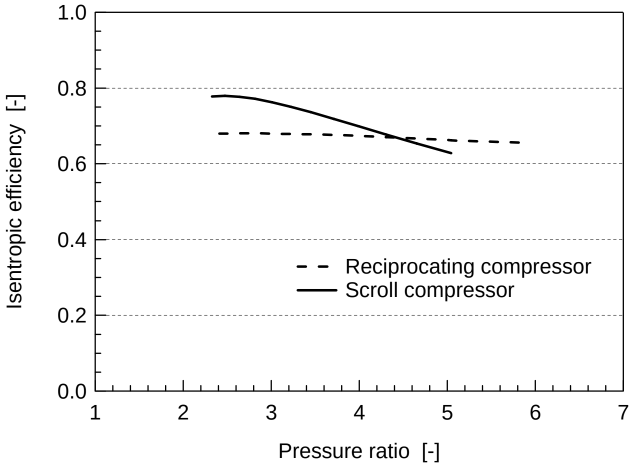

Fig. A 2: Isentropic compressor efficiency for scroll and reciprocating compressors

A2 Mathematical aspects concerning the pressure ratio

The pressure ratio used in Eq. (109) is consequently derived as follows. In general, the following is valid for $p_1 = p_E$ and $p_2 = p_C$:

$$\varphi = \frac{p_2}{p_1} = \frac{p_C}{p_E} \tag{108}$$

Using the *Clausius-Clapeyron* equation*,* the vapour pressure curve of the working fluid can be mathematically analysed. The following is valid:

$$p = p_0 \cdot e^{\frac{r}{R}\cdot\left(\frac{1}{T_0}-\frac{1}{T}\right)}$$

Consequently, according to *Clausius-Clapeyron,* the following is valid for the evaporation pressure p_E and the condensation pressure p_C :

$$p_C = p_2 = p_0 \cdot e^{\frac{r}{R}\cdot\left(\frac{1}{T_0}-\frac{1}{T_C}\right)}$$

$$p_E = p_1 = p_0 \cdot e^{\frac{r}{R}\cdot\left(\frac{1}{T_0}-\frac{1}{T_E}\right)}$$

By insertion in the Eq. (108), the pressure ratio as a function of the relevant process temperatures T_E and T_C is obtained:

$$\varphi = \frac{p_C}{p_E} = e^{\frac{r}{R}\cdot\left(\frac{1}{T_E}-\frac{1}{T_C}\right)} = e^{\frac{r}{R}\cdot\left(\frac{T_C-T_E}{T_E\cdot T_C}\right)} \approx e^{\frac{r}{R}\cdot\frac{\Delta T_{Lift}}{T_A{}^2}} \tag{109}$$

Using the Clausius-Clapeyron equation, the pressures p_E and p_C are thus eliminated from the pressure ratio and are replaced by the relevant process temperatures.

A3 Simplification of the exergy losses in the compressor

In a first step, the series expansion of the exponentials contained in Eq. (110) is examined. In this case, the scope of application must be determined and verified. For the series expansion of the exponential function, the following applies:

$$e^x = 1 + x + \frac{1}{2}x^2 + \frac{1}{6}x^3 + \frac{1}{24}x^4 + ...$$

In order to achieve an important simplification of Eq. (110), the series expansion must be broken off after the first term. The relative error of the simplified function in comparison with the exact exponential function as a function of x-values is shown in Fig. A 3.

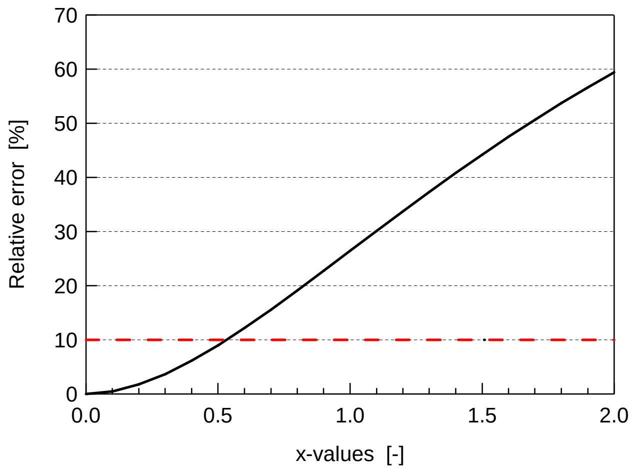

Fig. A 3: Relative error of the simplified function in comparison with the exact exponential function

In accordance with Fig. A 3, the range of valid x-values can be limited as follows:

$$e^x = e^{K \cdot \frac{r}{R} \cdot \left(\frac{1}{T_E} - \frac{1}{T_C}\right)} \Rightarrow x = K \cdot \frac{r}{R} \cdot \left(\frac{1}{T_E} - \frac{1}{T_C}\right) = 0...0.5$$

In order to check the range of validity for the x-values, a verification calculation for R407C is carried out: Operating conditions: $T_E = 259.15\,K$, $T_C = 312.15\,K$; Thermophysical properties of R407C: $K = 0.111$, $r = 230\,kJ/kg$, $R = 79.6\,J/kgK$.

According to the above equation, $x = 0.21$. The verification of the assumptions made shows that a series expansion of the exponential function with a truncation after the first term is permissible. With this approximation we obtain the result:

$$e^{K \cdot \frac{r}{R} \cdot \left(\frac{1}{T_E} - \frac{1}{T_C}\right)} \approx K \cdot \frac{r}{R} \cdot \left(\frac{1}{T_E} - \frac{1}{T_C}\right) + 1$$

Used in Eq. (110) the following is obtained:

$$e_{LCp} = T_A \cdot \left(c_{pg} \cdot \ln\left(\frac{1}{\eta_s} \cdot K \cdot \frac{r}{R} \cdot \left(\frac{1}{T_E} - \frac{1}{T_C}\right) + 1\right) - r \cdot \left(\frac{1}{T_E} - \frac{1}{T_C}\right)\right)$$

In order to provide a simple interpretation of the above equation, the logarithmic function is once more approximated using a series expansion. The following applies to the series expansion of the logarithmic function:

$$\ln(x) = (x-1) - \frac{1}{2}\cdot(x-1)^2 + \frac{1}{3}\cdot(x-1)^3 - \frac{1}{4}\cdot(x-1)^4 + \ldots$$

To simplify Eq. (110), the series expansion is once more broken off after the first term. Fig. A 4 shows the relative error as a function of the x-values and with reference to the exact function.

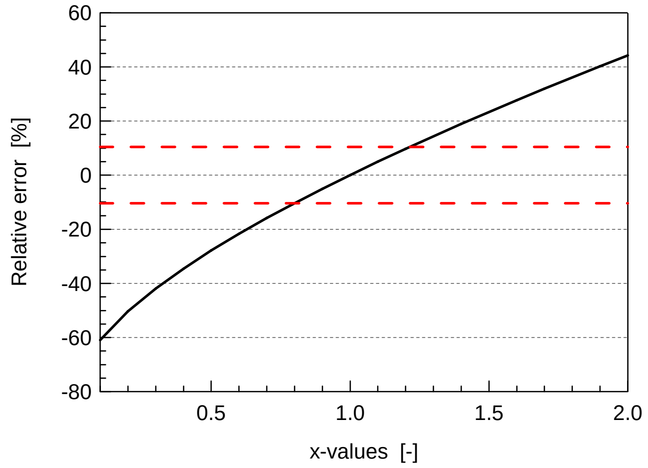

Fig. A 4: Relative error of the simplified function with reference to the exact logarithmic function

The validity of the range of x-values can in turn be determined as follows so that the relative error of the simplified function referring to the exact logarithmic function is not greater than 10%.

$$\ln(x) = \ln\left(\frac{1}{\eta_s}\cdot K\cdot\frac{r}{R}\cdot\left(\frac{1}{T_E}-\frac{1}{T_C}\right)+1\right) \Rightarrow x = \frac{1}{\eta_s}\cdot K\cdot\frac{r}{R}\cdot\left(\frac{1}{T_E}-\frac{1}{T_C}\right)+1 = 0.8\ldots1.2$$

Using the above-mentioned operating conditions and material properties (R407C), and assuming an isentropic compressor efficiency of 75%, an x-value of $x = 1.28$ is obtained. Although the x-value of the term to be developed is just outside of the range of validity, the series expansion is still carried out.

By including the identity according to Eq. (111) the following results:

$$e_{LCp} = T_A\cdot r\cdot\frac{\Delta T_{Lift}}{T_E\cdot\left(T_E+\Delta T_{Lift}\right)}\cdot\left(\frac{1}{\eta_s}-1\right) \tag{112}$$

The accuracy of this strongly simplified function for the calculation of the specific compression exergy losses will now be checked.

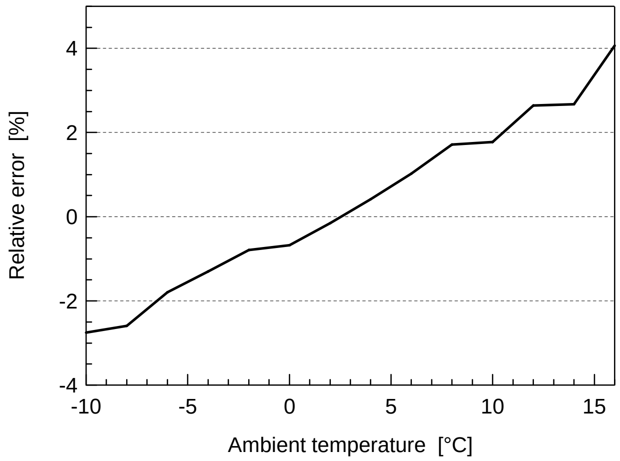

Fig. A 5: Relative error of the particular exergy losses of compression (Eq. (112)) with reference to Eq. (110)

In this case, the isentropic compressor efficiency required in Eq. (112) was modelled in accordance with appendix A1. The resultant errors are small: around 4% at the most. Consequently, Eq. (112) provides a good approximation for the calculation of the specific exergy losses of compression.

A4 Specific enthalpy and entropy after the expansion valve

In the following section, the specific enthalpy and entropy after the expansion valve are derived in a detailed manner.

In chapter 2.1, it was already shown that the energy flow and the enthalpy flow of a mass flow remains unchanged across the throttle (expansion valve). This means that the expansion valve operates - to a good approximation – *isenthalpically.* The denotations employed in the derivation are shown in Fig. A 6. The specific enthalpies are named analogously to the specific entropies.

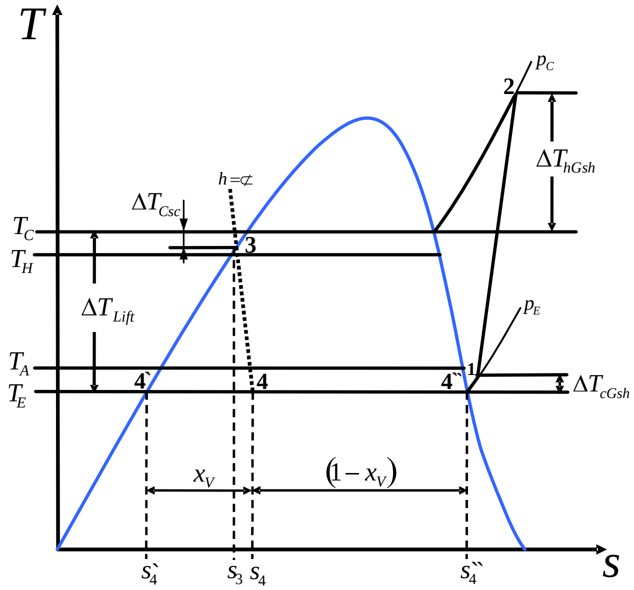

Fig. A 6: T,s-diagram with specific entropies

If the expansion valve works isenthalpically, the following is valid for the specific enthalpies before and after the throttle:

$$h_3 = h_4$$

State point 3 rests on the boiling line. Consequently:

$$h_3 = h_3'$$

State point 4 (exit of the expansion valve or entry to evaporator) lies in the wet steam area. Its specific enthalpy can be calculated using the vapour quality x_V. The vapour quality x_V in the wet steam area is defined using:

$$x_V = \frac{m''}{m' + m''} = \frac{m''}{m}$$

m' stands for the mass of the boiling liquid and m'' for the mass of the saturated vapour. Consequently, for the specific enthalpy h_4 the following is valid:

$$h_4 = h_4' + x_V \cdot (h_4'' - h_4')$$

with:

$$h_4'' - h_4' = r_E$$

This provides the Eq. (116) for the calculation of the specific enthalpy h_4 with the specific enthalpy of evaproation r_E at the corresponding evaporation pressure $p_E = p_1$.

$$h_4 = h'_4 + x_V \cdot \left(h''_4 - h'_4\right) = h'_4 + x_V \cdot r_E \tag{116}$$

As for the specific enthalpy h_4 at state point 4, the specific entropy s_4 can also be calculated at this state point in a similar way.

$$s_4 = s'_4 + x_V \cdot \left(s''_4 - s'_4\right)$$

whereby the following is valid:

$$s''_4 - s'_4 = s_E$$

The evaporation entropy s_E can be calculated using the specific enthalpy of evaporation r_E and the corresponding evaporation temperature T_E.

$$s_E = \frac{r_E}{T_E}$$

Equation (117) results for the calculation of the specific entropy s_4.

$$s_4 = s'_4 + x_V \cdot \left(s''_4 - s'_4\right) = s'_4 + x_V \cdot \frac{r_E}{T_E} \tag{117}$$

A5 Simplification of the exergy losses in the expansion valve

Equation (125) for the calculation of the specific exergy losses in the expansion valve contains a logarithmic function that complicates any simple interpretation of this equation.

This logarithmic function can be approximated by means of series expansion as follows. For the series expansion of the logarithmic function the following applies analogously to appendix A3:

$$\ln(x) = (x-1) - \frac{1}{2}\cdot(x-1)^2 + \frac{1}{3}\cdot(x-1)^3 - \frac{1}{4}\cdot(x-1)^4 + \ldots$$

With the aim of achieving an important simplification of Eq. (125), the series expansion has to be broken off after the first term. The resulting error of the simplified function with reference to the exact logarithmic function is shown in Fig. A 4 as a function of the x-values.

In order to ensure that the resulting relative error of the simplified function with reference to the exact function does not become larger than 10%, the range of validity can be limited as follows:

$$\ln(x) = \ln\left(\frac{T_E}{T_E + \Delta T_{Lift} - \Delta T_{Csc}}\right) \approx \ln\left(\frac{T_E}{T_C}\right) \Rightarrow x = \frac{T_E}{T_C} = 0.8\ldots1.2$$

Assuming $T_E = 259.15\,K$ and $T_C = 312.15\,K$, an x-value of $x = 0.83$ is obtained. Consequently, a series expansion of the logarithmic function with abortion after the first term is permissible. The following is therefore valid:

$$\ln\left(\frac{T_E}{T_E + \Delta T_{Lift} - \Delta T_{Csc}}\right) \approx \left(\frac{T_E}{T_E + \Delta T_{Lift} - \Delta T_{Csc}}\right) - 1$$

By insertion in Eq. (125) the following is obtained:

$$e_{LEx} \approx T_A \cdot c_{pl} \cdot \left(\frac{\Delta T_{Lift}{}^2}{T_E{}^2 + T_E \cdot \Delta T_{Lift}}\right)$$

The accuracy of this strongly simplified function for the calculation of the specific exergy losses of the expansion valve will now in turn be checked.

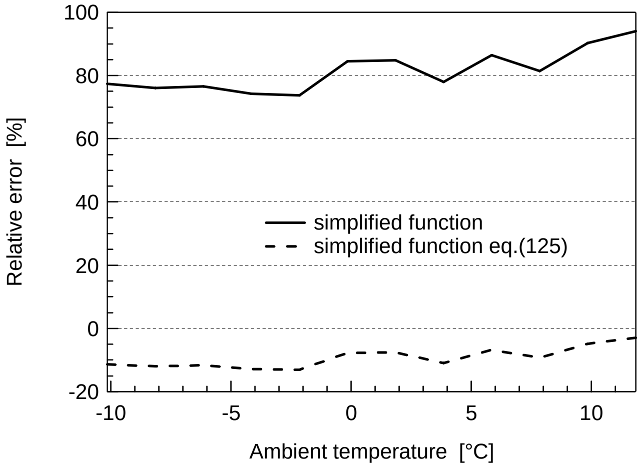

Fig. A 7: Relative error of the specific exergy losses of the expansion valve with reference to Eq. (125)

The relative errors shown in Fig. A 7 refer to unsimplified Eq. (125). The equation simplified by means of the series expansion delivers bad results. The relative error of 10% taken into account during series expansion influences the results of the simplified equation quite strongly. This can be demonstrated using an error propagation calculation.

If the simplified equation is corrected by a factor 0.5, the Eq. (126) results, which supplies good results and is easily interpretable. Consequently, Eq. (126) represents a suitable approximation for the calculation of the specific exergy losses of the expansion valve.

$$e_{LEx} \approx T_A \cdot c_{pl} \cdot \frac{1}{2} \cdot \left(\frac{\Delta T_{Lift}{}^2}{T_E{}^2 + T_E \cdot \Delta T_{Lift}} \right) \tag{126}$$

For use in simulation programs, Eq. (125) is recommended as it supplies the best results.

A6 Iterative process for the determination of the operating characteristic

The process equations required for the determination of the operating characteristic are discussed in chapter 5. Using the process equations (Eq. (164) - (191)), the self-adjusting operating point (evaporation and condensation temperatures, working fluid mass flow, heating capacity etc.) can be determined iteratively as a function of the ambient temperature. Within the framework of this study, an iteration program for the calculation of the operating characteristic was written in Maple 10.

Sequence of operations in the iteration program:

- Input of the required material properties and constants (e.g. heat exchanger surfaces, heat transfer coefficients, compressor characteristics etc.).
- Definition of initial values: As an initial value, the evaporation temperature is set to be equal to the ambient temperature; for the condensation temperature the supply temperature as defined by the heating curve is used. In this case, the supply temperature is - as for the return temperature - a function of the ambient temperature.
- Calculations are performed using Eq. (164) to (191) using the initial values described above.
- In a further step, new initial values for evaporation and. the condensation temperatures for the next iteration pass are calculated with the aid of Eq. (175) and (186).
- Subsequently, the calculations (points 3 and 4) are carried out once more and the recalculated values of the evaporation and condensation temperatures are used as initial values for the evaporation and condensation temperatures once more.
- This calculation loop is repeated until the differences in condensation and evaporation temperatures from pass n to pass n+1 is less than 0.001 K.
- As soon as this convergence criterion is fulfilled, the calculation loop is stopped and the relevant data (evaporation and condensation temperatures, heating capacity, compressor power, temperature differences for heat transfer, temperature lift etc.) are noted.

For better understanding, the iteration process can also be represented graphically.

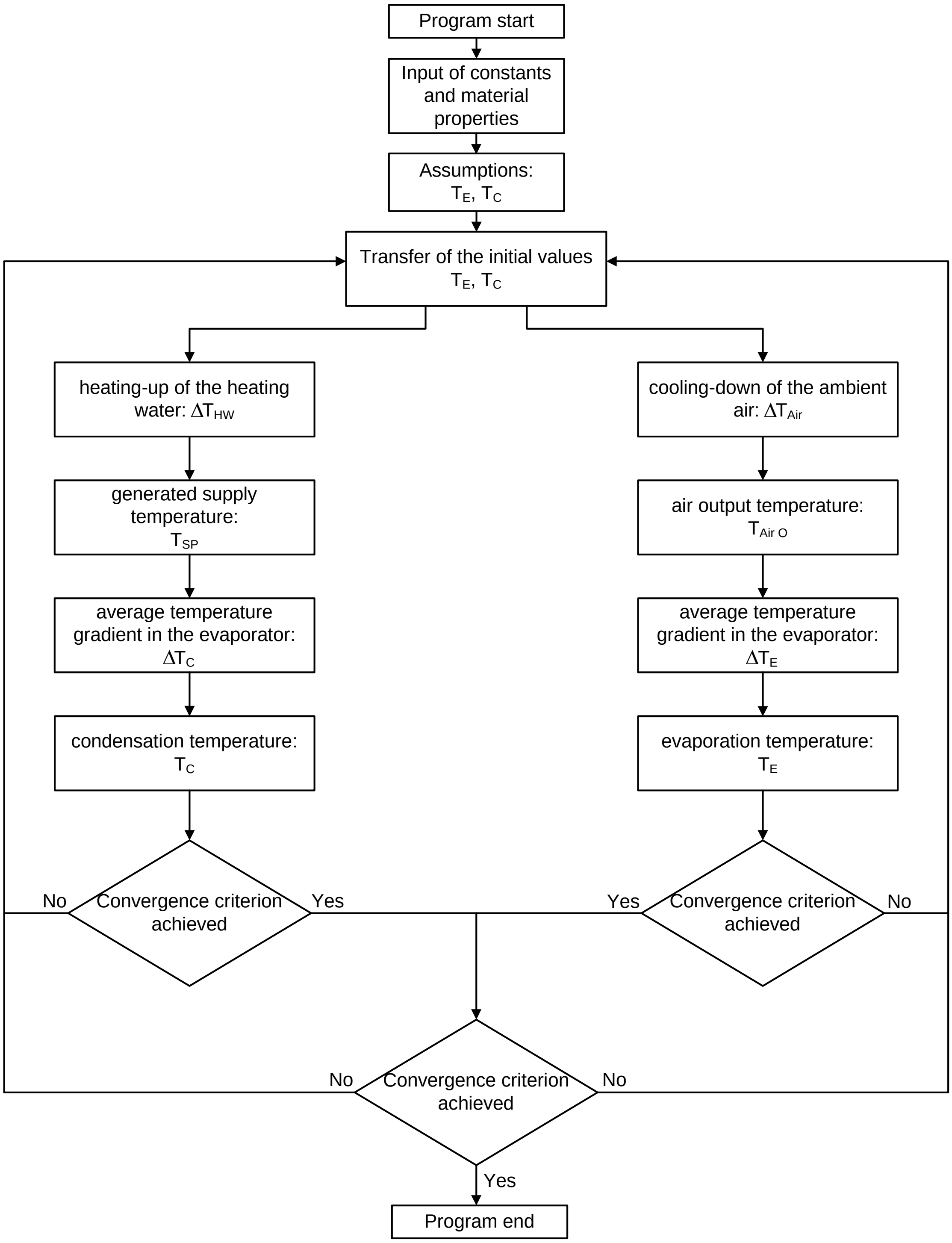

The resulting operating characteristic of the air/water heat pump is heavily dependent on the compressor model used. Consequently, it is absolutely necessary to make separate calculations for all compressor models examined.

A7 Specifications of the air/water heat pump simulated

Within the framework of this theoretical exergy analysis, the air/water heat pump with on/off control installed at the laboratory of the Lucerne University of Applied Sciences and Arts – Engineering & Architecture, Switzerland, was simulated and evaluated exergetically.

Model: Air/water heat pump PPL 401

Manufacturer: Steinmann Apparatebau AG
Alpenweg 4
3038 Kirchlindach

Technical data:

Working fluid: R 407C

Compressor: Scroll compressor - see appendix A1

Evaporator: Fin tube evaporator with a depth of 4 rows of tube
total heat transfer surface $A_E = 18.2\,m^2$

Condenser: Plate heat exchanger
total heat transfer surface $A_C = 0.92\,m^2$

A8 Evaporation and condensation of multi-component mixtures

In refrigeration technology, multi-component mixtures already have quite a long tradition. For multi-component mixtures, it can be distinguished between so-called azeotropic and zeotropic refrigerants. Azeotropic multi-component mixtures show a similar behaviour to single-component refrigerants during evaporation and condensation. In contrast to azeotropic mixtures (e.g. R134A, R502, R507A) which behave like single-component mixtures during the evaporation and condensation, the phase change in the case of zeotropic mixtures “glides” over a certain range of temperature. This temperature glide during evaporation and condensation can be more or less strongly pronounced [11].

In the heat pump process, the zeotropic behaviour leads to a slight temperature increase during evaporation and a small temperature drop during condensation. This behaviour is shown as a heat pump process in the log p,h-diagram in Fig. A 8 for the multi-component mixture R407C.

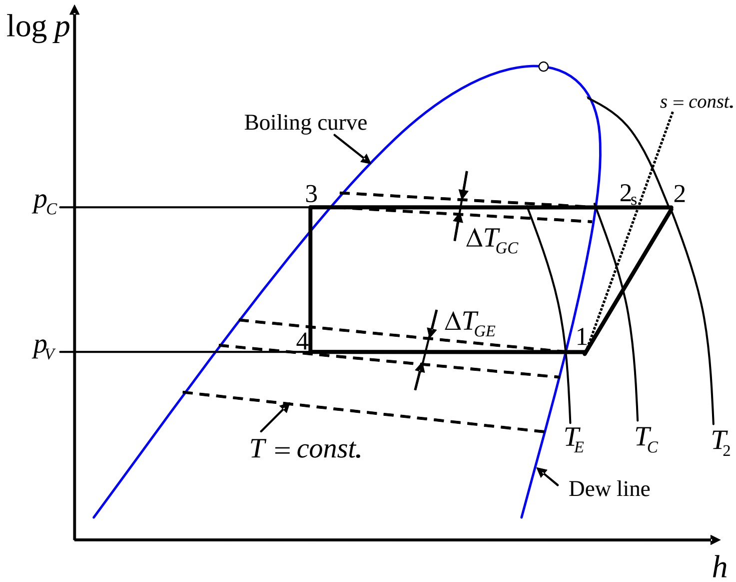

Fig. A 8: log p,h-diagram for a zeotropic mixture (e.g. R407C) with heat pump process

If the working fluid exhibits a temperature glide during the evaporation and condensation, the evaporation and condensation temperatures (T_E and T_C) refer to the respective temperatures on the dew line (cf. Fig. A 8).